The identification of miRNA biomarkers of chronic kidney disease and development of minimally-invasive methods of molecular detection

Cristina Beltrami, BSc MSc

Thesis presented for the degree of Philosophiae Doctor

2014

Institute of Molecular and Experimental Medicine (IMEM)
Institute of Nephrology
School of Medicine
Cardiff University
Heath Park
Cardiff
CF14 4XN

DECLARATION

This work has not previously been accepted in substance for any degree and is not concurrently submitted in candidature for any degree.

Signed..... (candidate) Date .....

STATEMENT 1

This thesis is being submitted in partial fulfillment of the requirements for the degree of PhD

Signed..... (candidate) Date .....

STATEMENT 2

This thesis is the result of my own independent work/investigation, except where otherwise stated.

Other sources are acknowledged by explicit references.
Signed..... (candidate) Date .....

STATEMENT 3

I hereby give consent for my thesis, if accepted, to be available for photocopying and for inter-library loan, and for the title and summary to be made available to outside organisations.

Signed..... (candidate) Date .....

STATEMENT 4: PREVIOUSLY APPROVED BAR ON ACCESS

I hereby give consent for my thesis, if accepted, to be available for photocopying and for inter-library loans **after expiry of a bar on access previously approved by the Graduate Development Committee.**

Signed..... (candidate) Date .....

To my parents, for your support and love.

Acknowledgements

I want to express my gratitude to my supervisors, Dr Timothy Bowen and Dr Donald Fraser, first of all for giving me the possibility to do my PhD in their laboratory but also for their support and guidance throughout my PhD. I would like to thank them for trying to keep me calm when the project ever went down and when I was stressed because the results were not enough for me. I am also very grateful to Professor Aled Phillips, for his help during the entire project from the beginning to the end and to Dr. Robert Steadman (Bob) for the precious advices.

I am grateful to Dr Alexa Wonnacott for consenting and collecting the urine samples from DN patients, to Dr Aled Rees for involving us in PCOS studies, to Dr Simon Satchell for kindly donating the CiGEnC and to Prof Susan Wong for the NOD mice RNA.

Thanks to all the people that shared the study office with me in these 3 years. For their essential advises, guidance, and ability to sort out experimental problems. For the intelligent conversations but even more for the less scientific chat because it made those times memorable. For encouraging me and making me feel part of a group. For listening to all my complaining and motivate me to never give up. Big thanks also to the lab manager and the secretaries for their essential assistance in dealing with any problems, especially bureaucracies.

A thank you goes also to my friends. To the old ones from Italy because, even if we see each other twice in a year, we know that we can count on each other. To the new ones, that I met during this experience in Cardiff and that made it special.

A special thanks goes to Tiago for becoming one of the most important and essential people in my life. Because your help, encouragemeny and love made this thesis and everything possible.

Finally, I want to say the greatest thanks to my parents. Because with their sacrifices I had the possibility to study. Because they are always next to me, even if we are in two different countries. Because they encourage and support any my decisions even when they are not completely happy with my choices.

Thesis Summary

Kidney biopsy is the current gold standard diagnostic test for intrinsic renal disease but requires hospital admission and carries a 3% risk of major complications. Current non-invasive prognostic indicators such as urine protein quantification have limited predictive value. Better diagnostic and prognostic tests for chronic kidney disease (CKD) patients are therefore a major focus for industry and academia. An alternative approach is the quantification of urinary microRNAs (miRNAs): short, non-coding RNAs that regulate gene expression post-transcriptionally.

This project investigated the utility of urinary miRNA expression analysis as a method for non-invasive diagnostic/prognostic testing for CKD. A technique was developed for quantifying miRNAs in urine samples from control subjects and diabetic nephropathy (DN) patients with a coefficient of variation below 10%. The stability of endogenous miRNAs was demonstrated in urine samples from unaffected individuals and DN patients. Two populations of urinary miRNAs were identified: those associated with exosomes and those associated with AGO2, a component protein of the RNA-induced silencing complex.

Expression of over 750 urinary miRNAs in pooled urine samples from DN patients was compared with that in corresponding control samples using TaqMan Array Human microRNA Card analysis. Statistically significant differences in expression of a subset of putative disease-associated miRNAs were then replicated in individual urine samples, and these data were supported by ROC curve analyses. Expression analysis of these target miRNAs in defined nephron segments was observed using laser capture microdissection of renal biopsy tissues followed by miRNA detection by RT-qPCR. Subsequent renal cell line analysis pinpointed miRNA cellular origins, and miRNA release into conditioned tissue culture medium in response to disease stimuli was also observed.

These experimental data reveal a pattern of urinary miRNA expression changes in DN and present putative mechanisms by which these differences in abundance might come about.

Publications and Presentations Arising From This Thesis

Peer-reviewed publications

Beltrami C, Simpson KA, Carrington CP, Jenkins RH, Corish P, Satchell SC, Phillips AO, Fraser DJ, Bowen T (2014). Altered urinary microRNA profiles in diabetic nephropathy. (manuscript in preparation).

Beltrami C, Clayton A, Jenkins RH, Corish P, Phillips AO, Fraser DJ, Bowen T (2014). Stability of urinary microRNAs is conferred by association with exosomes and argonaute 2 protein. (manuscript in preparation).

Publications

Jenkins RH, Davies LC, Taylor PR, Akiyama H, Cumbes B, Beltrami C, Carrington CP, Phillips AO, Bowen T, Fraser DJ.miR-192 induces G2/M growth arrest in Aristolochic Acid Nephropathy. *The American Journal of Pathology*, Vol. 184, No. 4, April 2014

Beltrami C, Clayton A, Phillips AO, Fraser DJ, Bowen T (2012). Analysis of urinary microRNAs in chronic kidney disease. *Biochemical Society Transactions* **40**, 875-879.

Oral presentations at conferences

Beltrami C, Clayton A, Phillips AO, Fraser DJ, Bowen T (2013). Urinary microRNAs are stabilised by association with argonaute 2 protein. Presented at the 1st Meeting on OMICS towards the Systems Biology approach in renal diseases and transplantation , Bari, Italy.

Beltrami C, Clayton A, Phillips AO, Fraser DJ, Bowen T (2013). Stability of microvesicle-free urinary microRNAs is conferred by complex formation with argonaute 2 protein. Presented at the Spring Meeting of the Renal Association, Bournemouth, UK.

Beltrami C, Clayton A, Phillips AO, Fraser DJ, Bowen T (2013). Urinary microRNAs are stabilised by association with argonaute 2 protein. Presented at the annual South West UK RNA Meeting, Cardiff University, UK.

Beltrami C, Clayton A, Phillips AO, Fraser DJ, Bowen T (2012). Analysis of urinary microRNAs in chronic kidney disease. Presented at the 27th Annual Life Science Postgraduate Research Day, Cardiff, UK

Beltrami C, Clayton A, Phillips AO, Fraser DJ, Bowen T (2012). Urinary microRNAs are stabilised by association with argonaute 2 protein. Presented at 2nd South West Regional Regenerative Medicine Meeting, Bristol, UK

Beltrami C, Clayton A, Phillips AO, Fraser DJ, Bowen T (2012). Urinary microRNAs are stabilised by association with argonaute 2 protein. Presented at RNA-UK 2012 Lake District, UK

Beltrami C, Clayton A, Phillips AO, Fraser DJ, Bowen T (2011). Analysis of urinary microRNAs in chronic kidney disease. Presented at the annual South West UK RNA Meeting, Exeter University, UK

Poster presentations at conferences

Beltrami C, Simpson KA, Carrington CP, Jenkins RH, Corish P, Satchell SC, Phillips AO, Fraser DJ, Bowen T (2014). Altered urinary microRNA profiles in diabetic nephropathy. Cardiff and Vale University Health Board Conference, Cardiff City Football Stadium, Cardiff, UK. (Prize Winning Poster)

Beltrami C, Simpson KA, Carrington CP, Jenkins RH, Corish P, Satchell SC, Phillips AO, Fraser DJ, Bowen T (2014). Altered urinary microRNA profiles in diabetic nephropathy. 27th Annual General Meeting of the EDNSG, Royal College of Physicians, London, UK

Beltrami C, Simpson KA, Carrington CP, Jenkins RH, Corish P, Satchell SC, Phillips AO, Fraser DJ, Bowen T (2014). Altered urinary microRNA profiles in diabetic nephropathy. Spring Meeting of the Renal Association, Glasgow, UK

Beltrami C, Fraser DJ, Bowen T (2013) urinary microRNAs are stabilized by association with Argonaute 2.Presented at ASN Kidney Week 2013 Annual Meeting, Atlanta, GA

Beltrami C, Clayton A, Phillips AO, Fraser DJ, Bowen T (2012) Analysis of urinary microRNAs in chronic kidney disease. Presented at the Spring Meeting of the Renal Association, Gateshead, UK

Beltrami C, Fraser DJ, Bowen T (2012). Analysis of urinary microRNAs in chronic kidney disease. Presented at Inaugural South West Regional Regenerative Medicine Meeting, 2011

Glossary of abbreviation

ACR	Albumin:creatinine ratio
AGE	Advanced glycosylation end product
AGO	Argonaute
AGO2	Argonaute 2
AKT	Protein kinase B
ALIX	Programmed cell death 6-interacting protein
AP-1	Activator protein-1
APO-E	Apolipoprotein E
AQP1	Aquaporin 1
AT1R	Angiotensin II receptor - 1
ATC	Human podocyte cell line
AUC	Area under the ROC curve
bFGF	Basic fibroblast growth factor
bp	Base pairs
BUN	Blood urea nitrogen
BSA	Bovin serum albumin
cAMP	Cyclic adenosine monophosphate
CD9	Cluster of differentiation 9
CD10	Cluster of differentiation 10
CD81	Cluster of differentiation 81
Cdc25A	Cell cycle regulator
cDNA	Complementary DNA
CiGEnC	Conditionally immortalised glomerular endothelial cells
CKD	Chronic kidney disease
Cp	Plasma creatinine
CREB	cAMP response element-binding protein
C_t	Threshold cycle
CTGF	Connective tissue growth factor
Cu	Urine creatinine
DBA/2	Dilute Brown Non-Agouti
DGCR8	DiGeorge Syndrome Critical Region 8
DN	Diabetic nephropathy
ECM	Extracellular matrix
eGFR	Estimated glomerular filtration rate
ECL	Enhanced chemiluminescence
EDTA	Ethylenediamine-tetraacetic acid
EMT	Epithelial to mesenchymal transition
EPO	Erythropoietin
ERK	Extracellular signal-regulated kinases
ESL	Endothelial surface layer
ESRD	End-stage renal disease
ET-1	Endothelin-1
ETS	E26 transformation-specific sequence
Exp-5	Exportin-5
FCS	Fetal calf serum
FFPE	Formalin-fixed paraffin embedded
FGF	Fibroblast growth factor
FSGS	Focal segmental glomerulosclerosis
FOG2	Friend of Gata - 2

GAPDH	Glyceraldehyde-3-phosphate dehydrogenase
GBM	Glomerular basement membrane
GFB	Glomerular filtration barrier
GFR	Glomerular filtration rate
GW182	Glycin-tryptophan protein of 182 kDa (official symbol TNRC6A)
h	Hour
HEK	Human Embryonic Kidney 293 cell
HK-2	Human proximal tubular epithelial cell line
HPV	Human papilloma virus
HUVEC	Human umbilical vein endothelial cell
ICAM-1	Intercellular Adhesion Molecule 1
IGF	Insulin-like growth factor
IGF-1	Insulin-like growth factor-1
IL-1	Interleukin-1
IL-1-ß	Interleukin-1- ß
IL-6	Interleukin-6
IL-18	Interleukin-18
INF-γ	Interferon gamma
JAK-STAT	Janus kinase/signal transducers and activators of transcription
JNK	c-Jun N-terminal kinase
kDa	Kilodalton
LCM	Laser capture microdissection
MAPK	Mitogen-activated protein kinases
miRNA	microRNA
MMC	Mouse mesangial cell
MMP9	Matrix metallopeptidase - 9
mRNA	messenger RNA
MP	Microparticle
MV	Microvesicle
ncRNAs	Non-coding RNA
NKF-KDOQI	National Kidney Foundation Kidney Disease Outcomes Quality Initiative
NF-κB	Nuclear factor κB
NO	Nitric oxide
NOD	Non-obese diabetic
nt	Nucleotide
PAI-1	Plasminogen activator inhibitor-1
PAGE	Polyacrylamide gel electrophoresis
PAZ	Piwi-Argonaute-Zwille
PBS	Phoshate buffer saline
PCC	Pearson correlation coefficients
PCOS	Polycystic ovary syndrome
PCR	Protein:creatinine ratio
PCR	Polymerase chain reaction
PDGFA	Platelet-derived growth factor subunit A
PDGFC	Platelet-derived growth factor subunit C
PDGFß-R	Platelet-derived growth factor-ß receptor
PECAM-1	Platelet endothelial cell adhesion molecule -1
PI3K	Phosphatidylinositol-3-kinase
PIK3R2	Phosphoinositol-3 kinase regulatory subunit - 2
PKC	Protein kinase C
PKD	Polycystic kidney disease

PKD2	Polycystic kidney disease- 2
pol II	Polymerase II
pol III	Polymerase III
pre-miRNA	Precursor miRNA
pri-miRNA	Primary transcript of microRNA
PTC	Proximal tubular cell
PTEN	Phosphatase and tensin homolog
qPCR	Quantitative polymerase chain reaction
RT-qPCR	Quantitative reverse transcription – polymerase chain reaction
RAAS	Renin-angiotensin aldosterone system
Ran-GTP	RAs-related nuclear protein-guanosine-5'-triphosphate
RIN	Regulatory interaction network
RISC	RNA-induced silencing complex
RNA	Ribosomal nucleic acid
RNase A	Ribonuclease A
RT	Reverse transcription
RT-NTC	Reverse transcription – non template control
ROC	Receiver-operator characteristic
ROS	Reactive oxygen specie
SDS-PAGE	Sodium dodecyl sulfate-polyacrylamide gel electrophoresis
SEM	Standard error of the mean
SDF-1	Stromal cell-derived factor - 1
STZ	Streptozotocin
SOCS1	Suppressor of cytokine signaling - 1
SOD2	Superoxide dismutase - 2
SPRED1	Sprouty-related protein
T1DM	Type 1 diabetes mellitus
T2DM	Type 2 diabetes mellitus
TIMP1	Tissue inhibitor of metalloproteinase - 1
TGF-ß	Transforming growth factor beta
TGF-ß1	Transforming growth factor beta -1
TNF-α	Tumour necrosis factor-alpha
TNFAIP3	Tumour necrosis factor, alpha-induced protein - 3
TNFR1	Tumour necrosis factor receptor - 2
TNFR2	Tumour necrosis factor receptor - 2
TRBP	Transactivating response RNA-Binding Protein
TRL	Toll-like receptors
TSG101	Tumour susceptibility gene
TXNRD2	Thioredoxin reductase - 2
UTR	Untranslated region
UUO	Unilateral ureteral obstruction
VCAM-1	Vascular cell adhesion molecule - 1
VEGF	Vascular endothelial growth factor
VEGFR2	Vascular endothelial growth factor receptor - 2
vWF	Von Willebrand factor
ZEB1	Zinc finger E-box-binding homeobox - 1
ZEB2	Zinc finger E-box-binding homeobox - 2

Chapter 1 – Introduction

The overall purpose of the work carried out during the PhD research project described in this thesis was to develop approaches to urinary miRNA quantification as novel, non-invasive biomarkers for the diagnosis and prognosis of diabetic nephropathy. In order to have a complete understanding of the potential of urinary biomarkers, in this introduction I have first considered how the kidney makes urine. To this end, before outlining the biogenesis and role of miRNAs in kidney disease, this introduction section will briefly describe the structure of the kidney and the different compartments of the nephron. As the basic structural and functional unit of the kidney, the nephron is ultimately responsible for urine production. The structural changes in diabetic nephropathy that subsequently result in functional impairment are also described.

1.1 Kidney

1.1.1 Kidney structure

The kidneys are a pair of organs located in the back of the abdomen that in a healthy adult human are approximately 10 cm in length, 6 cm wide and have a thickness of 3 cm. The surface of the kidneys is covered by the renal capsule, a connective tissue layer rich in fibroblasts and collagen fibres that preserves the structure of the kidneys and provides protection from injury. The peripheral part of the kidney consists of the cortex and the medulla. The medulla is composed of medullary pyramids with the base of each pyramid facing the renal cortex. It appears striated because it contains the straight tubular structures known as the descending and ascending limbs of the loop of Henle, the collecting tubule, and blood vessels. The cortex is the outer portion of the kidney and consists of renal corpuscles, convoluted tubules, descending and ascending straight tubules, and an extensive vascular supply.

The nephron is the basic structural and functional unit of the kidney. The afferent arteriole provides blood to the glomerular capillaries, which then leaves via the efferent arteriole. In the majority of glomeruli, the efferent arteriole then divides into a capillary network supplying the renal tubules. The nephron begins at the renal corpuscle, which is composed of the glomerulus with a tuft of capillaries surrounded by a double-layer of cup-shaped epithelial cells known as

the Bowman's capsule. The cavity of the capsule leads to the proximal renal tubule, which is separated into convoluted and straight sections. The straight part continues into the descending limb of the loop of Henle, which then ascends to become the distal tubule, firstly the straight part and then the convoluted distal tubule. The convoluted distal tubule is connected to the cortical collecting duct by a connecting tubule [1].

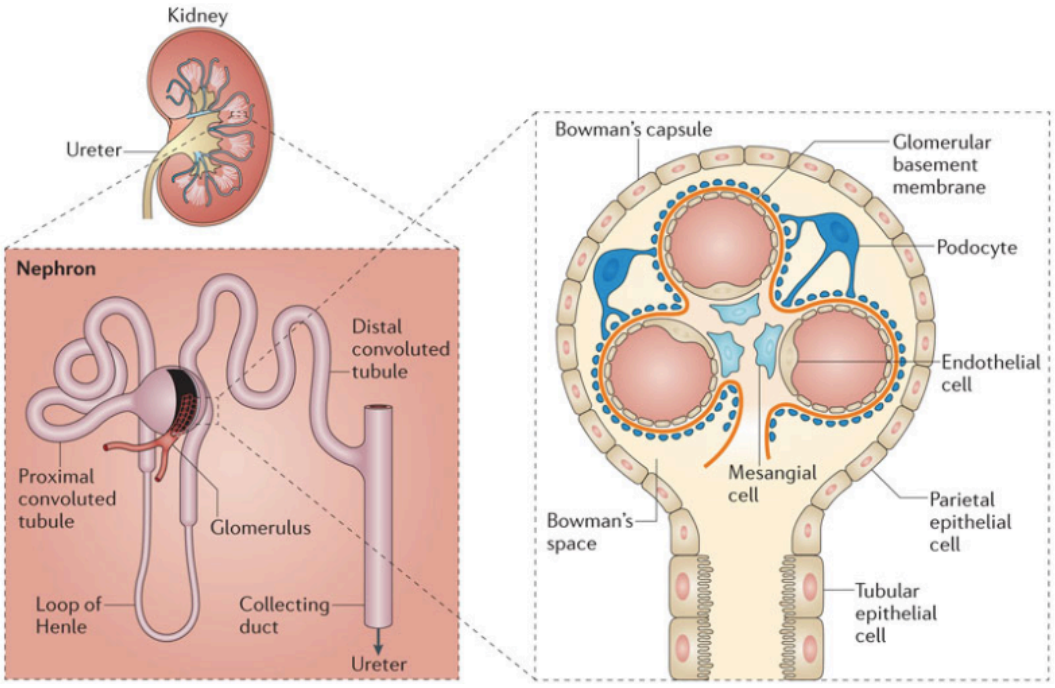

Figure 1.1. Basic kidney anatomy

The illustrations were adapted from the excellent review by Kurts and colleagues [2].

1.1.2 Nephron

1.1.2.1 Nephron compartments

As stated before, the first part of the nephron is composed of the glomerulus and Bowman's capsule, and functions as the filtration apparatus of the kidney. The glomerulus is composed of endothelial cells, mesangial cells and podocytes, while the Bowman's capsule is characterised by simple squamous epithelium. The glomerular filtration barrier (GFB) comprises 3 layers: a capillary endothelium, a basal lamina and a podocyte layer, with the basal lamina located between the other two layers.

The GFB defines the characteristic of the glomerular ultrafiltrate. Water, small and midsized solutes of mass <10 kDa can cross the GFB directly. For molecules of mass >10 kDa, passage is restricted and charge selection applies, while molecules >100 kDa cannot be filtrated. Fluid filtered through the glomerulus flows to the proximal convoluted renal tubule that consists of epithelial cells covered by densely packed microvilli, the loop of Henle that is made up of simple squamous epithelial cells, and the distal convoluted tubule lined with simple cuboidal cells [2].

The endothelium

The glomerular endothelial cells are responsible for haemostasis, trafficking of leucocytes and vasomotor tone regulation through the secretion of endothelin, platelet derived growth factor and the secretion of nitric oxide and prostacyclin [3]. Glomerular endothelial cells have the unique structural feature of fenestrations that constitute 20-50% of the endothelial cell surface and facilitate the exchange of substrate between intra and extravascular compartments [4]. The fenestrations are approximately 60 nm in diameter, and since albumin has a diameter of 3.6 nm, this suggests that endothelial cells are only partly responsible for the selective permeability of the glomerular barrier [5]. An endothelial cell surface layer (ESL) covers the luminal side of the blood vessel and this is implicated in processes such as blood coagulation, angiogenesis and capillary barrier function [6]. The ESL is composed of glycocalyx and endothelial cell coating. Glycocalyx is formed by soluble plasma components and is composed of large amounts of glycoprotein, such as proteoglycans, and/or

glycosaminoglycans. With a typical thickness of approximately 200 nm the glycocalyx plays an active role in restricting the passage of macromolecules and permitting the passage of water and small solutes [7]. The normal endothelium is also characterised by its capacity to maintain blood flow [8] and initiate the inflammatory centre by recruitment of leucocytes [9].

The mesangium

The mesangial cells are localised in the centre of the glomerulus and, together with the extracellular matrix (ECM), are responsible for maintaining the structure and function of the GFB. They are adjacent to endothelial cells on the opposite side of the glomerular basement membrane to the podocytes. They contract or relax in response to a number of vasoactive agents, and this event may modify the glomerular ultrafiltration coefficient [10]. Mesangial cells express platelet-derived growth factor-ß receptor (PDGFß-R) [11], together with transforming growth factor beta (TGF-ß), a key mediator in kidney disease progression, interleukin-1 (IL-1), and insulin-like growth factor (IGF) [11]. These cells also express angiotensin-II receptors [12] and produce mesangial ECM components [13].

The glomerular basement membrane (GBM)

The GBM is composed of the basal lamina, approximately 300-370 nm thick that lies between the glomerular endothelial cells and podocytes. The basal lamina is composed of laminin, type IV collagen, sulphate proteoglycans and glycoproteins.

These components are located in specific regions of the lamina:

- the lamina rara externa, on the podocyte side, is well provided with polyanions responsible for preventing the passage of negatively charged molecules;
- the lamina rara interna, on the endothelial side;
- the lamina densa, overlaps the rara externa and rara interna, and is characterized by the presence of type IV and XVIII collagen, perlecan and agrin responsible for both increasing the anionic charge and connecting the endothelial cells and podocytes to the membrane.

Molecules larger than 70 kDa, or with a radius greater than 3.6 nm, do not cross the filtration barrier, while those with a mass below 70 kDa that are negatively charged are also repulsed [1,14].

The podocyte

Podocytes are differentiated, highly specialized cells of mesenchymal origin, which subsequently undergo phenotypic transition and acquire a partial epithelial characteristic, an apical and a basolateral membrane. The podocyte cellular architecture is characterized by a cell body with interdigitating foot processes that are separated by a filtration slit approximately 25-60 nm wide, and covered by the slit diaphragm. Podocytes are connected to the GBM via foot processes that represent the basolateral domain, and are characterized by a contractile apparatus composed of myosin II, α-actin, talin and vinculin. The cell body is characterized by the presence of proteins such as vimentin and desmin, and small microtubules. The apical membrane is composed of glycoproteins, these are negatively charged and therefore play a role in regulating filtration across the GBM [6,15,16]. Proteins that form the slit diaphragm, such as the main protein component nephrin, are crucial for maintaining normal glomerular permeability and regulating passage of molecules across the GBM on the basis of the size, charge and physical configuration [17].

The parietal cell

The parietal cells form a single layer of simple squamous epithelium attached to the Bowman's basement membrane with a thickness of 0.1-0.3 μm. Like podocytes, they are derived from a common ancestral mesenchymal progenitor and have the ability to respond to injury by de-differentiating into an embryonic phenotype, while under homeostasis they differentiate into glomerular podocytes.

Between parietal cells, tight junction proteins and cadherins help to prevent the passage of proteins into the extra-glomerular space, and these cells are therefore considered a second glomerular barrier to filtered proteins [17-19]

The proximal tubular cell

The proximal tubule is the portion of the nephron that receives the ultrafiltrate from the glomerulus and leads to the loop of Henle and is divided into a convoluted and straight portion. Cuboidal epithelial cells make up the convoluted

proximal tubule, with the apical-luminal surface bordered with millions of microvilli that increase the surface area for absorption/transport. On the basolateral side, mitochondria supply energy for transport. Proximal tubular cells (PTC) have a key role in renal function: they are responsible for reabsorbing glucose, hormones, vitamins and peptides filtered by the glomerulus. These cells also control the acid-base balance and excrete metabolic end products [20].

The convoluted tubule is followed by the loop of Henle, which is organized into 3 sub-sections composed of squamous epithelial cells with limited cytoplasm and small numbers of mitochondria:

- The thin descending limb which is permeable to water but not to salt;
- The thin ascending limb that is impermeable to water and passively permeable to salt;
- The thick ascending limb which is responsible for the transport of salt from the lumen

The loop of Henle then becomes the distal convoluted tubule, which is composed of cuboidal cells. Shorter than the proximal tubule, the distal tubule shows infolding of the basolateral membrane and its cells are rich in mitochondria. The distal convoluted tubular cells are responsible for the final part of sodium and water reabsorption, and hydrogen and potassium secretion [21].

1.1.2.2 Functions of the nephron compartments

Nephrons are responsible for producing urine and maintaining homeostasis, via control of electrolytes, acid-base balance and removal of toxins and waste products. Additional roles include blood pressure regulation and production of hormones like renin, calcitriol and erythropoietin [8,21].

Urine production and maintenance of homeostasis

Filtration

Urine formation begins with blood filtration in the renal corpuscle. Blood arrives via the afferent arteriole, flows in the glomerulus under pressure, and is filtered through the GBM according to its composition. Molecules with a radius

below 1.8 nm such as water, ions, glucose or insulin pass through freely, while those with a radius between 1.8 and 4.2 nm, or above 4.2 nm, have restricted access or cannot pass through the barrier. In addition, the overall negative-charge of the GFB impedes passage of negatively charged molecules but facilitates the passage of positively charged ones. The non-filterable components of the blood, mainly blood cells, platelets and some plasma proteins, leave via the efferent arteriole.

Reabsorption

Reabsorption is the process by which approximately 60-80% of solutes and water that cross the GFB each day are absorbed again by endocytosis in the proximal convoluted tubule. It is regulated by active transport, osmosis and diffusion and is divided into two steps. Molecules are initially transported from the tubule to the interstitium, and subsequently to the peritubular capillaries.

The composition of the ultrafiltrate produced in the Bowen's capsule space changes in the proximal tubule due to the reabsorption of substances including glucose, amino acids, vitamins and electrolytes. Sodium is reabsorbed mainly at the proximal tubule, but in lower amounts also in the loop of Henle, distal tubule and collecting duct. Sodium reabsorption involves the Na^+/K^+ ATPase pump where Na^+ is primarily moved passively from the lumen to the tubular cells. Subsequently, Na^+ is actively transported from the tubular cell into the interstitial fluid within the lateral space and, finally, into the peritubular capillary.

Secretion

Substances such as toxins, antibiotics, hydrogen ions, creatinine or molecules present in surplus in the blood are secreted directly from the distal convoluted tubule. Secretion has two fundamental roles: to remove waste products and to maintain acid-base balance. The combination of these secreted substances with water and other waste products constitutes urine, which is then ready to move from the kidney to the bladder via the ureters in readiness for excretion [1,9-11,20,22,23].

Hormone secretion

In response to renal hypoxia, the renal mesangial and tubular cells produce erythropoietin (EPO), which promotes the formation of red blood cells in the bone marrow. In addition, the kidney is responsible for the formation of calcitriol, the active form of vitamin D, from cholecalciferol. Calcitriol has a role in regulating the concentration of calcium and phosphate in the bloodstream and bone remodelling. The juxtaglomerular apparatus, located near the vascular pole of the glomerulus, is an integral part of the maintenance of sodium homeostasis and renal haemodynamics by the renin-angiotensin aldosterone system (RAAS) [23-26].

1.2 Kidney diseases

1.2.1 Chronic kidney disease (CKD)

Chronic kidney disease (CKD) is characterised by a progressive loss of renal function, as evidenced by a reduction of the volume of glomerular filtrate produced per min, or glomerular filtration rate (GFR), to less than 60 mL/min per 1.73m^2 on at least 2 occasions for more than 3 months. A UK cross-sectional study conducted in over 130,000 adults indicated a prevalence of CKD stage 3-5 of 8.5%, higher in females (10.6%) than in males (5.8%) [28]. This value is likely to underestimate true CKD prevalence, since GFR is untested in a significant proportion of the population [27]. The prevalence of CKD in the USA has been estimated at 13% [28], and in Australia at 13.4% for stages 1–5 and 7.8% for stage 3–5 [29]. The estimated cost of CKD to the NHS in England in 2009-2010 was £1.4 billion / year, 1.3% of the total NHS annual budget [30].

The National Kidney Foundation Kidney Disease Outcomes Quality Initiative (NKF-KDOQI) classified CKD into 5 stages on the basis of kidney damage and level of renal function estimated as GFR [31].

- Stage 1, GFR more than 90 mL/min per 1.73m^2
- Stage 2, GFR between 60-89 mL/min per 1.73m^2

  Both of these stages require the presence in urine of persistence of protein (proteinuria), albumin (albuminuria) or red blood cells (haematuria), or structural abnormalities.
- Stage 3, GFR between 30-59 mL/min per 1.73m^2
- Stage 4, GFR between 15-29 mL/min per 1.73m^2
- Stage 5, GFR less than 15 mL/min per 1.73m^2. This stage may be described as established renal failure or end stage renal disease (ESRD).

In general, CKD stages 1 and 2 are asymptomatic. Indeed, its presence may not become obvious until disease is well established, and has led to CKD being referred to as a “silent killer” [32].

1.2.1.1 CKD biomarkers

GFR is used to estimate renal function, providing a measure of how well the kidneys are working, and is usually approximately 120 mL/min. Since GFR cannot be measured directly, it is estimated as endogenous creatinine clearance, the volume of blood plasma that is cleared of creatinine per unit of time. Creatinine is a molecule produced during normal muscle breakdown. It is proportional to the muscle mass, and is filtered and not absorbed by the kidney.

Creatinine clearance is calculated by multiplying the creatinine concentration in the collected urine sample (Cu) per the urine flow rate (V) and dividing by creatinine concentration in plasma (Cp) i.e. GFR = (Cu x V) / Cp. Creatinine clearance is frequently corrected for body surface area and compared to the average size of an adult male (mL/min/1.73 m^2). However, the variation in creatinine clearance is not sensitive enough to detect CKD, since it is susceptible to non-renal and/or analytical effects such as ingestion of cooked meat, inaccuracies in urine collection or method/analyser used, and there is inter-laboratory variation [33]

The upper limit of protein in urine is around 150 mg/24 h, equal to a protein:creatinine ratio (PCR) of 15 mg/mmol. Albumin, one of the main proteins in the blood, is the most abundant protein detectable in urine in most nephropathies. A normal mean value for albuminuria is 10 mg/day, microalbuminuria is defined as 30–300 mg/day, equivalent to an albumin:creatinine ratio (ACR) of >2.5 mg/mmol in men and >3.5 mg/mmol in women. Macroalbuminuria is defined as an urinary albumin output exceeding 300 mg/day (ACR >30 mg/mmol) [31,34,35].

New biomarkers have emerged for monitoring renal function including cystatin-C and uric acid [36]. Cystatin-C has a molecular weight of 13 kDa and is normally filtered and reabsorbed, in pathological conditions its serum levels increase. In normal conditions, uric acid is eliminated through the kidney, but during CKD its levels raise [37]. Additional biomarkers for kidney cellular injury include nephrin and podocin, podocyte-specific markers, that are found at elevated levels in the urinary sediment of diabetic nephropathy patients [38]. The main biomarkers used for renal disease, including those that have been recently discovered, have been expertly and comprehensively reviewed in the context of pathophysiological processes [39].

Currently, the gold standard diagnostic test for kidney disease is the renal biopsy, an invasive procedure where a small sample of tissue is removed and in 3% of the cases complications such as bleeding or infection may occur. The CKD biomarkers described above have been useful, but additional biomarkers are needed, particularly for diagnosis of early stage CKD, since current disease markers are not specific and sensitive enough to predict the outcomes of individual CKD patients. In many cases, outcome will be influenced by factors involved in renal perfusion, and presently available biomarkers are not capable of discriminating either the cause or the location of the injury.

Albuminuria has been used as a marker for glomerular disease but lacks specificity, by the time significantly increased albuminuria is detectable extensive renal damage may already be present. In addition, slower progression of CKD may be accompanied by a reduction in proteinuria, while a faster decline may be associated with a proteinuria increase [40]. Blood urea nitrogen (BUN) and cystatin-C are influenced by non-renal events such as protein intake, dehydration, liver activity, gastrointestinal bleeding and steroid use, or muscle mass, age and sex. Given both the complexity of this pathology and the multitude of factors involved in the progression/complications of CKD, more informative biomarkers are under study/in demand for efficient classification of disease progression, morbidity, and mortality.

1.2.1.2 CKD progression

Many conditions and factors that damage the kidney contribute to CKD progression. Diabetes is the most important cause of renal disease, followed by vascular disease (primarily hypertension) [41]. Other conditions that cause CKD include glomerulonephritis, pyelonephritis, polycystic kidney disease, and systemic lupus erythematosus.

The national kidney foundation found additional risk factors that correlated with CKD included old age (> 60 years old), genetic factors, autoimmune disease, obesity, sedentary life style, drug abuse and family history of kidney disease [34]. Irrespective of their origins, most kidney diseases appear to share common pathways to glomerular and tubular fibrosis via mechanisms involving common signalling pathways and cytokines such as TGF-ß, platelet-derived growth factor (PDGF), fibroblast growth factor (FGF), connective tissue growth factor (CTGF)

and endothelin. Disease progression is also characterised by increased ECM synthesis [42].

1.2.2 Diabetic Nephropathy

Diabetic nephropathy (DN) is the principal cause of CKD in the UK and the second most common cause of end-stage renal disease (ESRD), constituting 20-50% of all patients requiring renal replacement therapy or kidney transplantation. Classification of DN is determined by urinary albumin excretion along with increase in blood pressure and decline in GFR [43,44].

Morgensen and co-workers classified DN into 5 stages:

Stage 1 – Early hypertrophy and hyperfunction associated with excretion of albumin in the urine

Stage 2 – Glomerular lesion without sign of clinical disease and elevation of GFR and urinary albumin excretion

Stage 3 – Development of DN with higher albumin excretion

Stage 4 – Clear DN characterised by persistent proteinuria (> 0.5g/24h)

Stage 5 – End-stage renal failure with uraemia [45]

DN can occur following either type 1 diabetes (T1DM) or type 2 diabetes (T2DM). Presentation of DN in T1DM is ascribable to the above classification, while the DN in T2DM is frequently accompanied by the presence of other chronic diseases or conditions such as obesity, hypertension or cardiovascular disease [46,47]. Differences in the patterns of renal damage caused by T1DM or T2DM have also been reported [47]. In T1DM, renal damage is the consequence of long-term exposure to hyperglycaemia, and it is characterized by the accumulation of ECM proteins that leads to increased mesangial size [48]. Glomerular and tubular basement membrane thickening and tubulointerstitial fibrosis and glomerulosclerosis are also seen. Initially, subjects exhibit hyperfiltration (high value of GFR), and possibly, microalbuminuria, while when the disease progress (usually after 15-20 years), GFR decreases gradually and microalbuminuria is succeeded by moderate proteinuria. Eventually, severe proteinuria is seen in the final pathological stage [48].

In pure T2DM, classical DN is seen in a minority of cases, often those with diabetic retinopathy and normal body mass index (BMI). Other patients may manifest a more complex renal injury, including tubulointerstitial and vascular lesions. Approximately 30% of T2DM patients have hypertension [49,50].

1.2.2.1 Factors involved in development and progression of DN

Glucose

Hyperglycaemia is the leading cause of DN and, together with hypertension, is one of the main reasons for renal hypoperfusion, glomerular hypertension and hyperfiltration [51]. Glomerular hypertrophy is one of the first consequences of elevated circulating glucose levels, followed by an accumulation of ECM proteins that causes a thickening of the glomerular and tubular basement membranes. Later, capillary barrier and basement membrane are affected by non-enzymatic glycosylation factors. In addition, concomitant ECM accumulation of collagen IV, fibronectin, laminin and thrombospondin with collagen I and III cause mesangial matrix hypertrophy [52,53].

High circulating glucose concentrations cause oxidative stress and the production of reactive oxygen specie (ROS) that is, in turn, responsible for DNA damage and upregulation of TGF-ß, plasminogen activator inhibitor-1 (PAI-1), ECM protein expression and the induction of apoptosis [54]. Metabolic abnormalities in mesangial cells have been reported following treatment with high glucose concentrations of 23-30 mM [54]. This condition induces TGF-ß production that leads to increased expression of GLUT1 mRNA and protein, causing enhancement of glucose uptake [55]. Another effect of TGF-ß induction in mesangial cells is an increase in collagen IV and laminin production [56]. Further work in the same cells has shown that PDGF, which has an important role in angiogenesis, is also activated after incubation with high glucose and causes an increase of TGF-ß1 expression [57]. Hyperglycaemia also up-regulates vascular endothelial growth factor (VEGF) expression in podocytes and vascular permeability [58].

Advanced glycosylation end products (AGE) are glycosylated proteins formed following onset of hyperglycaemia and have a key role in the progression of DN. Galler and colleagues showed that ESRD patients have double the amount of tissue AGEs in comparison with healthy subjects [59]. AGE accumulation in the GBM and ECM modifies ECM-ECM and ECM interactions [60]. AGEs regulate different intracellular events, such as the activation of protein kinase C (PKC), mitogen activated protein kinase (MAPK), and transcription factors such as nuclear factor κB (NF-κB) [61,62].

The PKC family is a group of enzymes responsible for phosphorylation of serine and threonine residues on intracellular proteins involved in basement membrane regulation or growth factor expression [63]. Enhancement of PKC activity was identified in diabetic rats and cells treated with high glucose concentrations [63]. It has also been shown that high PKC expression is responsible for endothelial dysfunction with reduction of nitric oxide production and up-regulation of endothelin-1 and VEGF [64]. PKC activation also results in increased endothelial permeability to albumin, kidney hypertrophy, inhibition of mesangial cell proliferation and accumulation of mesangial ECM [62,65-67].

Hypertension

Hypertension is another main risk factor for renal disease. It has been reported that 70% of diabetic patients are affected by hypertension, but DN is also the main cause of hypertension in subjects with T1DM [68]. Damage to kidney vasculature occurs as a result of increased blood pressure, which reduces the capacity of the kidney to filter fluid and waste products, resulting in increased proteinuria [69]. High blood pressure can also be a consequence of CKD, and may result from a reduction in kidney function due to other factors, along with increased blood volume [70].

Factors associated with hypertension include increased renal sodium reabsorption, activation of the RAAS, up-regulation of ET-1 and ROS, and down-regulation of nitric oxide (NO). It has been reported that increased extracellular fluid volume resulted in loss of salt balance and RAAS activation, leading to a direct reduction of NO which, in turn, effected vasoconstriction and loss of vasodilator effect [69]. Increased angiotensin II production is attributable to prolonged hyperglycaemia, which increases the production of mesangial matrix proteins and inhibition of mesangial matrix degradation [69]. Another consequence of angiotensin II induction is the production of TGF-ß in resident renal cells that concurs with ECM accumulation [71]. Moreover, angiotensin II stimulates synthesis in vascular smooth muscle cells of proteins such as collagen I, but not collagen IV, and increases levels of insulin-like growth factor 1 (IGF-I), PDGF-A, basic FGF and TGF-ß [13].

In high glucose conditions, angiotensin II binds to its type 1 receptor (AT1R) activating extracellular signal-regulated kinases (ERK), c-Jun N-terminal kinase (JNK) and p38 MAPK signaling, and production of activator protein-1 (AP-1) and

cyclic adenosine monophosphate (cAMP) response element-binding (CREB) protein are enhanced. The result is an increase of ECM synthesis and cell growth. Association of angiotensin II with its AT1R is also responsible for vasoconstriction in vascular smooth muscle cells and increased sodium reabsorption in the PTCs [72].

In normal conditions, vascular endothelial cells release substances that have opposite effect than the RAAS. These cells produce nitric oxide (NO) that induces relaxation and vasoconstriction in vascular smooth muscle cells. Hypertension and hyperglycaemia increase oxidative stress and decrease excretion of NO, there reducing its vasodilator function [72].

ET-1 is produced in the vascular endothelium and stimulates mesangial cell proliferation and hypertrophy, ET-1 expression is increased in insulin resistant type 2 diabetic subjects [73].

Inflammation

Inflammatory processes are also important in DN pathogenesis, with leukocyte infiltration and cytokine activity apparent at every disease stage [2]. Hypertension and hyperglycaemia stimulate ET-1 production and activate neutrophils, induce monocyte chemoattractive factor-1 synthesis by endothelial cells, and increase expression of cell adhesion molecules such as intercellular adhesion molecule 1 (ICAM-1) [74]. Different stimuli, such as hyperglycaemia, hyperinsulinemia, AGEs, ROS and angiotensin II act on different kidney cell types, inducing intracellular signalling cascades such as MAPK and JAK-STAT pathways. Each of those pathways involves circulating inflammatory cells, driving the development and progression of DN [75].

NF-κB is a transcription factor that has been implicated in inflammation in DN, and activates inflammatory cytokines as well as cell adhesion proteins [75]. NF-κB is stimulated by oxidative stress and plays a role in mesangial cells activation leading to renal injury [76]. In DN patients, NF-κB drives the transcription of genes encoding chemokines, effector molecules of immunity, inflammatory cytokines and cell adhesion molecules, as well as metalloproteinases and tissue factors [75]. Hasegawa and colleagues have demonstrated that both tumour necrosis factor-alpha (TNF-α) and IL-1, produced by AGEs, may have a role in development of DN [75,77]. Sassy-Prigent and co-workers have demonstrated an increase of IL-1 in the renal cells of DN rats which induced the expression of

other proinflammatory molecules such as ICAM-1, VCAM-1 and E-selectin [78]. The latter chemokines increase vascular endothelial permeability [75] and have been implicated in early structural abnormalities such as glomerular basement thickening [79]. IL-1-stimulated mesangial cell proliferation leads to increased expression of fibronectin and ECM proteins [79].

IL-18, an immunoregulatory cytokine member of the IL-1 family, is also more abundant in the serum and urine of DN patients. IL-18 concentration has been correlated with urinary albumin excretion rate and plays a key role in early renal dysfunction [80]. Miyauchi and colleagues have shown increased expression of IL-18 in renal biopsies from DN patients, and the same workers also found that this increase was due to TGF-ß–stimulated MAPK activation [81]. IL-18 is secreted by monocytes/macrophages and stimulates expression of interferon gamma (INF-γ), IL-1 and TNF-α, as well as endothelial cell apoptosis and up-regulation of ICAM-1 [82].

Increased IL-6 expression was found in the serum of DN patients with macroalbuminuria [76] and also in mesangial, interstitial and tubular cells from DN biopsy samples [83]. IL-6 expression also has a role in renal disease progression and is correlated with mesangial proliferation, tubular atrophy and increase of fibronectin [84].

TNF-α is a proinflammatory chemokine that is produced by monocytes and macrophages, but also by renal cells such as mesangial, endothelial and PTCs [85-87]. The effects of TNF-α are mediated by its two specific receptors: the ubiquitously expressed epithelial-cell receptor tumour necrosis factor receptor 1 (TNFR1), and tumour necrosis factor receptor 2 (TNFR2), a myeloid-cell receptor. Receptor activation induces the signaling pathways responsible for apoptosis and necrosis, reduction of glomerular filtration, increase of endothelial permeability, promotion of oxidative stress culminating in an increase in albumin's permeability and renal hypertrophy [75]. TNF-α-induced hemodynamic instability between vasodilatory and vasoconstrictive mediators leads to intraglomerular blood flow and GFR alterations [88]. Up-regulated TNF-α expression has been shown in glomerular and epithelial tubular cells in a diabetic rat model [89], as well as in human renal cortex and urine samples, where it is also correlated with urine albumin extraction [75]. TNF-α also induces expression of cell adhesion molecules ICAM-1 and VCAM-1. ICAM-1 is mainly expressed in endothelial, epithelial and mesangial cells in the kidney, while VCAM-1 in endothelial and

smooth muscle cells. ICAM-1 and VCAM-1 have a pivotal role in T-cell migration into the kidney, and increased ICAM-1 and VCAM-1 expression has been shown in several DN models, and is associated with DN progression [90,91].

1.3 miRNA

1.3.1 miRNA discovery

The first miRNA identified was *lin-4* in *C. elegans* by Victor Ambros and his colleagues in 1993. They discovered that this gene, important for controlling *C. elegans* larval development, did not encode a protein but two small transcripts of approximately 61 and 22 nucleotides (nt) in length. The longer one was predicted to fold into a stem loop and it was suggested to be the precursor of the shorter one which had antisense complementarity to multiple sites in the 3' UTR on target messenger RNAs (lin-14) in order to block its gene expression [92].

After this discovery, no similar noncoding RNAs were found in nematodes or other species until 2000 when Reinhart and Slack [93,94] found *let-7* in *C. elegans.* This new miRNA was considered a heterochron switch gene that encodes for a 21nt RNA complementary to the 3'UTR of different genes (*lin-14*, *lin-28, lin-41, lin-42* and *daf-12)* and that may control the temporal sequence of events in *C. elegans* development [93]. In the same year, Pasquinelli identified that the same miRNA, *let-7*, was conserved in samples from a wide range of species as vertebrate, ascidian, hemichordate, mollusc, annelid and arthropod, [95] implicating a more universal function for these genes in animals.

1.3.2 miRNA biogenesis and regulatory functions

miRNAs can be situated both in previously not annotated regions of the genome and in introns or exons of protein coding genes with the same orientation as the predicted mRNA. The first are generally classified as “intergenic” and are regulated by an independent promoter, while the second, called “intronic”, are controlled by the promoter of the host gene [96,97]. However, some reports, suggest that even these intronic miRNAs may be transcribed by their own promoter [98]. miRNAs can also be located in clusters in the genome and usually these are co-regulated and expressed sharing also the primary transcript [99]. However recently it was discovered that miRNAs located in clusters of a host gene’s intron can be transcribed independently and different pri-miRNAs can be the result of alternative splicing situated near these regions of the genome [97].

The biogenesis starts in the nucleus with the transcription by the polymerase II (pol II) or polymerase III (pol III) of a primary miRNA transcript (pri-miRNA), a single stranded RNA a few thousand of nucleotides long and characterised by a stem-loop structure [100,101]. The pri-miRNA is then cleaved into a small hairpin structure the pre-miRNA long 60-70 nt containing both the 5’ and 3’ arm of the mature miRNA. This process is performed by a protein complex know as “the microprocessor”. It is constituted of an RNase III endonuclease Drosha, a 160 kDa protein, composed by two tandem RNase III domains and a double-stranded RNA-binding domain and a cofactor, DiGeorge syndrome critical region gene 8 (DGCR8) that it is believe to assist Drosha in substrate recognition [102,103].

The process described above is typical of the intergenic miRNAs, instead, the coding-intronic miRNA situated in an intron of a protein coding gene are transcribed by pol II as part of the precursor mRNA (pre-mRNA). Subsequently, the pre-mRNA through a splicing process, still not fully clear, produces the miRNA [104].

The pre-miRNA is then actively transported from the nucleus to the cytoplasm by export receptor Exportin-5 and a Ran-GTP. The hydrolysis of Ran-GTD to Ran-GDP allows the release of RNA in the cytoplasm while the exportin-5 helps in the cytoplasm translocation process and prevents the nuclear degradation by stabilising the pre-miRNAs [105,106].

Once in the cytoplasm the pre-miRNA is cleaved by a second polymerase III, Dicer, into a small double strand RNA duplex 21-24 nt long and composed by

both the mature miRNA and its complementary strand. Dicer contains a long N-terminal ATPase/Helicase domain, a DUF283 domain, two tandem RNase III nuclease domains at the C-terminal and a PAZ domain, named after the proteins Piwi, Argonaute and Zwille, that bind to the 3' end of the small RNAs [102,107].

After the production of a 21-24nt miRNA duplex, one strand is loaded into the miRNA-induced silencing complex (RISC) composed by the transactivating response RNA-Binding Protein (TRBP) that recruits Argonaute 2 (AGO2), a major component of the RISC complex and other proteins. Usually the RISC complex selects the single strand RNA that has the lowest thermodynamic stability at its 5' terminus and it is considered the guide. Originally it was considered that the other strand not incorporated in the RISC complex and denominated as star (*) was degraded. However, it was shown that also this strand could be loaded into the Argonaute complex and target mRNAs [102,108,109].

miRNAs's function is to regulate the expression of their mRNA target mainly by two post transcriptional mechanisms: mRNA cleavage or translational repression. Both mechanisms involve the presence of Ago proteins (AGO1-4), core components of RISC complex. These proteins contain four domains:

- N-terminal
- PAZ (Piwi-Argonaute-Zwille) domain that anchors the 3' end of guide miRNA
- MID domain that has high specificity for the 5' end of the miRNA and also can discriminate between the four bases at that extremity
- PIWI element that has endonuclease activity and mediates RNA cleavage [100].

During the cleavage process, the miRNA binds the mRNA with a perfect or near perfect match via a Watson-Crick base paring mechanism in a sequence between their 2nd and 8th nucleosides of their 5' extremity, called the seed sequence. However recent advances in miRNA studies reported that alternative mechanisms of miRNA regulation also exist. These include the binding in the 5'UTR of the mRNA as well as in the open reading frame or also the possibility that miRNA may also activate gene expression by binding to the promoter of the target gene [110,111]. mRNA degradation occurs via endonucleolytic cleavage by AGO2 protein [112] or because the mRNA poly(A) tail is removed by deadenylases guided by a partial complementarity with miRNA [113].

During translational repression, miRNA and mRNA are associated with some mismatch in the target sequence causing a repression of the mRNA target. This semi-complementarity between miRNA and mRNA allows that one miRNA can recognise and therefore inhibit a large number of mRNA simultaneously and one mRNA can be identified by multiple miRNA [102] (Figure 1.2).

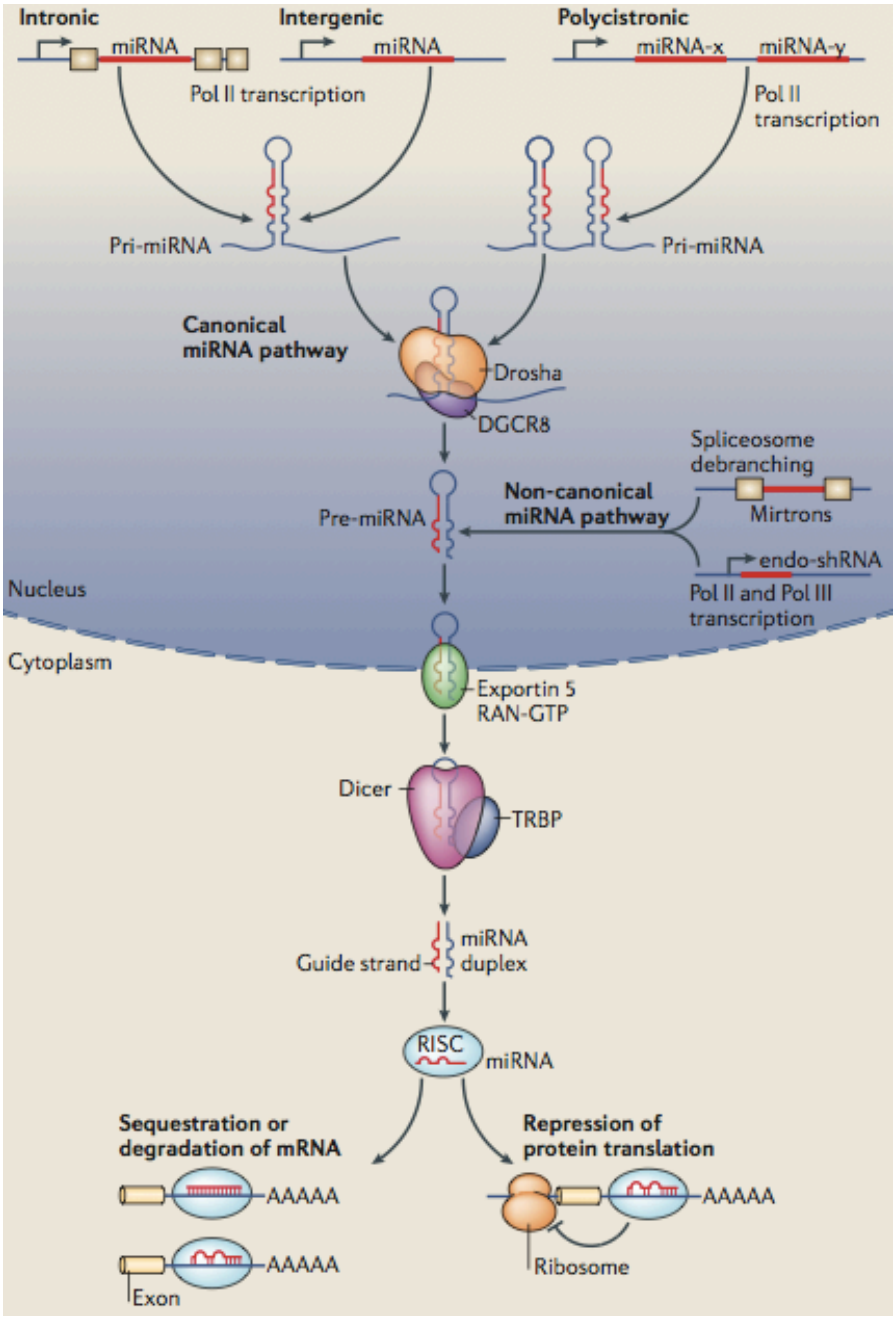

Figure 1.2. miRNA biogenesis pathway

MicroRNAs, produced by canonical biogenesis pathway, are transcribed from genomic DNA in the nucleus as long primary microRNAs (pri-miRNA) by RNA polymerase II (Pol II). The pri-miRNA transcript acquires a stem–loop structure and it is processed by Drosha in association with DGCR8 RNase III complex into a precursor miRNA (pre-microRNA). In the non-canonical miRNA pathway, miRNA are transcribed directly as endogenous short hairpin RNAs (endo-shRNAs) or derive directly by splicing from introns (mirtrons) [114]. Pre-miRNAs are then exported by Exportin-5 and RAN-GTP-dependent process to the cytoplasm. In the cytoplasm, pre-microRNAs are processed by Dicer and transactivation-response RNA-binding protein (TRBP) RNase III enzyme complex into the mature double-stranded RNA complexes. The mature microRNAs (single-stranded RNA) are incorporated into the RNA-induced silencing complex (RISC) complexes and are ready to interact with specific mRNA targets. The illustration was adapted from [115].

1.3.3 miRNA and the kidney

miRNAs are detectable in a wide range of body fluids and usually their expression is also tissue specific [116]. Several studies also revealed that kidney tissue is rich in miR-192, miR-194, miR-215, miR-216, miR-146a, miR-886 and miR-204 [25]. Some miRNAs, such as miR-192, miR-126, miR-145 and miR-30 are more expressed in the renal cortex, glomerular endothelium, mesangial and podocytes respectively [117,118]. miRNAs involvement in kidney regulation and development is now evident. Indeed knockdown of Dicer, DGCR8 or miR-30a-5p causes defects in pronephric tubules and delayes epithelial differentiation of the pronephric duct [119]. Other miRNAs, such as miR-335 and miR-34a are linked to kidney senescence, as their overexpression in mesangial cells inhibits the expression of superoxide dismutase 2 (SOD2) and thioredoxin reductase 2 (Txnrd2) and consequent increase of ROS [120].

Renal biopsies of patients with hypertensive nephrosclerosis have higher expression of miR-200a, miR-200b, miR-141, miR-429, miR-205 and miR-192. In the same work it was also shown that zinc finger E-box-binding homeobox 1 (ZEB1), the transcriptional repressor of e-cadherin, was also negatively regulated by miR-429 while E-box-binding homeobox 2 (ZEB2) was inversely regulated with miR-200a, miR-200b and miR-429 [121]. miR-200b targets also the Na/H exchange factor-1, a regulator of ion transport in apical membrane, while miR-302a controls two proteins important for the water homeostasis, aquaporin 1 and 4 [122].

Most of the miRNAs involved in renal disease are TGF-ß regulated [123]. miR-200 family for example, targets ZEB1 and ZEB2 , two regulators of the epithelial-mesenchymal transition and collagen deposition [124]. Reduction of miR-200a was observed in fibrotic kidneys in diabetic nephropathy and in cells that had undergone epithelial to mesenchymal transition (EMT) in response to TGF-β, while over-expression of this miRNA suppresses renal fibrosis [125].

miR-21 is also up-regulated in response to TGF-ß signalling and implicated in fibrosis. Knockdown of miR-21 corresponds to a reduction of mesangial expansion by affecting collagen I/IV and FN1 expression, while miR-21 inhibition corresponds to a decrease in Akt phosphorylation mediated by TGF-ß [126,127]. Increase of miR-21 expression was also detected in renal transplant patients with fibrotic kidney disease [128] and in urine of renal fibrosis in patients with IgA

nephropathy [129]. miRNAs participation in salt-induced hypertension and renal injury in Dahl salt-sensitive rats show that miR-29b regulates genes involved in extracellular matrix formation (as collagen genes, matrix metalloproteinase 2 and integrin beta 1) and mediates protection from renal medullary fibrosis in those rats [130]. Decrease of miR-29b level was found in proximal tubular cells, primary mesangial cells, and podocytes treated with TGF-ß1, while the extracellular matrix proteins were increased [130]. miR-29b was also found to be correlated with proteinuria and renal function in IgA nephropathy [129] but decreased in serum of diabetic patients [131].

It was also reported that miRNAs control the polycystic kidney disease (PKD) genes and they also mediated functional effects. For example, polycystic kidney disease 2 (PKD2) gene is targeted by miR-17 and the same miRNA can promote cell proliferation in HEK cells by targeting PKD2 [132]. miR-15 is another miRNA involved in the regulation of the expression of cell cycle regulator Cdc25A in both rat polycystic kidney disease (PKD) model and patients in cystic liver tissues [133].

1.3.3.1 miRNA and diabetic nephropathy

The first work of miRNAs involvement in diabetic nephropathy was published in 2007 and described an increase of miR-192 in the glomeruli isolated from C57BL/6 mice injected with STZ. miR-192 expression was up-regulated after treatment of mesangial cells with TGF-ß and this led to an increase of collagen 1-alpha 2 synthesis by direct inhibition of ZEB2 by miR-192 [134]. Similar results were shown also by Chung et al. in rat PTCs via a Smad3-dependent mechanism [135]. An anti-fibrotic instead of a pro-fibrotic role of miR-192 was demonstrated by Krupa in human renal PTCs after incubation with TGF-ß. This miRNA down-regulated ZEB1 and ZEB2 and suppressed E-cadherin expression. This study, originating from our group, also showed that miR-192 expression was down-regulated in renal biopsies from advanced diabetic nephropathy patients and this was correlated with both structural (tubulointerstitial fibrosis) and functional (reduced estimated glomerular filtration rate) indicators of renal damage [136]. Similar results to Krupa were shown by Wang et al. in PTCs and in kidneys from diabetic apoE (apolipoprotein E)-deficient mice and rat. Also in this study

reduction of miR-192 was linked to TGF-β1-mediated repression of E-cadherin [137].

As just described, miR-21 is a pro-fibrotic miRNA whose expression increases after TGF-ß treatment and in renal cortices of type 1 and type 2 diabetic mouse models [126,137] and it contributes to renal fibrosis by mediating MMP9/TIMP1 [138]. These results were also confirmed by Fiorentino et al. in kidneys from diabetic mice compared to control, in a mesangial cell line grown in high glucose conditions and also in kidney biopsies from diabetic patients compared to healthy controls [139]. miR-21 abundance was also found in urinary sediment of chronic kidney disease patients and correlated with the rate of renal function decline and risk of progression to dialysis-dependent renal failure [140].

An opposite role is played by miR-29, which is considered an anti-fibrotic miRNA and plays a protective role during renal injury. Mesangial cells, tubular epithelial cells and podocytes under diabetic conditions and treated with TGF-ß show a reduction in miR-29 levels and in contrast it was shown that kidney cell lines treated with an inhibitor of the miR-29 promoter, stimulate the expression of fibrotic markers [141-143]. Human miR-29 family is formed by 3 mature members: miR-29a, miR-29b and miR-29c, encoded by two gene clusters, sharing a common seed region sequence and target overlapping sets of genes but it is known that they may have different regulation and subcellular distribution [144]. Also miR-29a, as well as miR-29b, decreased in a human epithelial cell line after treatment with high glucose condition and lead to increased collagen IV expression [142]. An opposite role is played by miR-29c that was found to be highly expressed in glomeruli from db/db mice and endothelial cells and podocytes cultured under high glucose conditions [145]. The same work showed also that miR-29c inhibition decreases albuminuria and mesangial matrix accumulation in db/db mice.

miR-200 family (miR-200a, miR-200b, miR-200c, miR-429, and miR-141) are miRNAs amply studied for their role in maintaining epithelial differentiation in non-renal contexts and their expression is reduced in cells that are treated with TGF-ß and that undergo EMT [124]. Decrease of miR-200a and miR-141 was found in a mouse model of diabetic nephropathy [146]. However opposite results were shown for miR-200b and miR-200c in glomeruli from type 1 (streptozotocin) and type 2 (db/db) diabetic mice and in mouse mesangial cells treated with TGF-ß *in vitro* [147].

Other miRNAs implicated in diabetic nephropathy are miR-124 and miR-93. The first was found to be up-regulated in kidney of diabetic rats while the second one is down-regulated in db/db mice glomeruli and podocyte/endothelial cells subjected to high glucose concentrations [148].

1.3.4 miRNA as possible biomarkers

An ideal biomarker should fulfil multiple criteria. It should exhibit specificity and sensitivity, ability to differentiate pathologies from healthy states and be present at early stages of the disease. It should in addition be obtainable via a non-invasive method but still capable of being detected in a rapid and precise way [149]. Since miRNAs can fulfil most of those criteria, lately, there is a great and growing interest in the use of miRNAs as possible biomarkers in different kinds of disease [150,151]. Also it is possible to detect them outside the cells and more specifically in the serum, plasma, urine and most of the biologic fluids [116,152].

For example, miRNAs are being explored as potential biomarkers for cardiovascular disease, including different circulating miRNAs patterns for myocardial infarction, heart failure, atherosclerotic disease, T2DM and hypertension [153]. Zampetaki and colleagues, while analysing the miRNAs profile in plasma of 80 patients with T2DM, found that miR-126, miR-15a, miR-29b and miR-223 were reduced while miR-28-3p was elevated. Interestingly, reduction of miR-126, miR-15a and miR-223 were already detectable years before any diabetes manifestation. miR-126 was not the only miRNA mainly associated with this pathology, but was also down-regulated in atherosclerotic CAD [154,155]. miRNAs dysregulation have been associated also with other diseases, including different cancers [156,157], chronic lymphocytic leukaemia [158] and nervous system diseases [159].

Recently, miRNAs were detected in urine, urinary sediment and serum of patients with kidney disease [128,140,160-162]. Some of the previously mentioned miRNAs such as miR-21, miR-29 and miR-93 were detectable in urine and considered a biomarker of fibrosis in IgA nephropathy patients [128]. Other miRNAs, miR-10a and miR-30d, were identified in urine samples, but not in serum, of a mouse model of renal ischaemia-reperfusion and streptozotocin-diabetes induced renal injury. Their expression and correlation with the degree of kidney injury, make these 2 miRNAs a novel urine-based biomarker for this injury [163]. Argyropoulos et al. found that urinary miRNA profiles vary across the different stages of DN. In this study it was found that 27 miRNAs are differently regulated in different stages of diabetic renal disease. Decrease of miR-323b-5p and increase of miR-429 were associated with appearance of micro-albuminuria,

while miR-589 and miR-323b-5p showed an increasing trend in the urine of patients with nephropathy [164].

Another study conducted on 159 children affected by nephrotic syndrome, reported that miR-30a-5p, miR-151-3p, miR-150, miR-191, and miR-19b in serum and miR-30a-5p in urine were found to be increased in this syndrome and suggested the possible utility of those miRNAs as potential diagnostic and prognostic biomarkers [165].

1.3.5 miRNA packing in body fluids

What makes miRNAs so attractive as possible biomarkers is their apparent stability in tissues and biological fluid, even under extreme pH and temperatures, RNase activity, extended storage and multiple freeze–thaw cycles [166,167]. This protection from degradation may occur as result of different events that involve RNA sequence structure, packing in extracellular vesicles such as microparticles (MP) and exosomes [168], incorporation in apoptotic bodies [169] or association with RNA binding proteins [170] or lipoprotein complexes [171].

1.3.5.1 miRNA and extracellular vesicles (EVs)

Extracellular vesicles are membrane vesicles of endosomal or plasma membrane origin and their classification is based on their origin and biological function or biogenesis. Based on cellular origin and biological function it is possible to identify vesicles secreted by neutrophils or monocytes (Ectosomes), by platelets or endothelial cells in blood (Microparticles), by cardiomyocytes (Cardiosomes), purified from serum of antigen-fed mice (Tolerosomes), extracted from seminal fluid (Prostatosomes) or linked with adeno-associated virus vectors (Vexosomes) [172].

Classification based on the biogenesis identified microvesicles (MVs), exosomes and apoptotic bodies. Microvesicles (MVs) are small plasma membrane derived particles that are released from different cell types into the extracellular space by outward budding and fission of the plasma membrane. Their size varies from 100nm to 1µm and they are formed by exocytotic budding of cell membranes and characterised by a plasma membrane rich in negatively charged phospholipids while on the surface these exhibit antigens of the cells from which they originate [173]. Exosomes have an endosomal origin, derived from the endolysosomal pathway and have a size ranging from 30 to 100nm. They are retained within the multivesicular bodies as a result of endosome compartmentalization and are released when the latter fuse with the cell membrane while microvesicles are shed from the plasma membrane surface [174]. Apoptotic bodies are the biggest vesicles with a size between 1 and 5 µm and are formed in the last step of apoptosis [175]. All EV can be found in different

body fluids such as urine, blood (plasma and serum), ascites, breast milk [176] and they have a direct role in different biological process by directly activating receptor on the surface of different cells via protein binding or lipid ligands and their effectors are released into recipient cells [168,172,177]. Recently it was shown that exosomes participate in different biological functions including angiogenesis, cell proliferation, tumour cell invasion or immune response to neighbouring or distant cells [178]. It has also been shown that in diverse biological functions, protein, mRNA and miRNAs are transferred between cells in a selective way [179,180] and functionally active extracellular miRNAs can be taken up and affect gene expression in the recipient cells [168]. Interestingly, it was shown that the exosome RNA profile is different from the RNA profile of the parental cells, suggesting that this packing is selective [181]. Circulating exosomal miRNAs are studied also as possible biomarkers in different pathologies as colon cancer [182], pituitary tumors [183] or pulmonary diseases [184]. It was shown that exosome secreted into the urine may originate from different nephron segments [185,186] with an RNA integrity profile alike the mRNA of kidney. Furthermore, a study of proteomic analysis of urinary vesicles confirmed the presence of 21 proteins known to be involved with specific renal diseases [186]. Differently, miR-29c and miR-200 expression in urinary exosomes were identified by Lin-Li in patients with diabetic nephropathy, focal segmental glomerulosclerosis and IgA nephropathy [187] suggesting also the possible use of urinary exosome miR-29c as a possible non-invasive marker for renal fibrosis since it correlated with both renal function and the degree of histological fibrosis [160]. An increment of miR-145 in exosomes was detected in patients with microalbuminuria, in an animal model of early diabetic nephropathy and mesangial cell-derived exosomes treated with high concentrations of glucose [188].

1.3.5.2 miRNA and RNA-binding proteins

Recent studies have highlighted that miRNAs stabilization might be also due to association with RNA-binding protein and not only with microparticles as firstly demonstrated by Arroyo and Turchinovich [170,189]. Arroyo, using differential centrifugation and size exclusion chromatography showed that the 90% of the miRNAs were not incorporated in microvesicles but bound to a ribonucleoside complex, specifically with Argonaute2 (AGO2). This association was also responsible for miRNAs stability in plasma [170]. Similar results were also showed in Turchinovich paper where most of the plasma and cell culture media miRNAs have a non-vesicular origin and were associated with AGO proteins [189]. Following studies showed that circulating miRNA in human blood plasma can be immunoprecipitated with AGO1 and AGO2 antibody, however AGO-specific miRNA profiles in blood cells differed from the ones in plasma suggesting that most of the circulating miRNAs may originate from non-blood cells [190]. In HEK-293 cells, it has been shown that GW182 also plays a key role in protecting AGO-bound miRNAs from being degraded [191]. A recent article demonstrated also that human platelets, activated by thrombin, release miR-233 associated with AGO2 to endothelial cells via microparticles, suggesting an even more complex mechanism of intercellular exchanges and stability of miRNAs [192]. Moreover, another study established that for 3 weeks miRNAs associated with Argonaute complex are stable and ready to be recruited into RISC complex after external stimuli activation [193]. miRNAs stability and exportation can also be due to association with other RNA-binding proteins as for example nucleophosmin. Wang and colleagues showed that conditioned serum-free tissue culture medium, from a variety of cell types, contained 197 proteins, 12 of which were known as RNA-binding proteins. One of these, nucleophosmin, mainly located in the nucleolus, was shown by immunoprecipitation to bind to miRNAs and in addition, incubation of this protein with the synthetic miR-122 proved that this protein was involved in miRNAs protection from RNase A digestion and not only in the exporting process [194].

1.4 Aims

The aim of this thesis was to investigate the potential of miRNAs as novel, non-invasive biomarkers for the diagnosis and prognosis of DN.

The aim of my studies was to contribute to development of biomarkers for CKD patients. These are needed since those available at present are not sufficiently sensitive and specific enough to predict disease outcome. At the beginning of this PhD project, miRNAs were known to play a key role in regulation of gene expression in a number of diseases. However, comparatively little was known about the abundance of urinary miRNAs. Indeed, an established, robust method for urinary miRNA extraction and detection was not available.

The specific objectives were:

- To develop a robust and non-toxic technique for extraction and detection of urinary miRNAs
- To establish the stability of endogenous urinary miRNAs in samples from unaffected individuals and DN patients
- To investigate differences in urinary miRNA expression profiles between diabetic nephropathy patients and healthy individuals, and thereby identify potential disease biomarkers
- To locate the nephron tissue compartments, and more precisely the kidney cell types, expressing the putative disease-associated miRNAs identified by the above aims
- To analyse expression of selected miRNAs in cells and conditioned media from *in vitro* diabetic nephropathy models

CHAPTER 2 – Materials and Methods

2.1 Samples

2.1.1 Urine samples collection and preparation

Second morning urine samples were collected from 20 DN patients admitted to the University Hospital of Wales, Cardiff, between January and May 2012, and 20 urine samples from unaffected volunteer control subjects from the Institute of Nephrology, School of Medicine, Heath Hospital, Cardiff. All donors gave informed written consent. pH, glucose, ketones, leucocytes, nitrite, protein, blood and haemoglobin were detected through test strips (Combure 7 Test, Roche) for whole urine samples. Urine samples were centrifuged at 2,000 *g* for 10 min at 4°C to remove living cells.

The supernatants were divided as followed:

- 3 aliquots of 300 µl each for RNA extraction
- 3 aliquots of 800 µl for protein:creatinine ratio
- residual urine was stored in a fresh sterile universal container

and were stored at -80° until experiments.

Information on renal function (defined as eGFR), protein:creatinine ratio, CKD stage, blood glucose level, age, sex and date of collection were obtained for all the patient samples.

2.1.2 Urine sample and preparation (PCOS)

Urine samples were collected from 17 patients with PCOS (Polycystic ovary syndrome) admitted to the University Hospital of Wales, Cardiff between February and September 2012, and 15 control subjects. Urine collection from these patients and controls was part of collaboration with Dr. Aled Rees at the Centre for Endocrine and Diabetes Sciences, Cardiff University School of Medicine. All donors gave informed written consent. pH, glucose, ketones, leucocytes, nitrite, protein, blood and haemoglobin were detected through test strips (Combure 7 Test, Roche) for whole urine samples. Urine samples were processed as described in 2.1.1.

2.1.3 Tissue sample collection and preparation by laser capure microdissection (LCM)

Five formalin-fixed paraffin embedded (FFPE) archived renal biopsies from unaffected people were used to isolate glomeruli, proximal tubular and distal tubular profiles using the Arcturus Pixcell IIe infrared laser enabled LCM system (Applied Biosystems). From each biopsy, two 6-µm sections were obtained. One of these was stained with an antibody anti-CD10, while the other section was used to isolate glomerular, proximal tubular and distal tubular nephron compartments. CD10 staining was used to identify these structures as the CD10 antigen is expressed at the surface of glomerular and proximal tubular cells, but not distal tubular cells. This staining was carried out by Mr. Dilwyn Havard at the Histopathology Department, University Hospital of Wales, Cardiff. The tissues were cut, placed in the middle third of an uncharged, uncoated glass slide (VFM White coat slides CellPath Ltd) and stained according to the method by Espina et al. [195].

Using infrared laser, the target tissue was bonded to a polymer membrane located on a cap (Arcturus ® Capsure ® Macro LCM caps – Applied Biosystems) placed onto the slide which when lifted removes the highlighted tissue. These experiments were carried out with guidance from Dr. Christopher Carrington at the Institute of Nephrology, Cardiff University School of Medicine.

2.1.4 Cell culture

2.1.4.1 Human conditionally immortalised glomerular endothelial cells (CiGEnC)

Two T75 flasks of human conditionally immortalised glomerular endothelial cells (CiGEnC) were kindly donated by Dr. Simon Satchell from the Academic Renal Unit at the University of Bristol. Dr Satchell's research group have successfully conditionally transformed normal human glomerular endothelial cells using a technique restoring functional telomerase activity and introducing the simian virus 40 large tumour antigen (SV40LT). A temperature-sensitive (ts) SV40LT construct was used to allow conditional immortalization (ci), that is, enhanced proliferation at a permissive temperature, while the SV40LT element can be "switched off" by transfer to a non-permissive temperature. At this temperature, cells take on a mature phenotype not seen in cells constitutively expressing SV40LT [196].

Cells were cultured in endothelial growth medium 2 microvascular (EGM-2-MV, CC-3202, Lonza) containing foetal calf serum (5%) and growth factor as supplied, excepting VEGF unless otherwise stated.

Cell were grown to confluence at 33°C, trypsinized, and reseeded in a fresh flask at a dilution 1:3. Cell were grown to confluence before transferring to incubation at the non-permissive temperature of 37°C [197].

2.1.4.2 CiGEnC stimulation

CiGEnC at 33°C were seeded in 12-well plates; after 5 d cells were transferred to 37°C and, after further 5 d, were growth arrested for 24 h and then treated with TNF-α (10 ng/mL), VEGF (20 ng/mL), TGF-ß1 (1 ng/mL) or IL-6 (1 ng/mL) at either 5 mM or 25 mM glucose concentration for 24 h. The cells obtained from each well were used for RNA extraction as described on page 42.

2.1.4.3 Human proximal tubular epithelial cell line HK-2 and podocyte cell line

HK-2 cells

The human proximal tubular epithelial cell (PTC) line HK-2 (human kidney-2) was established by transduction of primary proximal tubule cells from adult human kidney with human papilloma virus (HPV 16) E6/E7 genes [198]. Cells immortalized this way retain many features of primary cells, are not tumorigenic in experimental animals, and do not grow in soft agar and exhibit contact inhibition [198].

HK-2 cells show close similarities to the phenotype and function of primary PTCs [199,200]. For instance, they are positive for alkaline phosphatase, gamma-glutamyl transpeptidase, leucine aminopeptidase, acid phosphatase, cytokeratin, integrin alpha-3 beta-1 and fibronectin; but negative for factor VIII-related antigen, 6.19 antigen and CALLA endopeptidase [199,200]. They also exhibit PTC characteristics such as sodium dependence, pholorizin-sensitive sugar transport and increased production of cAMP in response to parathyroid, but not to antidiuretic hormone. Moreover, many aspects of PTC biology, including those directly relevant to this project, have been studied in this laboratory and shown close similarity between HK-2 and primary PTCs [199,200].

HK-2s were maintained in a 1:1 mixture of Dulbecco's Modified Eagle's Medium (GIBCO/Invitrogen, Paisley, UK) and Ham's F12 (Sigma, Poole, UK), supplemented with 10% (v/v) fetal calf serum (FCS) (Biosera, Ringmer, UK), 20 mM HEPES, 2mM L-glutamine, 5 µg/ml transferrin, 5ng/ml sodium selenite and 0.4µg/ml hydrocortisone (Sigma). Fresh growth medium was added to cells every two d until confluent. Cells were cultured at 37°C in a humidified incubator (Cll House 170, Heto Holten, Derby, UK) in an atmosphere of 5% CO_2 and then they were used in experiments, or subcultured at ratio 1:3.

For subculture, 10X solution of trypsin/EDTA (Sigma) diluted with PBS (1:10) was added to the cells. After 10 minutes, equal volume of culture medium containing 10% (v/v) FCS was added, cell suspension transferred to a tube, and

centrifuged for 5 minutes at 1200 g at room temperature. The cells were resuspended in culture medium and seeded into new culture flask or plates.

Podocytes

A human podocyte cell line (ATC) exhibiting temperature dependent expression of SV40-T gene has previously been developed by Professor Moin Saleem at the Academic Renal Unit, University of Bristol. In brief, at the permissive temperature (33°C) these cells proliferate. However, on transfer to the non-permissive temperature of 37°C, they enter growth arrest and express markers of *in vivo* differentiated podocytes such as nephrin, podocin, CD2AP and synaptopodin, as well as slit diaphragm markers [201].

Podocytes were propagated and seeded at 33°C in RPMI – 1640 medium (Sigma) with 10% FCS (Biosera, Ringmer, UK), 100X Insulin Transferrin Selenium G supplement (Invitrogen) diluted 1 in 100, 100X L-Glutamine 200mM (Invitrogen) diluted 1 in 100 and Penicillin/ Streptomycin (Invitrogen) diluted 1 in 100 in medium.

When cells were approximately 60% confluent they were incubated at 37°C for 14 d during which time they underwent growth arrest and differentiated into “mature” podocytes. Stimulation experiments were performed on these differentiated or so-called “mature” podocytes.

2.2 RNA analysis

2.2.1 RNA extraction

2.2.1.1 RNA extraction urine samples

At the start of this project, there was no clearly validated protocol for urinary miRNA extraction. Initial experiments using three isolation protocols on control urine samples were compared to identify the best one to take forward. Two commercially available kits for RNA and/or miRNA extraction from urine samples were used: the Norgen kit (Cat. No 29000) was used according to the manufacturer's recommendations, while the Qiagen miRNA-easy mini kit (Cat. No 217004) was used with minor modifications recommended by Andreasen et al., using 1 μg of Carrier RNA (MS2 RNA, Roche Cat. No 10165948001) per 750 μl of QIAzol reagent [202]. The third protocol used TRI-Reagent RNA Isolation Reagent (Life Technologies, Cat. No AM9738) and chloroform extraction according to manufacturer's guidelines.

Total RNA/miRNA extracted and mean A_{260}/A_{280} purity ratios from each extraction protocol varied. TRI-Reagent provided the greatest RNA recovery, but yields were highly variable. It was not possible to accurately estimate RNA yield and purity using the above Qiagen protocol since carrier RNA was used. Following the results obtained from this first study (see 3.2.1.1) the Qiagen protocol was used for further analyses.

For RNA isolation using the chosen Qiagen miRNeasy kit (Qiagen), urine samples from DN Patients and PCOS patients and controls were processed according to the manufacturer's recommendation with the following modifications. After mixture and incubation at room temperature for 5 min of 750 µl of QIAzol plus Carrier RNA (MS2 RNA, Roche) with 250 µl of urine sample, 0.5 pM of spike in *Caenorhabditis elegans* (cel-miR-39) (Ambion, Cat. No 4464066, Part No. MC10956) was added to each sample. Subsequently, 200 µl of chloroform was added per sample, and samples were incubated at room temperature for 2 min and then spun for 15 min at 12,000*g* at 4°C. At that point, the manufacturer's protocol was followed, with the entire aqueous phase from each sample loaded onto a single affinity column. RNA extracts were then stored at -80°C until analysed.

2.2.1.2 RNA extraction tissue sample from LCM samples

The polymer membrane on the LCM caps was removed and miRNAs were extracted using RecoverALL™ Total Nucleic Acid Kit according to the manufacturer's protocol with the following two main modifications. Firstly, deparaffinisation step was not carried out, as this was previously performed before LCM. Secondly, 1 µg of carrier (MS2 RNA Roche) was added during the nucleic acid isolation stage.

2.2.1.3 RNA extraction from CiGEnC cell line

Total RNA was prepared with TRI-Reagent from CiGEnC, human lung fibroblasts (a kind gift from Dr. Adam Midgley at the Institute of Nephrology, Cardiff University School of Medicine), human PTC line HK-2 and podocytes. TRI Reagent combines phenol and guanidine thiocyanate in a monophasic solution to rapidly inhibit RNase activity. Cells were lysed in 1 ml of TRI-Reagent solution and incubated at room temperature for 5 min to allow for complete dissociation of nucleoprotein complexes. The homogenate was then separated into aqueous and organic phases by addition of 200 µl of chloroform and centrifuged at 12,000x*g* for 15 min at 4ºC. Then, the RNA was precipitated from the aqueous phase by adding 500 µl of isopropanol and repeating the centrifugation step after 10 min of incubation at room temperature. The samples were then washed 3 times with 75% ethanol and centrifuged for 5 min at 12,000*g*. RNA was then eluted in 15 µl of nuclease-free water. Purity and concentration of RNA samples were assessed using the NanoDrop ND-1000 Spectrophotometer (Thermo Scientific). An equal volume (1 µl) of sample was measured at 260 nm and 280 nm.

2.2.2 miRNA detection

miRNAs were analysed in whole samples by two-step quantitative reverse transcription – polymerase chain reaction (RT-qPCR).

2.2.2.1 Reverse transcription

To evaluate recovery of RNA/miRNA using different extraction procedures, miRNAs were assayed using two different methods according to the respective manufacturer's instructions:

- High Capacity cDNA Reverse Transcription Kit (Applied Biosystems) using a specific primer for each miRNA
- miRCURY LNA™ Universal RT microRNA PCR system (Exiqon) following the manufacture's protocol

High Capacity cDNA Reverse Transcription Kit

Reverse transcription (RT) was performed using the High-Capacity cDNA Reverse Transcription Kit (Applied Biosystems, Cat. No 4368814). The RT master mix for one reaction was composed of: 4.25 µl of water, 1.5 µl 10 x Reverse Transcription Buffer, 0.15 µl 100mM dNTP, 0.1 µl 40 U/µl RNase Inhibitor (New England BioLabs® Inc, Cat. No M0307S,), 1 µl 50 U/µl MultiScribe Reverse Transcriptase and 3 µl 5x RT-primer specific for each miRNA. Then, 10 µl of the RT master mix was added to 4 µl of water plus 1 µl of RNA for the urine samples or 5 µl containing 10 ng total RNA for the cell lines, and incubated on ice for at least 5 min. The RT non-template control (RT-NTC) negative control reaction contained an equal volume of water instead of RNA. The following thermal cycler profile was used: 30 min at 16°C, 30 min at 42°C, 5 min at 85°C, followed by cooling to 4°C. The cDNA was diluted with water 1:3, and 4 µl were used in qPCR, performed as described in the section 2.2.2.2.

2.2.2.2 Quantitative polymerase chain reaction

For each gene analysed, the master mix for each reaction was prepared by combining 1 µl of gene-specific set of PCR-primers and TaqMan probe for each

miRNA (designed and supplied by Applied Biosystems), 5 µl of water and 2 x Universal PCR Master Mix with No AmpErase UNG composed of an optimized solution of thermostable DNA polymerase, deoxynucleotides, and the passive reference dye ROX (Applied Biosystems, Cat. No 4440047). A total of 16 µl of gene-specific master mix was distributed to appropriate wells on an Optical 96-Well Fast Plate (Applied Biosystems) and subsequently, 4 µl of pre diluted cDNA or water for the NTCs was added. The plate was sealed with a MicroAmp Optical Adhesive Film (Applied Biosystems) and qPCR was performed on a ViiA7 Real-Time PCR System (Life Technologies), using the manufacturer's recommended cycling parameters: 10 min at 95°C, followed by 40 cycles of 15 s at 95°C and 1 min at 60°C. The list of TaqMan assays used in this study is given in Table 2.1, below.

miRNA assay	Catalogue Number
cel-miR-39	Part. Number 4427975 Assay ID 000200
hsa-miR-16	Part. Number 4427975 Assay ID 000391
hsa-miR-192	Part. Number 4427975 Assay ID 000491
hsa-miR-191	Part. Number 4427975 Assay ID 002299
hsa-miR-126	Part. Number 4427975 Assay ID 002228
hsa-miR-29b	Part. Number 4427975 Assay ID 000413
hsa-miR-200b	Part. Number 4427975 Assay ID 002251
hsa-miR-212	Part. Number 4427975 Assay ID 000515
hsa-miR-155	Part. Number 4427975 Assay ID 002623

Table 2.1. TaqMan assays used in this study

2.2.2.3 RT-QPCR data analysis

For qPCR data analysis, Viia 7 software and GraphPad Software version 5.0a were used. Relative expression was calculated using the 2-ΔΔCT method [203].

2.2.2.4 miRNA profiling in urine samples by TaqMan®Array Human MicroRNA Cards

Urine procession and RNA extraction

Urine samples were processed as describe in section 2.1.1 and RNA was isolated using the miReasy kit (Qiagen) as described in 2.1.1.1.

Reverse transcription (RT) and pre-amplification

miRNAs were reverse transcribed using the Megaplex Primer Pools (Human Pools A v2.1 and B v3.0) with a predefined pool of up to 381 reverse transcription (RT) primers for each Megaplex Primer Pool. To assess the level of specific miRNAs in individual urine samples, a fixed volume of 3 µl of RNA solution was used as input in each RT reaction. Each RT reaction was performed according to the manufacturer's recommendations: 0.8 µl of pooled primers were combined with 0.2 µl of 100 mmol/L dNTPs including dTTP, 0.8 µl of 10 x RT Buffer, 0.9 µl of $MgCl_2$ (25mmol/L), 1.5 µl of Multiscribe reverse transcriptase (50 U/µl) and 0.1 µl of RNAsin (20 U/µl) to a final volume of 7.5 µl.

Each RT reaction was set up in an Applied Biosystems 7900HT thermo cycler as follows: 16°C for 2 min, 42°C for 1 min and 50°C for 1 s for 40 cycles, followed by incubation at 85°C for 5 min.

RT reaction products were then amplified using Megaplex PreAmp Primers (Primers A v2.1 and B v3.0). A 2.5 µl aliquot of the RT product was combined with 12.5 µl of Pre-amplification Mastermix (2 x) and 2.5 µl of Megaplex PreAmp Primers (10 x) to a final volume of 25 µl. The pre-amplification reaction was performed by heating the samples at 95°C for 10 min, 55°C for 2 min and 72°C for 2 min, followed by 12 cycles of 95°C for 15 s and 60°C for 4 min. Finally, samples were heated at 99.9°C for 10 min to ensure enzyme inactivation.

Pre-amplification reaction products were diluted to a final volume of 100 µl and the diluted pre-amplification products from controls and DN were pooled as follows:

Pool 1 control = 5 female urine samples; average age= 44.8
Pool 2 control = 5 female urine samples; average age= 57.6

Pool 3 control = 5 male urine samples; average age= 35.2

Pool 4 control = 5 male urine samples; average age= 53.2

Pool 1 Patient = 5 CKD urine sample; stage 3 and eGFR between 43.3 and 36 mL/min per 1.73m^2

Pool 2 Patient = 5 CKD urine sample; stage 3 and eGFR between 35 and 31 mL/min per 1.73m^2

Pool 3 Patient = 5 CKD urine sample; stage 4/5 and eGFR between 27.3 and 23 mL/min per 1.73m^2

Pool 4 Patient = 5CKD urine sample; stage 4/5 and eGFR between 22 and 12.9 mL/min per 1.73m^2

TaqMan miRNA array

TaqMan®Array Human MicroRNA Cards A and B were used to quantify 754 human miRNAs. In each array, three endogenous controls and a negative control were included. Card A focused on more highly characterized miRNAs, while Card B contained many of the more recently discovered miRNAs along with miR* (miR star) sequences. Initial microarray screening was carried out using pools of diluted pre-amplification product from 20 individuals with DN, and from 20 controls. The expression profiles of miRNAs in urine samples were determined using the Human TaqMan miRNA Arrays A v2.1 and B v3.0 (Applied Biosystems). PCR reactions were performed using 450 µl of the TaqMan Universal PCR Master Mix No AmpErase UNG (2X) and 9 µl of the diluted pre-amplification product to a final volume of 900 µl. Aliquots of 100µl of this PCR mix were dispensed to each port of the TaqMan microRNA Card. The fluidic card was then centrifuged and mechanically sealed. qPCR was carried out on an Applied Biosystems 7900HT thermo cycler using the manufacturer's recommended program. The list of these products is in Table 2.2, below.

Products	Catalogue Number
TaqMan® Array Human MicroRNA A+B Cards Set v3.0	4444913
Megaplex™ RT Primers, Human Pool Setv3.0	4444745
Megaplex™ PreAmp Primers, Human Pool A v2.1	4399233
Megaplex™ PreAmp Primers, Human Pool B v3.0	4444303
TaqMan® PreAmp Master Mix Part Number	4391128

Table 2.2. TaqMan miRNA array products

2.2.3 mRNA detection

2.2.3.1 Reverse transcription

The cDNA was generated using High Capacity cDNA Reverse Transcription Kit (Cat. No 4368814, Life Technologies) from 1 µg of RNA of each sample. Briefly, 1 µg of total RNA in 10 µl of water was added to 10 µl of the RT mix containing 2 µl of 10 x RT buffer, 0.8 µl of 25 x dNTP Mix (100 mM), 2 µl of 10 x RT random primers, 1 µl of MultiScribe™ Reverse Transcriptase, 1 µl of RNase inhibitor and 3.2 µl of nuclease-free water. The thermal profile used was: 10 min at 25°C, 2 h at 37°C and 5 s at 85°C, followed by cooling at 4°C. RT reactions were diluted by adding 60 µl of water, and then used for the qPCR or stored at -20°C as required.

2.2.3.2 Quantitative polymerase chain reaction.

qPCR was performed on a ViiA7 Real-Time PCR System (Life Technologies). GAPDH, VEGFR-2, vWF, PECAM-1, PAI-1 reaction products were quantified by Power SYBR® Green PCR Master Mix (Cat. No 4367659, Life Technologies) with 300 nM gene-specific primers. The amplification of a single PCR product was confirmed by melting curve analysis. The nucleotide sequences of the used primer pairs can be found below:

Gene	Primer Reverse	Primer Forward
GAPDH	TGACGAACATGGGGGCATCA	AGCCGCATCTTCTTTTGCGT
VEGFR2	CCAGTGTCATTTCCGATCACTTT	GGCCCAATAATCAGAGTGGCA
vWF	GCCCTGGTTGCCATTGTAATTC	AGCCTTGTGAAACTGAAGCAT
PECAM1	TCGGAAGGATAAAACGCGGTC	CCAAGGTGGGATCGTGAGG
PAI-1	CGGTCATTCCCAGGTTCTCT	TCTCTGCCCTCACCAACATTC

The primers were designed using Primer-BLAST, against mRNA sequences taken from the NCBI database, to amplify all known splice-variants. To avoid amplification from DNA genomic, primers were designed to span intron-exon junctions. PCR product length was ideally around 100-150 bp.

2.3 Analysis of urinary miRNA stability

2.3.1 Addition of urine to the RT step

Exogenous *C. elegans* cel-miR-39 (0.05 pM) was spiked into 4 control urine samples during the RNA extraction step (see 2.2.1.1). Subsequently, different percentages of urine (0, 0.1, 0.5, 1 and 5%) were added to the RT reactions. The endogenous miR-16 and the exogenous cel-miR-39 were then detected by RT-QPCR as previously described (see 2.2.2.1 and 2.2.2.2).

2.3.2 Room Temperature analysis urine analysis over 24 h

Urine samples from 6 control subjects and 4 proteinuric DN patients were collected as previously described (see 2.1.1). Subsequently, *C. elegans* cel-miR-39 was spiked into each sample at time zero and the urine samples were stored at room temperature over 24 h. Aliquots of 250 µl from each sample were isolated after 0, 1, 2, 4, 8 and 24 hours RNA extracted, the endogenous miR-16 and the exogenous cel-miR-39 were detected by RT-qPCR as described previously (see 2.2.2.1 and 2.2.2.2).

2.3.3 RNase treatment of urine

Two 2.5 ml aliquots were taken from each of 5 urine samples from control subjects and 5 from proteinuric DN patients. Negative control reactions were composed of urine aliquots, 0.5 pM of cel-miR-39 and 250 µl of RNase storage buffer were added, the latter replaced by 0.1 mg/ml of RNase A (RPA Grade; Life Technologies (Ambion), AM2272) in the treated samples. Following incubation of 1 control sample in duplicate at 37°C, aliquots of 250 µl were removed after 1, 5, 10, 15, 30, 60 min, 750 µl of QIAzol plus 1 µg of carrier RNA added, and stored at -80°C. RNA was isolated and miR-16 detected as described above (see 2.2.2.1 and 2.2.2.2). Following analysis, the experiment was then repeated at the 30 min time-point using 10 samples.

2.3.4 Proteinase K treatment of urine

Urine samples from 2 control subjects and 5 proteinuric DN patients were incubated at 55°C +/- 50 µg/ml of proteinase K (P-2308; Sigma-Aldrich, Gillingham, Dorset, UK). Aliquots of 250 µl were removed after 0, 10, 20, 30, 40, 50 and 60 min, 750 µl of QIAzol plus 1 µg of carrier RNA added, and samples were stored at -80ºC. RNA was isolated and miR-16 detected as described above (see 2.2.2.1 and 2.2.2.2). Following analysis, the experiment was then repeated at the 30 min time-point with urine samples from 5 control subjects and 5 proteinuric DN patients.

2.4 Exosome isolation and characterization

2.4.1 Purification of extracellular vesicles from urine samples

Typically, 300 ml of pooled urine samples from control subjects was subjected to centrifugation at 400*g* for 10 min to pellet cells, followed by a further 2,000*g* for 10 min to remove cellular debris. The resultant supernatant was then centrifuged at 200,000*g* for 1 h in order to collect all extracellular vesicles, after which pellets were re-suspended in 100–150 µl of PBS and their total protein quantified by micro-BCA protein assay (Pierce/Thermo Scientific).

2.4.2 Determination of extracellular vesicle density

Extracellular vesicle pellets (see above) were overlaid onto a continuous sucrose gradient of 0.2-2.5 M sucrose. Samples were centrifuged at 4°C overnight at 210,000*g* using an MLS-50 rotor in an Optima-Max ultra-centrifuge (Beckman Coulter). The refractive index of collected fractions was measured at 20°C in an automatic refractometer (J57WR-SV, Rudolph Scientific) and from this, the density was calculated as previously described. Fractions were washed in PBS by ultracentrifugation at 150,000*g* in a TLA-110, and pellets resuspended in a small volume before being aliquoted into 3 different microtubes: MES buffer was added to the first prior to coupling to microbeads for flow cytometric analysis, SDS loading buffer was added to the second prior to Western blot analysis and the last was used for miR extraction.

2.4.3 Flow cytometric analyses of exosome-coated beads

For analysis of sucrose gradient fractions, 10 µl (of a total of 40 µl) of each fraction was coupled to 0.5 µl of stock beads (surfactant-free, aldehyde sulfate 3.9 µm beads, Interfacial Dynamics) that had been washed twice in MES buffer (0.025 M MES, 0.154 M NaCl, pH 5). Exosome beads were incubated in a final volume of 100 µl of MES buffer at room temperature for 1 h on a shaking platform, followed by rolling overnight at 4°C. Beads were blocked by incubating them with MES buffer + 1% BSA for 2h at room temperature. Blocking buffer was

washed away and beads were resuspended in MES buffer + 0.1% BSA. Primary monoclonal antibodies against CD9 (R&D Systems, Abingdon, Oxfordshire, UK) and CD81 (AbD Serotec, Kidlington, Oxfordshie, UK) were used (at 2–10 μg/ml) for 1h at RT. After one wash, goat anti-mouse Alexa Fluor 488-conjugated antibody (Invitrogen, Life Technology) diluted 1:200 in MES buffer + 0.1% BSA was added for 1h. After washing, beads were analysed by flow cytometry using a FACS-Canto instrument configured with a high throughput sampling module running FACSDiva Version 6.1.2 software (BD Biosciences, Oxford, UK), and median fluorescence values were plotted.

2.4.4 Western blotting

One half of each gradient fraction was analysed by Western blotting. Proteins were solubilised by the addition of 50 mM Tris-HCl, 2% SDS, 20 mM DTT and 0.002% (w/v) bromophenol blue. Samples were electrophoresed through 4 –12% Bis-Tris gels (Invitrogen, Life Technology) and transferred to PVDF membranes. Blots were blocked overnight (3% non-fat milk, in PBS + 0.05% Tween 20) then probed with antibodies against classical exosome markers TSG101 and Alix (Santa Cruz Biotechnology via Insight Biotechnology, Wembley, Middlesex, UK). After 3 washes (PBS + 0.05% Tween 20) blots were stained with goat anti-mouse IgG-HRP conjugated antibody (1:15,000 in PBS + 0.05% Tween 20, Santa Cruz Biotechnology). Bands were visualized using the ECL+ system and photographic film (GE Healthcare, Chalfont St Giles, Buckinghamshire, UK).

2.4.5 Nanoparticle tracking analysis (NanoSight^{TM})

Vesicles present in urinary samples were analysed by nanoparticle tracking using the NanoSight LM10 system (NanoSight Ltd, Amesbury, Wiltshire, UK) configured with a 405 nm laser and a high sensitivity digital camera system (OrcaFlash2.8, Hamamatsu C11440, NanoSight Ltd). Videos of 60s were collected and analysed using NTA-software (version 2.2) with the minimal expected particle size set to 30 nm, and minimum track length and blur set to automatic. Each sample was diluted in nanoparticle-free water (Fresenius Kabi, Runcorn, Cheshire, UK) to a concentration of between 2 x 10^8 and 9 x 10^8

particles/ml. This was carried out in triplicate for pre-ultracentrifuged urine, and for 4 replicates following 200,000*g* ultracentrifugation.

2.5 Protein analysis

2.5.1 Argonaute 2 (AGO2) immunoprecipitation

For each sample, 200 µl of Magna Bind goat anti-mouse IgG Magnetic Beads (Thermo Scientific, Cat. No 21354) were washed 3 times with PBS solution (300 µl), and incubated with 10 µg of mouse monoclonal anti-Ago2 (ab57113; Abcam) or mouse IgG (Santa Cruz Biotechnology, Cat. No sc-2025) antibodies for 2 h at 4°C. The preincubated beads and antibody were then added to 400 µl of urine (prepared as previously described) and incubated overnight at 4°C. Beads were washed 3 times with 1% Nonidet P-40 buffer (1% Nonidet P-40, 50mM Tris-HCL, pH 7,4, 150mM NaCl, 2mM EDTA), resuspended in 200 µl of PBS and then split in half. One half of each sample was eluted in Loading Buffer, followed by SDS/PAGE and immunoblotting. The other half of each sample was eluted in 750 µl of QIAzol plus Carrier RNA (MS2 RNA, Roche) and processed for RNA isolation miR-16 detection. The cell line HEK-293 was used as positive control for AGO2 in the immunoblotting. Rabbit polyclonal anti-AGO2 antibody (ab32381; Abcam) was used to detect AGO2 in the immunoblotting

2.5.2 Albumin immunoprecipitation

For each sample 50 µl of Dynabeads Protein G (Invitrogen Cat. no. 10003D) were incubated with 10 µg of Anti-Human Serum Albumin antibody (ab10241; Abcam) or mouse IgG (Santa Cruz Biotechnology) antibodies diluted in 200 µl 0.1% PBS-Tween-20 for 15 min at room temperature. 400 µl of Control and Patient urine samples were added to the preincubated beads and antibody and incubated for 4 h at 4°C. The respective manufacturer's instructions were followed. Dynabeads-Ab-Ag complex were resuspend in 100 µl of washing buffer, transferred to a clean tube and then split in half. One half of each sample was eluted in Loading Buffer, followed by SDS/PAGE and immunoblotting. The other half of each sample was eluted in 750 µl of QIAzol plus Carrier RNA (MS2 RNA, Roche) and processed for RNA isolation and hsa-miR-16 detection. Human serum was used as positive control for Albumin in the immunoblotting. Albumin Antibody (H-126) (sc-50535 Santa Cruz Biotechnology) was used to detect Albumin in the immunoblotting.

2.5.3 Western blotting

Immunoprecipitated AGO2 and albumin were detected by Western blotting.

SDS-PAGE

Sodium dodecyl sulfate-polyacrylamide gel electrophoresis (SDS-PAGE) was performed by the method of Laemmli [204]

Composition of polyacrylamide gel – Resolving gel 7.5%

Water	9.9 ml
Resolving Buffer: 1.5M Tris-HCl pH 8.8	4.5 ml
10% (w/v) SDS	180 µl
40% Acrylamide/Bisacrylamide	3.37 ml
10% APS (Ammonium Persulfate) (0.05g/0.5ml of water)	90 µl
TEMED	12 µl

Composition of polyacrylamide gel – Stacking gel

Water	6.45 ml
Stacking buffer 0.5M	2.5 ml
10% (w/v) SDS	100 µl
40% Acrylamide/Bisacrylamide	980 µl
10% APS (Ammonium persulfate) (0.05g/0.5ml of water)	75 µl
TEMED	10 µl

Composition of loading buffer – reducing buffer 1 x

Water	4 ml
Stacking buffer 0.5M	1 ml
Glycerol	0.8 ml
10% (w/v) SDS	1.6 ml
0.05% Bromophenol blue	0.2 ml
ß-mercaptoethanol	0.4 ml

Composition of running buffer 10 x

0.25 M Tris-HCl	30 g/l
1.92 M Glycine	144 g/l
1% SDS	10 g/l
pH 8.3	

Composition of transfer buffer 10 x

0.25 M Tris-HCl	30 g/l
1.92 M Glycine	144 g/l
pH 8.3	

Composition of transfer buffer 1 x

Transfer buffer 10 x	100 ml/l
Methanol	200 ml/l

Immunoprecipitates were resuspended in 30 µl of 1 x reducing buffer, heated at 95°C for five minutes and cooled on ice. The tubes were placed on the magnet and the supernatant/samples were loaded onto a gel. Additionally, prestained protein ladder, broad range 10-230 kDa (Cat. No P7711s, New England bio labs) was loaded in one of the wells. The electrophoresis was carried out in a BioRad Mini Protein II apparatus, in (1X) Running Buffer, firstly at 100 V for 20 min and then 150 V for 40 min.

Protein transfer to nitrocellulose membrane

Following SDS-PAGE, separated proteins were transferred onto nitrocellulose membrane (GE Healthcare, Amersham, UK) using BioRad Mini Blot II apparatus. The membrane, filter paper, and pads were pre-soaked in 1X Transfer Buffer. The transfer cassette was assembled in the following order:

(-ve charge) – pad – paper – gel - membrane – paper – pad – (+ve charge)

The cassette was placed in the holder, and then in the transfer apparatus filled to the top with pre-chilled 1 x transfer buffer and containing an ice pack and stirring bar. The transfer was performed for 1 h at 100 V.

Incubation with antibody

The nitrocellulose membrane was blocked to prevent non-specific antibody binding for 1 h with 5 % (w/v) skimmed milk in PBS containing 0.1 % (v/v) Tween-20. Subsequently, the membrane was incubated overnight at 4°C with primary antibodies in PBS-Tween (0.1 %) and 1 % bovine serum albumin (BSA). After 3 quick washes and additional 3 x 15 min washes with PBS-Tween (0.1%), an

appropriate horseradish peroxidase (HRP)-conjugated secondary antibody solution in PBS-Tween (0.1%) and 1% BSA was added to the membrane. This step was completed with incubation at room temperature for 1 h, 3 quick washes and 3 x 15 min washes.

Detection

Antibody binding was visualised using enhanced chemiluminescence (ECL) detection (Luminogen, GE Healthcare). The substrate for HRP was prepared by mixing reagents A and B, and added to the drained membrane and left for 1 min. Then, the membrane was wrapped in cling film and exposed to Amersham Hyperfilm ECL (GE Healthcare) for 0.5 - 5 min, as required.

2.6 Statistical analysis

Data from the miRNA profiling experiment were analysed using DataAssist™ Software, NormFinder Software and GraphPadPrism 5 version 5.0a.

Pearson Correlation Coefficients (PCC) was used to detect clusters of similarity in miRNA Ct between each pool group in patients, and between each pool group in controls. Relative quantification of miRNA expression to normalization to a suitable reference gene is routinely used to compensate for experimental variation in RT-qPCR analyses. NormFinder is an algorithm for identifying the optimal normalization gene among a panel of putative reference genes. This algorithm ranks each candidate according to its stability of expression in analysis of the same experimental samples.

To identify a suitable reference gene for the normalization of miRNA expression in this study, the NormFinder algorithm was applied to the expression data obtained from the Human TaqMan miRNA Arrays A v2.1 and B v3.0. Using DataAssist Software, the Ct levels of the first 10 miRNAs with the lowest stability value i.e. the most stability expressed candidate reference genes were evaluated. In addition, this analysis also included miR-16, RNU-48 and MammU6, the endogenous controls included in the Array Card A for data normalization, and RNU-48, U6, the endogenous controls included in the Array Card B for data normalization.

Analysis comparing miRNA levels between subjects with DN and controls was carried out using GraphPad Prism version 5.0. Linear regression analyses were performed for matched miRNAs expression levels and the following variables: eGFR, Proteinuria, Creatinine and Blood Glucose levels. p-values <0.05 were considered statistically significant.

2.7 *In silico* network analysis

All networks were created using Cytoscape (National Institute of General Medical Sciences, NIH, US), a general-purpose modelling environment for integrating bimolecular interaction network and states [205]. Molecular species were represented graphically as nodes and intermolecular interactions as links (edges) between nodes. Parameters describing network topology were computed using the Network Analyzer plug-in for this software. CyTargetLinker is a Cytoscape plugin that extends biological networks with regulatory interaction as miRNA-target gene information. The regulatory interaction network (RIN) is derived from an online interaction database; these consists of two nodes, a source and target biomolecule, which are connected through one directed edge.

The RINS used in this study to create the miRNA network were:

- TargetScan (release 6.2) [206]
- microcosm (version 5)
- miRTarbase (release 3.5) [207]
- miRecord [208]

Chapter 3 – Isolation of urinary miRNA and investigation of their stability

3.1 Introduction

Diabetic nephropathy is the leading cause of chronic kidney disease in the UK and the second one of end-stage renal disease. Since the classical indicators of diabetic nephropathy, namely GFR, proteinuria, macroalbuminuria and creatinine clearance, are not specific and sensitive enough to predict the outcome for individual CKD patients, new biomarkers to help predict outcome in this disease are required [43]. An ideal biomarker requires robust and reproducible assays that work in clinically available samples as well as archived material.

miRNAs are endogenous, short, non-coding single-stranded RNA transcripts that regulate gene expression at the post-transcriptional level and unlike mRNAs and long ncRNAs, appear to be stable in tissue and biological fluids, even under adverse conditions such as extreme pH, long-term room temperature storage, multi freeze-thaw cycles and RNase activity [166,167,170]. Urine represents an important biological sample type for investigating the potential of miRNAs as biomarkers, since it is easy and non invasive to obtain in large amounts and its composition also reflects directly changes in the functions of the kidney and urogenital tract [209]. At the beginning of this study not much was known about miRNA abundance, efficiency and reproducible recovery in urine samples and moreover a well-established urinary miRNAs extraction and detection protocol was not available. Bravo and colleagues, in 2007, studied the stability of four murine miRNAs, belonging to different miRNAs families, and their cDNAs, in RNA preparation using mouse insulinoma ß-cell line and mouse liver. Three days after RNA isolation these molecules were significant degraded, and they concluded that the preparation method yielded highly unstable miRNAs [210]. Further article published in 2009 investigated the miRNAs stability in clinical samples of B lymphocytes using different RNA isolation methods after 14 days and over a period of 10 months at -80°C. Their findings were completely different from Bravo, the extraction using TRIzol/TRI-Reagent was a robust reproducible method and miRNAs and their cDNAs were highly stable [211]. Therefore it was clear to us that the quality and reproducibility of miRNA expression profiles obtained by quantitative reverse transcription PCR (RT-qPCR) would depend largely on the RNA extracted and isolation method. Because of their small size, standard molecular techniques were modified to allow for the detection of small

miRNAs species. The main approaches available at the beginning of this study for miRNAs isolation were:

- A monophasic solution of phenol and guanidinium isothiocyanate (e.g. TRI Reagent) considered a standard approach for extraction of mRNA and miRNA for analysis. Urine was homogenised with TRI Reagent solution by repeated pipetting, and the mixture was separated into aqueous and organic phases by addition of chloroform and centrifugation. RNA was partitioned to the aqueous phase, DNA to the interphase, and proteins to the organic phase. RNA was then precipitated from the aqueous phase using isopropanol, and was finally washed with ethanol and then solubilized. However, it was unknown whether such precipitation-based extraction techniques would be robust in the context of tiny quantitates of RNA found in urine samples.
- Norgen's urine microRNA Purification kit that uses Norgen's proprietary resin as the separation mix. A Lysis Solution lysed the urine sample and after adding ethanol the microRNA bound to the column's resin while most of the contaminating cellular proteins are removed in the flow through or retained on top of the resin. The bound RNA is then washed to remove any remaining impurities and the purified urinary microRNA is finally eluted.
- miRNeasy Mini (Qiagen) that integrates phenol/guanidine-based lysis of samples with silica-membrane–based purification of RNA from approximately 18 nucleotides. Initially the sample is lysed and the RNases solution inhibits by the phenol-guanidine thiocynate solution. DNA and proteins are then removed from the lysate by organic extraction and RNA/miRNAs are purified using the spin columns.

Real time PCR is the main technique used for studying expression of single miRNAs or to validate observations resulting from genome wide expression profiling of miRNAs [212]. Although alternative techniques, such as Northern Blotting, may be used to quantitate miRNAs, these require input amounts of RNA that preclude their use in small samples such as those obtained from clinical isolates. There are two main systems:

- The Exiqon product, miRCURY LNA™ Universal RT microRNA PCR. This is a system designed for miRNA detection by quantitative real-time PCR using SYBR® Green. The method is based on universal reverse

transcription (RT) where a poly-A tail is added to the mature miRNA template; cDNA is synthesized using a Poly-T primer with a 3' degenerate anchor and a 5' universal tag. The cDNA template is then amplified using miRNA-specific and LNA™-enhanced forward and reverse primers, while SYBR® Green is used for detection.

- The quantification using Applied Biosystems TaqMan® Small RNA Assays. This is done using two-step RT-PCR. The cDNA is reverse transcribed from total RNA samples using a small RNA-specific, stem-loop RT primer that binds to the 3′-portion of miRNA molecules. In the PCR step, PCR products are amplified from cDNA samples using the TaqMan® Small RNA Assay. The assay contains primers specific (forward and reverse) for the target miRNA and a probe that contain a report dye (FAM™ dye) linked to the 5' end of the probe, a minor groove binder (MGB) at the 3' end of the probe and a non-fluorescent quencher (NFQ) at the 3' end of the probe.

Publications detecting mainly RNA or miRNAs in urine samples as potential markers of different pathologies or diseases were available but none of them described a reliable miRNA detection protocol. In most cases, these early papers describe analysis of miRNA expression in urinary sediment obtained after a spin at 3000g for at least 20 minutes, and not in the supernatant as our focus was [213-217]. Therefore the first aim of the present chapter was to investigate a robust and non-toxic technique for urinary miRNAs extraction and detection.

As already discussed in chapter 1 (see 1.3.5) protection of miRNAs from degradation may occur as a result of packing in microparticles such as exosomes, microvesicles and apoptotic bodies; or by association with RNA-binding proteins, or lipoprotein complexes [168,169,218]. The second aim of this chapter was then to study the stability of urinary endogenous miRNAs in samples from unaffected individuals and CKD patients, since an investigation of the physiological state of circulating miRNA in human urine had not yet been reported.

3.2 Results

3.2.1 Development of a robust technique for urinary miRNA detection

3.2.1.1 Optimisation of extraction of urinary miRNAs

In order to establish a robust and non-toxic technique for urinary miRNA detection, three different approaches for RNA isolation and two different approaches for miRNA detection were tested on control urine samples, and the quality and reliability of extracted RNAs was compared (2.1.1 and 2.2.1). Evaluation was based both on the amounts of total RNA/miRNA measured and the mean A260/280 ratio (RNA integrity) obtained with the different extraction protocols.

TRI-reagent solution combines phenol and guanidine thiocyanate in a monophasic solution to rapidly inhibit RNase activity. TRI Reagent recovered the highest RNA yield, but with wide yield variability. Achieved concentrations of RNA were low (Fig 3.1). Lack of a visible RNA pellet during the extraction, and unreliable precipitation of such low concentration RNA may have contributed to the variability.

Norgen purification was based on spin column chromatography using a proprietary resin as the separation matrix binding RNA in an ionic concentration-dependent manner.

Small RNA molecules were preferentially purified from other cellular components such as ribosomal RNA without the use of phenol or chloroform. Our data show a difference in RNA recovery (range between 3.27 and 59.78 ng/µl) and a low A260/A280 ratio (range between 0.61 and 1.34) indicating probable protein contamination.

Followed by these observations, and previous work suggesting that in low abundance clinical samples, affinity column-based RNA extraction offers advantages [202], miRNeasy Mini (Qiagen) protocol with minor modifications (see 2.2.1.1) was selected for further analyses (Figure 3.1).

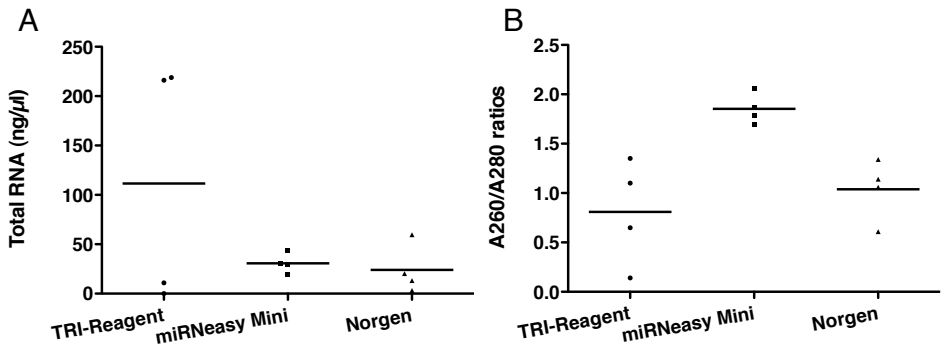

Figure 3.1. RNA/miRNA extraction using three different protocols

RNA/miRNA was extracted using three different approaches: Tri-Reagent, miRNeasy Mini (Qiagen) and Norgen. **A:** The graph shows the mean value of total yield. Standard Error of the mean (SEM) is respectively 61.25, 5.062 and 12.38 **B:** mean A260/A280 ratios: this ratio is used as a measure of RNA purity. A ratio of 2 signifies appropriate purity to analyse. SEM is respectively 0.26, 0.07 and 0.15.

Two different RT-qPCR techniques, Applied Biosystems and Exiqon, were then used to detect miR-16 and thereby evaluate RNA/miRNA extracted by the three methods described above. miR-16 was selected since it is a ubiquitously expressed miR and it is commonly used as a reference miRNA to normalize RT-qPCR expression data [219].

Figure 3.2 represents the Ct of miR-16 obtained using RNA extracted by the three different techniques described above, and provides a comparison of the recovery of urinary miRNAs using these three different isolation methods. There was no statistically significant difference in abundance of miRs detected, suggesting that there was no important difference in efficiency of extraction by the three methods. However, a consistent observation in my experiments was that the miRNeasy kit led to the lowest level of variance in the data, suggesting that this approach gave the most consistent RNA extraction (Fig 3.2). Similarly, although similar Ct values were achieved using both TaqMan and LNA/SYBR Green-based detection approaches, the data obtained using TaqMan chemistry were consistently less variable. Therefore, for my future work, I used the TaqMan approach.

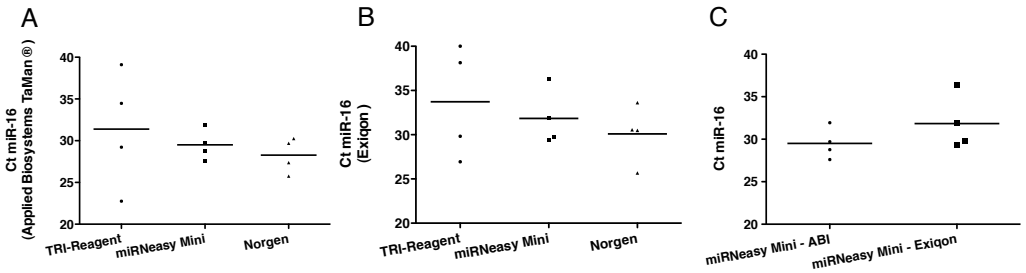

Figure 3.2. Ct value for miR-16 obtained using two different RT-qPCR techniques

Ct values for miR-16 obtained using two different RT-qPCR techniques, Applied Biosystems TaqMan (**A**) and Exiqon (**B**), on RNA samples isolated using three approaches described above. Graphs show the mean of four replicates. Difference were not statistically significant but miR extraction with miRNeasy Mini appeared more robust and with less SEM in both RT-qPCR techniques. (**A**) Standard error: TRI-Reagent = 3.51, miRNeasy Mini = 0.91, Norgen = 1.04. (**B**) Standard error: TRI-Reagent = 3.16, miRNeasy Mini = 1.59 Norgen = 1.64. (**C**) Comparison of mean of miR-16 CT between Applied Biosystems TaqMan® (ABI) and Exiqon with miRNeasy Mini isolation protocol. Statistical differences were not observed, but lower Ct values and reduced SEM was achieved with Applied Biosystems's reagent. SEM: Applied Biosystems TaqMan® (ABI) = 0.91 Exiqon = 1.59. RTqPCR was performed in duplicate. SEM= standard error of the mean.

Determination of the RT-qPCR assay efficiency is critical for accurate data interpretation. A PCR efficiency of 100% corresponds to a slope of –3.32, as determined by the following equation:

$$\text{Efficiency} = 10^{(-1/\text{slope})} - 1$$

Ideally, the efficiency (E) of a PCR reaction should be 100%, meaning that the template doubles after each cycle during exponential amplification. Calculation of actual reaction efficiency provides valuable information. The presence of PCR inhibitors in one or more of the reagents can produce efficiencies of greater than 110%. A good reaction should have efficiency between 90% and 110%, which corresponds to a slope of between –3.58 and –3.10.

To calculate RT efficiency, serial dilutions from one urinary total extract were used to perform qPCR following the protocol (2.2.2.2) (Figure 3.3 A). The slope was 3.288 with an efficiency of 101.44%. qPCR efficiency was calculated using serial dilutions from 1 sample following reverse transcription, data show a slope of 3.230 with an efficiency of 103.98% (Figure 3.3 B).

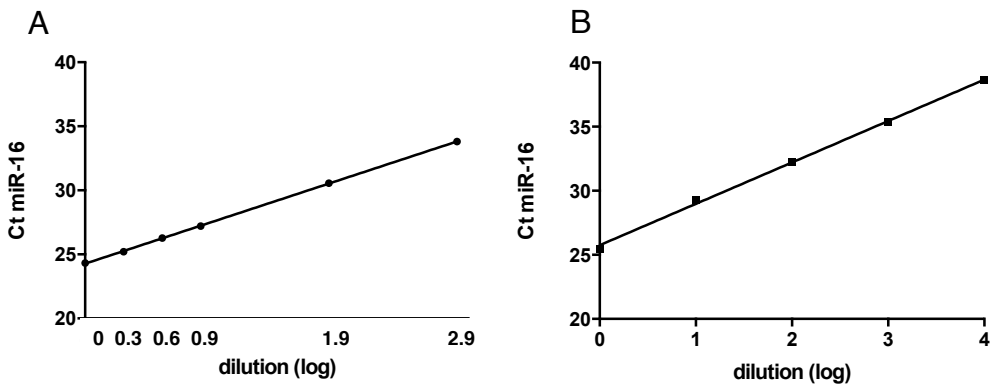

Figure 3.3. Calculation of RT and PCR efficiency

A: Serial dilutions were generated from a RNA sample isolated using miRNase Mini approach and added on the RT step to evaluate the retrotranscription's efficiency. Later, Ct for miR-16 at the indicated dilution points were detected using qPCR. **B:** Serial dilutions were produced from a RT product to analyse qPCR's efficiency for miR-16.
Both graphs show the log of made dilutions. RT's efficiency (**A**)= 101.44% and r^2= 0.9999 while qPCR's efficiency (**B**)= 103.98% and r^2= 0.9981.

3.2.1.2 Extraction assay variability studies

In order to quantify the robustness and reproducibility of RT-qPCR of urinary miRNAs, of RT-qPCR technique, intra-assay variability and biological variability in miRNA detection in urine samples were investigated and coefficients of variation (CV) were calculated. CV (standard deviation / mean) is a measure of the variability of the result for the same sample evaluated repeatedly in the same assay run, and in separate assay runs, respectively. The goal for any assay is the smallest possible coefficient of variation; generally a variability of less than 10 to 15% is acceptable. miR-16 and miR-192 were analysed since miR-16 is expressed abundantly and ubiquitously ,while miR-192 was chosen as previous work from our laboratory has demonstrated that it is down-regulated in diabetic nephropathy [220]. Intra-assay variability was determined by performing a sextuplicate reverse transcription reaction on RNA extracted from one urine sample followed by duplicate qPCR analysis, the coefficients of variation were 0.47% for miR-16 and 0.78% for miR-192. In addition, to assess the stability of miRNAs, RT-qPCR analysis was performed for miR-16 and miR-192 from freshly isolated RNA samples stored at -80°C over 6 days. The coefficients of variation were again less than 10% for all control samples; respectively 3.9%, 6.49% and 1.95% for miR-16 3.64, 7.33 and 3.94% for miR-192. Experimental data (Figure

3.4) show that miRNA stored under these conditions did not degrade and small differences appeared to be secondary to technical variability of the RT-qPCR itself.

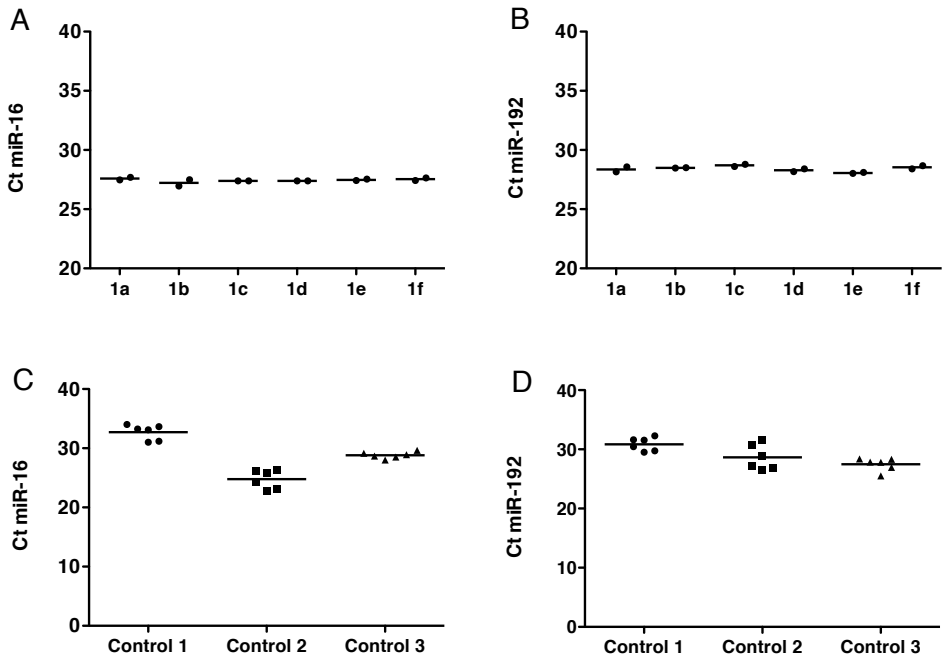

Figure 3.4. Study of the extraction variability assay

A-B: Reverse transcription reaction performed in sextuplicate and qPCR in duplicate to evaluate intra-assay variability for miR-16 and miR-192 detection from one control urine sample. The scatter dot plot represents the mean of the Ct value for miR-16 and miR-192; the CV are respectively 0.48 for miR-16 and 0.78 per miR-192. **C-D:** RT-qPCR analysis of miRs from control urine samples stored at -80°C over 6 days. The coefficients of variation were less than 10 % for all control samples; respectively 3.9% for control 1, 6.49% for control 2 and 1.95% for control 3 for miR-16, and 3.64, 7.33 and 3.94% for miR-192.

Biological variability for miR-16 and miR-192 was evaluated using RT-qPCR from fresh urine samples collected every day for 6 days from the same 4 volunteer control subjects. The coefficients of variation for biological variability for the 4 samples were 6.28, 4.78, 5.63 and 8.58% for miR-16 and 2.08, 5.52, 8.39,4.49% for miR-192 (Figure 3.5).

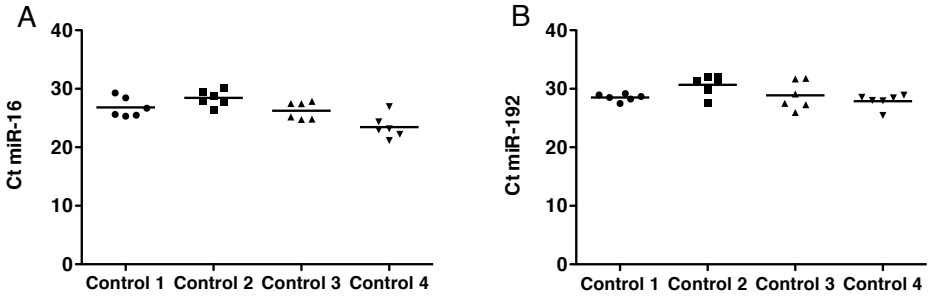

Figure 3.5. Analysis of biological variability

RT-qPCR analysis of miRNA samples from fresh urine samples from the same individuals over 6 days. The graphs represent the mean of miR-16 and miR-192 Ct. CV were calculated found to be below 10% for all samples.

3.2.1.3 RT-qPCR tolerance to urine

Molecular diagnosis, where nucleic acids are measured in the context of a disease, is a multistep process requiring collection, storage, and extraction of a sample prior to analysis. Urine, as already discussed, has advantages in this context, being easy to collect and homogeneous. Since PCR has been used by scientists, qPCR inhibitors have been an obstacle to success since a RNA sample that is not clean and free from any residual buffers or urine components may have repercussions on the entire process and/or modify the salt concentration of the buffer. This is usually not a problem when using spin column kits instead of manual extraction techniques.

In order to exclude important inhibition of RT-qPCR efficiency by carryover of urinary components, different percentages of urine were added in the reverse transcription reaction as possible qPCR inhibitor. Synthetic *C. elegans* miR-39 stem-loop (cel-miR-39) was spiked-in to provide an internal control for RNA isolation, cDNA synthesis and PCR amplification. To be certain that the spike in control did not itself alter miRNAs detection, exogenous cel-miR-39 was spiked into a control urine sample at 0.05, 0.5, 5 and 50 pM. Endogenous hsa-miR-16 and exogenous cel-miR-39 were then detected by RT-qPCR, and showed that the introduction of the synthetic miRNA into the RNA extraction resulted in no significant difference in detection (Figure 3.6 A). Exogenous 0.05pM cel-miR-39

was then spiked into 4 control urine samples. RNA was extracted and then different percentages of urine (0, 0.1, 0.5, 1 and 5%) were added to the RT (reverse transcription) step to analyse inhibition. Endogenous miR-16 and exogenous miR-39 were then detected by RT-qPCR and the data normalized versus 0% of urine. As showed in figure 3.6, percentages of urine between 0.1 and 5 in the RT step did not interfere and did not have consequences on miR-16 or miR-39 expression.

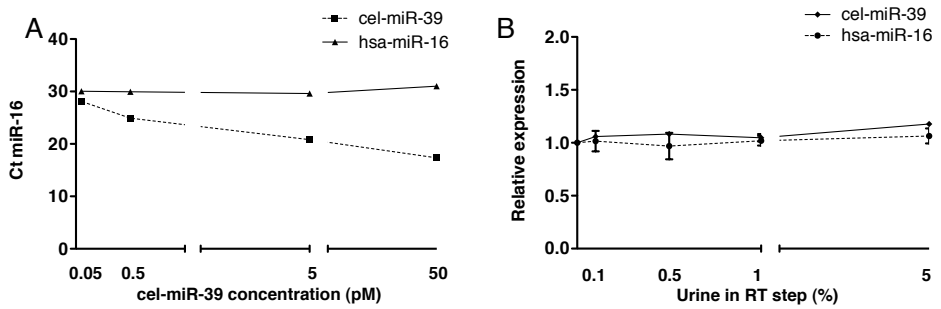

Figure 3.6. Analysis of RT-qPCR tolerance to urine

A: Exogenous cel-miR-39 was spiked into control urine sample at 0.05, 0.5, 5 and 50 pM. miR-16 and cel-miR-39 were detected by RT-qPCR**. B:** Exogenous cel-miR-39 was spiked into 4 control urine samples at 0.05pM. Urine at 0, 0.1, 0.5, 1 and 5% were added to the RT step to analyse inhibition. Endogenous miR-16 and cel-miR-39 were detected by RT-qPCR and data were normalized to 0% urine.

3.2.2 Stability of urinary miRNAs

3.2.2.1 Endogenous urinary miRNAs are resistant to RNase digestion

Having developed a robust technique for urinary miRNA detection, samples from control subjects and proteinuric patients were analysed in order to determine whether proteinuria altered miRNA stability. Human urine contains active ribonuclease (RNase) [221]; to test if miRNAs are protected from this ribonuclease action, urine samples from control and diabetic nephropathy patients were maintained at room temperature for 24h. Furthermore, to understand if this mechanism was exclusive to endogenous urinary miRNA, spiked-in exogenous synthetic cel-miR-39 was added to all urine samples and monitored under the same conditions. Synthetic cel-miR-39 was spiked-in at time zero into the urine samples and detection of ubiquitously expressed endogenous control miR-16 and exogenous cel-miR-39 was compared after 1, 2, 4, 8 and 24 hours (Figure 3.7). In urine samples from controls and patients > 60% of the time zero miR-16 signal was detected by RT-qPCR analysis after 24h at room temperature (Figure 3.7 A, B), while cel-miR-39 expression decreased to <10% of its time zero signal after 1 hour (Figure 3.7 C, D). These data suggest that a room temperature dwell-time of 4 hours is acceptable for studies of urinary miRNAs expression. Second, the data suggest that there are specific mechanisms of stabilisation that pertain to endogenous urinary miRNAs, and not to exogenous or spiked-in miRNAs. miRNAs stability is specific to endogenous miRNAs and not, more generically, a miRNA's characteristic.

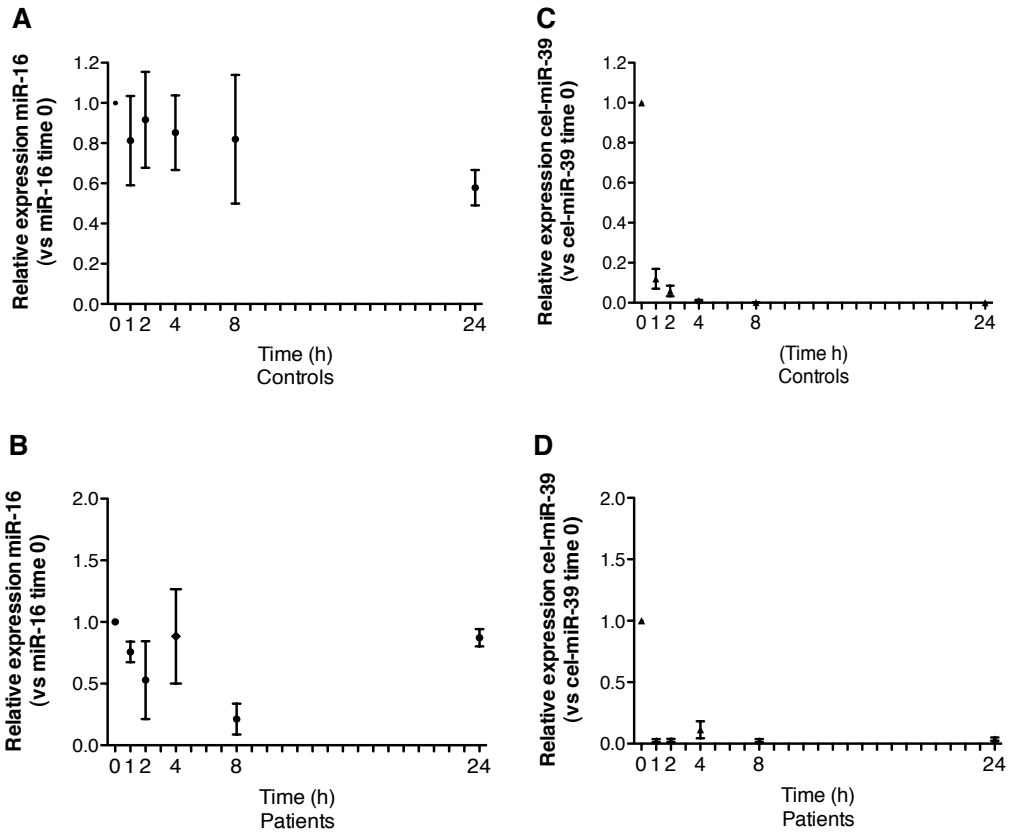

Figure 3.7. Stability of urinary miRNAs

Relative expression of miR-16 **(A-B)** and cel-miR-39 **(C-D)** in urine samples from control subjects **(A-C)** and diabetic nephropathy patients **(B-D)** stored at room temperature over 24 h. The data represent mean ± SEM of urine samples from 6 control and 4 diabetic nephropathy patients normalized against each respective zero time-point. SEM= standard error of the mean

Since urine contains active RNases, detection of miRNAs suggested that these transcripts are resistant to RNase digestion. Data in Figure 3.7 showed that miR stability was not intrinsic to their small size or chemical structure but suggested that it occurred by additional external factors. To investigate this observation further, RT-qPCR detection of endogenous miR-16 and exogenous miR-39 was compared in urine samples from control subject treated and not treated with exogenous RNase at time points up to 1 h incubation at 37°C, followed by analysis of both control and patient urine samples at the 30 min time point. Results in Figure 3.8 show that synthetic cel-miR-39 expression decreases rapidly both in the presence or absence of RNase being wholly degraded after 10 min in the absence of RNase, and after 1 min in the presence of enzyme (Figure 3.8 D-F). miR-16 expression detection was stable in urine untreated with RNase

(Figure 3.8 A); after 15 min RNase treatment around 15% of miR-16 expression was still detectable (Figure 3.8 A). Endogenous urinary miRNAs were resistant to exogenous RNase both in patient and control urine samples with a significant difference of p=0.04 in patients' urine and p=0.02 in controls' urine. (Figure 3.8 B-C)

These results confirmed the sensitivity of synthetic exogenous miRNAs to degradation in urine and that endogenous transcripts exist in a form that is partially resistant to urinary RNase activity.

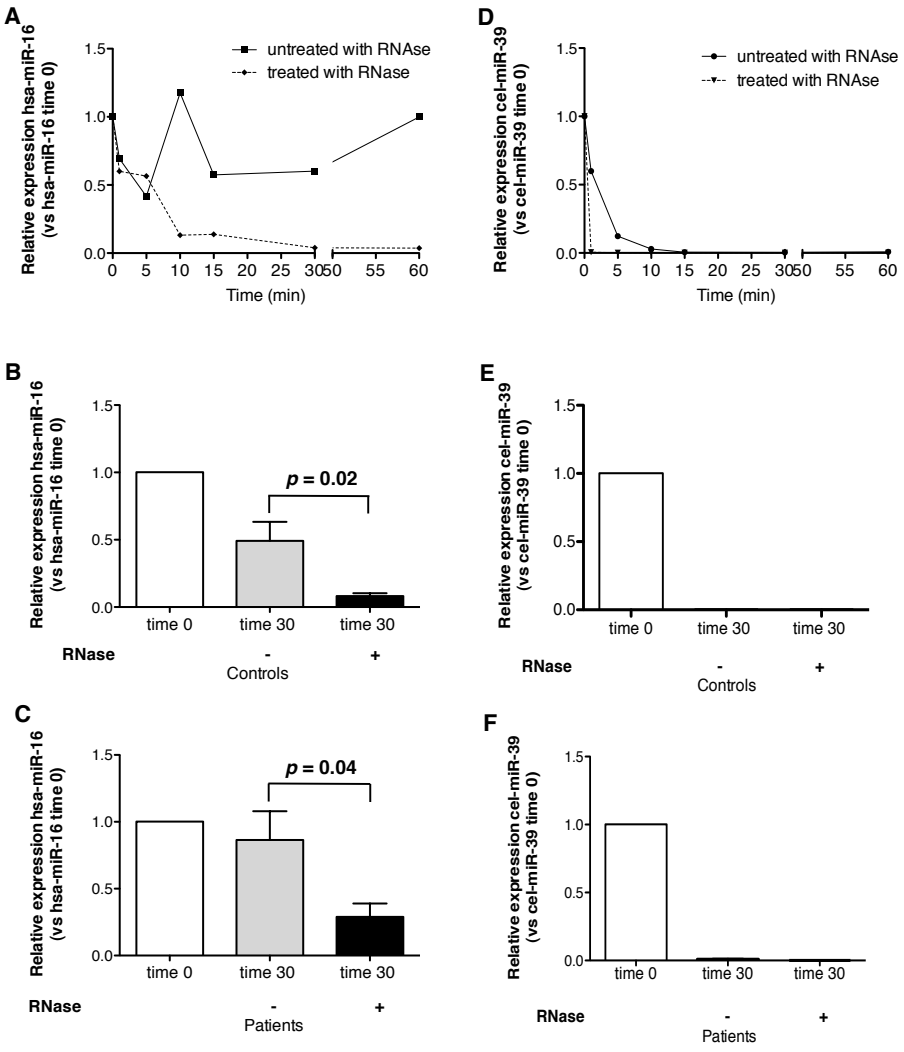

Figure 3.8. Treatment of urine samples with RNase

Relative expression of endogenous miR-16 (**A-C**) and exogenous cel-miR-39 (**D-F**) in urine samples from 6 control subjects and 4 diabetic nephropathy patients following treatment with RNase A. Data are normalized to their respective zero time-points and they are presented as mean value ± SEM. SEM= standard error of the mean

3.2.2.2 Urinary exosomes isolation

In the absence of a stabilising influence, degradation of urinary miRNAs would be predicted. Mechanisms by which urinary miRNAs are protected from endogenous RNase degradation were therefore investigated. Firstly, urinary extracellular vesicles were isolated from control samples and analysed by nanoparticle tracking (see 2.4). This method visualises and analyses particles in liquids by relating the rate of Brownian motion (random moving of particles suspended in a fluid) to particle size. Movement is related only to the viscosity of the liquid and is not influenced by temperature, particle density or refractive index. This technique provides a size distribution and particle count. The data demonstrated that ultracentrifugation pelleted ≈88% of urinary nanoparticles and that the majority of these nanoparticles were detected in the typical exosomal range around 100 nm (Fig 3.9).

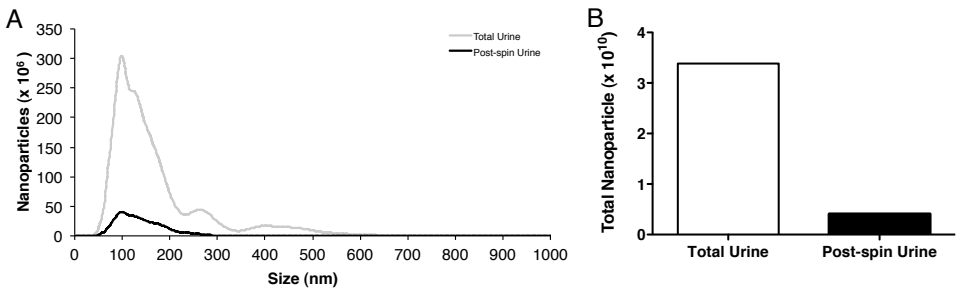

Figure 3.9. Nanoparticles analysis by NanoSight

Urinary nanoparticles were analysed using the NanoSight LM10 system, data (**A**) reveal that that the majority of nanoparticles was recovered around the size of 100nm, typical of exosomes while the graph in (**B**) shows that approximately 88% of urinary nanoparticles were pelleted using this protocol.

The total post-spin urine pellet was applied to a continuous sucrose gradient and ultra-centrifuged at 4°C overnight at 210,000*g* to obtain sub-fractions and to isolate urinary exosomes. Since it is know that the classical exosome density range is between 1.1-1.2 g/ml [222]; to find out which sub-fractions contain exosomes, refractive index of each subfraction was detected in each samples and density was calculated. These data suggested that fractions 3-5 contained vesicles with the typical exosome density (Figure 3.10). In addition, flow cytometric analysis showed that classical exosomally-expressed tetraspanins

CD9 and CD81 were abundant in fractions 3, 4 and 5, as were multivesicular bodies markers tumour susceptibility gene (TSG)101 and programmed cell death 6-interacting protein (Alix), detected by Western blotting analysis.

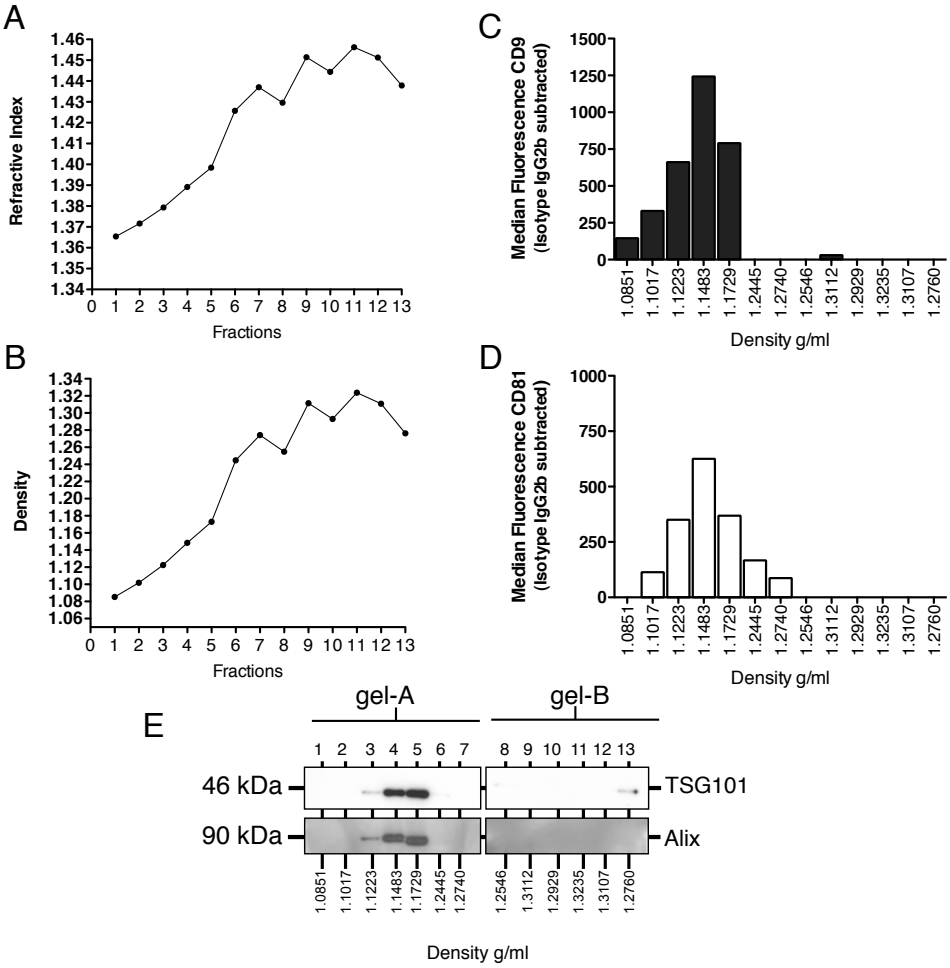

Figure 3.10. Exosomes characterization

Extracellular vesicle pellets were overlaid onto continuous sucrose gradients of 0.2-2.5 M sucrose and their refractive index (**A**) and density (**B**) determined to identify fractions containing exosomes. Since exosome-density range is between 1.1-1.2 g/ml the exosomes were isolated in fraction 3,4 and 5. Validation of these data was carried out using exosome-expressed tetraspanins CD9 and CD81 identified by flow cytometry (**C** and **D**) and identification of multivesicular body markers TSG101 and Alix by Western blotting (**E**). (**C** and **D**) Graphs represent the median fluorescence intensity for CD9 and CD81 with of IgG2b isotype control subtracted.

3.2.2.3 Protein association stabilises extra-vesicular urinary miRNAs

Detection of miR-16 and miR-192 was then carried out in the fractions prepared by density gradient ultracentrifugation. High relative abundances of these two miRNAs were detected in these exosomal fractions (Figure 3.11 A and B), suggesting that in urine, these miRNAs were protected from endogenous RNase degradation via association with exosomes.

miR-16 and miR-192 were also detected in the non-sedimented urinary miRNAs in the supernatant. Data obtained via RT-qPCR showed detection of supernatant miRNAs with a Ct=34.09 for miR-16 and Ct=36.02 for miR-192. The Ct average from the total pellet for miR-16 was 32.2, and 32.09 for miR-192, showing that detectable portions of urinary miRNAs were likely protected from RNase degradation by association with proteins. A more conservative conclusion was that urinary miRNAs were detected both in sedimented and non-sedimented urinary fractions.

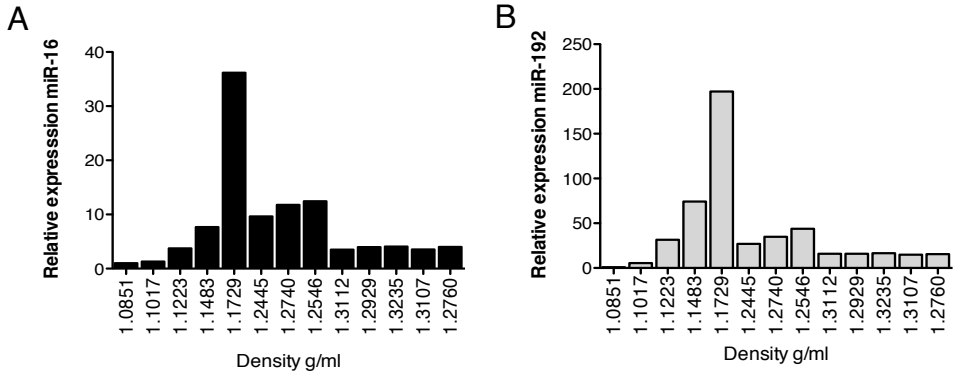

Figure 3.11. miR-16 and miR-192 detection is sedimented urinary miRNAs

(**A** and **B**) miR-16 and miR-192 were detected using RT-qPCR from extracellular vesicles fraction obtained by ultracentrifugation.

To investigate if the non-sedimented miRNAs were protected from degradation by association with proteins, we compared miR-16 recovery in control and patient urine samples incubated at 55°C over 60 min alone, or in the presence of proteinase K. Results in Fig 3.12, show that endogenous miRNA was

destabilised and not detected following proteinase K digestion while around 100% of miR-16 was recovered in urine samples not treated with proteinase K. Further analysis at the 30 min time-point showed that this effect was statistically significant in control and patient urine samples. These data suggest support the hypothesis that non-sedimented miRNAs resist RNase degradation via association with ribonucleoprotein complex.

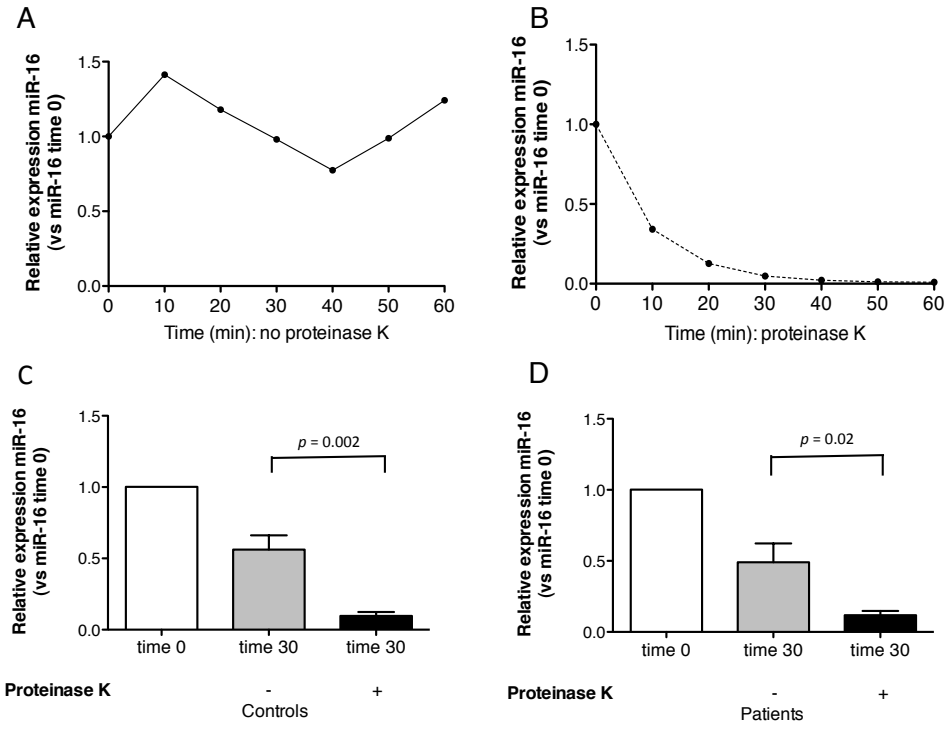

Figure 3.12. Treatment of urine samples with Proteinase K

(**A** and **B**) Control urine untreated (**A**) or treated (**B**) with proteinase K over 60 min at 55°C resulted in degradation of endogenous urinary miR-16. (**C** and **D**) The same experiment was repeated using 5 control and 5 CKD patient urine samples, data showed that this effect was statistically significant in control (p=0.002) and patient (p=0.02) urine samples. Data were normalized to the respective zero time-point.

3.2.2.4 Urinary miRNAs are associated with AGO2

Although not yet studied extensively in urine, it is well established that miRNA function involves association with the multi-protein RNA-induced silencing complex (RISC). Argonaute (AGO) proteins are the core effectors of the miRNA pathway and effectors of RNAi that incorporate mature miRNAs following processing of their respective primary transcripts [170,223]. To establish if AGO2 protein was present in urine and if miRNAs were associated with it, RNA-immunoprecipitation was performed followed by immunoblotting from controls urine samples (Figure 3.13). Detergent was not added during immunoprecipitation to avoid potential lysis of urinary vesicles. Western blotting analysis and quantification of these data by densitometry showed a significant difference (p=0.008) between urinary AGO2 immunoprecipitate and the negative control mouse IgG reactions. RT-qPCR analysis for miR-16 and miR-192 in these samples revealed that it was significantly recovered in greater abundance in the AGO2 immunoprecipitation than in the negative control mouse IgG with respective p-values of 0.01 for miR-16 and 0.02 for miR-192.

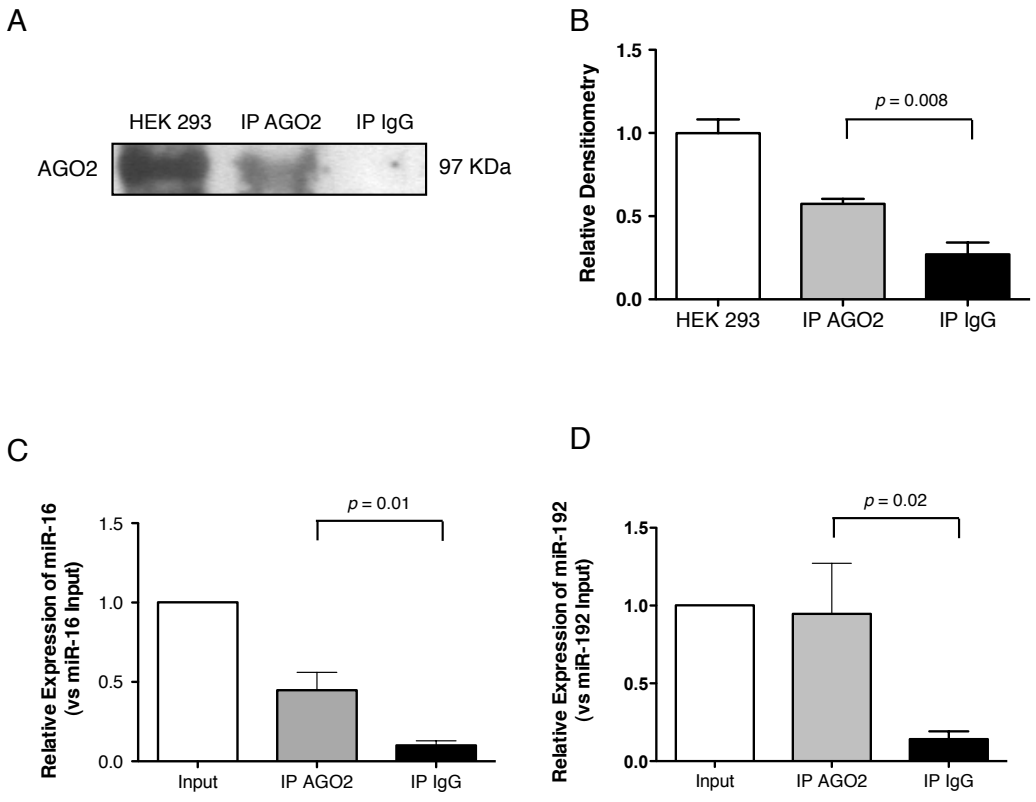

Figure 3.13. Urinary AGO2 immunoprecipitation

(**A**) Immunoprecipitation (IP) from urine sample using anti-AGO2 antibody detected AGO2, with negative normal mouse IgG and positive HEK-293 control reactions. The blot shown here is representative of a total of 5 experiments, each of which yielded similar results. (**B**) Densitometry analysis of AGO2 immunoprecipitation data from all 5 experiments. (**C** and **D**) RT-qPCR detected increased miR-16 and miR-192 in Ago2 immunoprecipitates in comparison with untreated urine input and mouse IgG reactions. Error bars represent mean ± SEM.

3.2.2.5 Urinary miRs are not associated with albumin

The appearance of increased quantities of urinary albumin is an important sign of damage of the glomerular filtration barrier. Albumin is a type of protein found in large amounts in the blood. Because it is a small molecule, it is one of the first proteins able to pass through the kidney into the urine when there are kidney problems. The presence of a small amount of albumin in the urine is called microalbuminuria. As the amount of albumin the urine increases, the condition progress from microalbuminuria to albuminuria or proteinuria. Detection of microalbuminuria is used widely as a biomarker for renal injury in diabetes and other disease-related contexts. Patients with conditions leading to glomerular damage such as diabetic nephropathy may exhibit grossly increased urinary protein losses of several grams per day, in sharp contrast with an average value of <100 mg/day in unaffected individuals. To investigate if miRNAs were associated with albumin under normal or grossly proteinuric conditions an RNA-immunoprecipitation of urinary human albumin was performed. Data in Figure 3.14 show that albumin was recovered by immunoprecipitation from both control and patient urine samples, a statistical significant difference was found between specific recovery in comparison to negative control data in both control (p=0.0004) and patients (p=0.004). In contrast with data regarding AGO2 recovery (Fig. 3.13), miR-16 and miR-192 were detected in very low quantities in both albumin immunoprecipitation samples (Fig 3.13 E-H). Figure 3.14 A and C show the presence of albumin concentration in the urine of unaffected individuals. This event is not unexpected since, with a molecular weight of 67 KDs, complete exclusion by the glomerular filtration barrier (GFB) is far less effective than for larger proteins like AGO2 (97KDa).

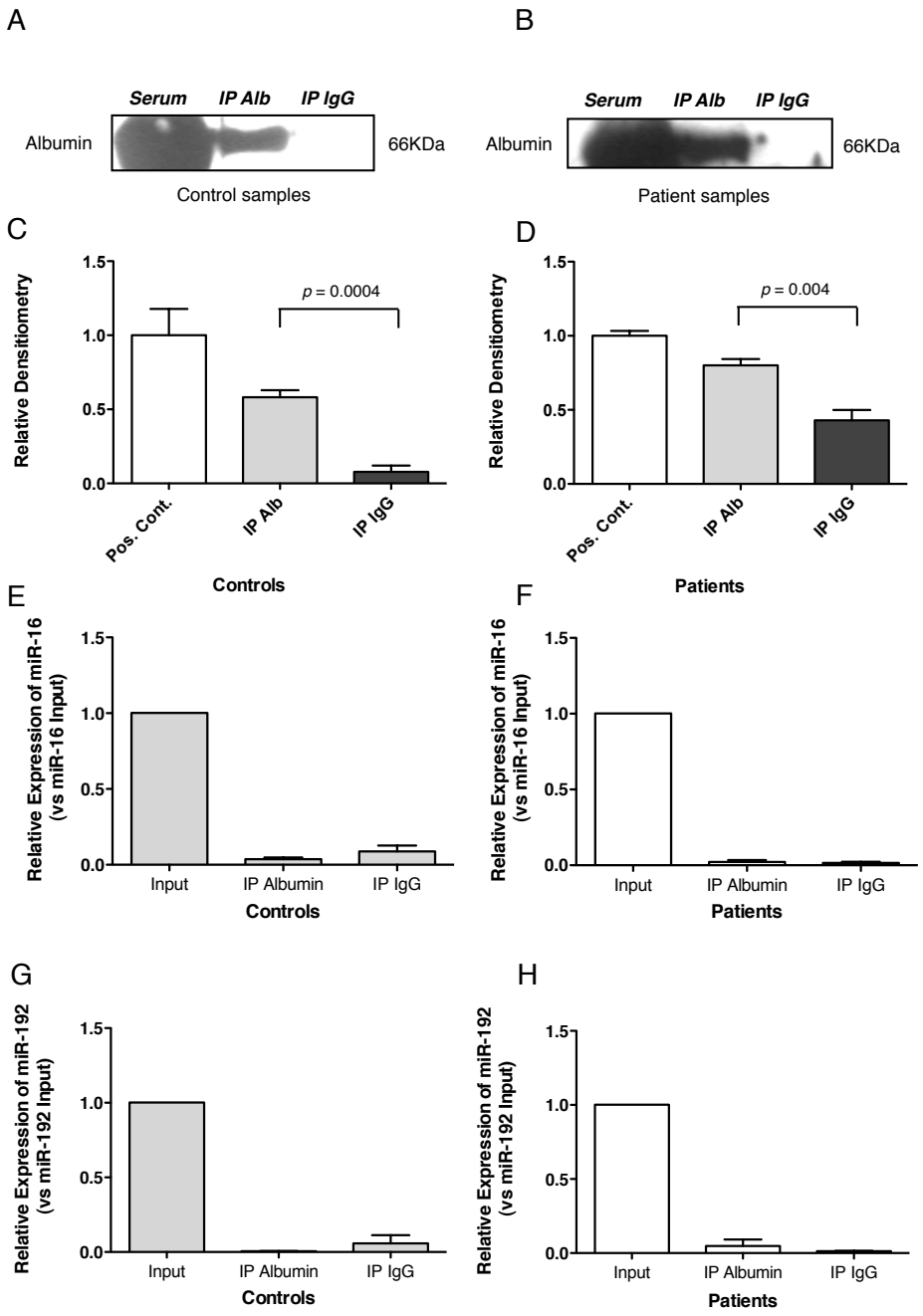

Figure 3.14. Urinary albumin immunoprecipitation

(**A** and **B**) Immunoprecipitation (IP) detection of albumin in control and patient urine samples, using IgG as negative control and human serum as positive control. The gels shown are representative from a total of four experiments, all of which yielded similar results. (**C** and **D**) Relative densitometry analysis of albumin immunoprecipitation data. (**E**-**H**) miR-16 and miR-192 were detected using RT-qPCR in whole albumin immunoprecipitates samples, in the untreated urine used as input and mouse IgG negative control reactions. Data were normalized versus the input and are presented as mean values ± SEM.

3.3 Discussion

At the beginning of this project, the utility of urinary miRNAs as biomarkers for non-invasive diagnostic/ prognostic testing for CKD had not been established. However, recovery of sufficient miRNAs of appropriate purity, following RNA extraction from biological fluids, for effective quantitative downstream analyses could to be problematic. The work carried out in this chapter therefore provided a starting point by establishing a robust protocol for the extraction of urinary miRNAs.

Development of a RT-qPCR protocol for the quantification of individual urinary miRNAs was followed by investigation of intra- and inter-assay variation, and urinary miRNA stability. Three different RNA extraction protocols were compared and RT-qPCR was used to assess recovery of miRNA species.

The most valid and reproducible technique for extracting and detecting miRNAs from urine was the miRNeasy Mini (Qiagen) protocol followed by Applied Biosystems TaqMan® detection. This method was robust and provided consistent results when used to study intra-assay and biological variability in different urine samples. Coefficients of variation were calculated at less than 10%, showing that the assay was sufficiently robust for the subsequent work described in this thesis.

Having established a robust urinary miRNA detection protocol, endogenous urinary miRNA stability in urine samples from unaffected individuals and CKD patients was investigated. Preliminary data showed that urinary miR-16 degraded over extended storage at room temperature. Given that samples have likely been stored in the bladder at 37°C for several hours prior collection, this result appeared surprising. However, in the light of this finding, the approach for urine collection was modified. Second pass, rather than overnight urine samples were used to minimise bladder dwell time, after which samples were placed on ice and processed immediately.

Concordance of miRNA expression in urine samples collected from the same individual on successive days was demonstrated, showing that the modified collection protocol yielded robust expression data. Indeed, in urine stored at room

temperature over 24 h; more than 50% of the time zero miR-16 signal was still detected. On the basis of the above data, a maximum room temperature dwell-time of 4h was included in our standard urinary miRNA analysis protocol.

The finding that the degradation of urinary miRNAs following the addition of exogenous RNase was lower when compared to spiked-in cel-miR-39 controls provided compelling evidence of a stabilising mechanism, or mechanisms, protecting endogenous urinary miRNAs from degradation.

Following 16 h ultra-centrifugation at 200,000 g, sedimented urinary miRNAs were associated with microvesicles, including exosomes, while a percentage of non-sedimented urinary miRNAs remained in the supernatant. Microvesicle association provided a readily conceivable means of protection from RNase degradation, but the persistence of the apparently “free” miRNAs required a different mechanism.

In an early study, Diederichs and Haber showed that argonaute proteins enhance production or stability of mature miRNAs. In addition, using AGO2 mutation, they demonstrated that direct interaction between miRNA and AGO2 increased expression of mature miRNAs [223]. In the present study, protein-conferred urinary miRNA stabilization was tested by incubation with proteinase K, and increased miRNA degradation suggested that at least some of the non-sedimented urinary miRNAs were stabilised in this way. RNA immunoprecipitation analysis identified RISC component protein AGO2 as a urinary binding partner that appeared to be responsible for protection from miRNA degradation.

Association between miRNA and Ago2 has been reported previously in plasma [170,189]. Arroyo et al. confirmed that some plasma miRNA, obtained by size-exclusion chromatography, were microvesicle-associated, but these represented a minority of total plasma miRNAs [170]. Indeed, more than 90% of miRNA in the plasma and serum were bound to a ribonucleoprotein complex and transcript degradation increased following proteinase k digestion, suggesting that association with the protein complex was a stabilising mechanism for miRNA in the RNase-rich circulation [170].

Results obtained by Turchinovich et al. conducted in human peripheral blood and cell culture media showed that >97% of miRNAs were exosome-free and that only small amounts of miRNAs were sedimented by centrifugation. These authors also reported that extracellular miRNAs were bound to 96kDa AGO proteins, AGO2 in particular [189].

Li and colleagues analysed 8 miRNAs with high expression levels in human plasma that remained stable after treatment with 20 µg/ml of RNase A. Following separation of plasma into (MV) multivesicular and multivesicular-free fractions, they found that most of them were localized in the MV. MV disruption using 0.1% Triton X-100 and subsequent RNase A treatment led to decreased miRNA detection, but resistance to degradation by RNase A was still apparent. Indeed, only after adding proteinase K were all miRNAs were degraded, and AGO2 was identified as a key protein apparently protecting the secreted miRNAs in the MV fraction. Together, these results suggest that both MVs and protein contributed to the resistance to RNase A of secreted miRNAs [224].

By contrast, recent work found that plasma-borne miRNAs from patients with stable coronary artery disease, as well as acute coronary syndrome were associated with microparticles, and that only a small proportion of the total miRNA component was microparticle-free [225]. Similarly, Gallo et all reported that the majority of the miRNAs in human biologic fluids were not freely circulating but enclosed in microvesicles, primarily exosomes [226]. Elsewhere, protection of urinary miRNAs from degradation may be a product of association with extracellular vesicles such as exosomes [227]. The above reports describe different mechanisms for miRNA protection from RNase degradation, with most of these studies carried out in cell lines and/or plasma or serum samples.

Understanding the molecular mechanisms stabilising urinary miRNAs has important implications for the utility of urinary miRNAs as a novel class of non-invasive CKD biomarker. Association with microvesicles such as exosomes would be predicted to result in exclusion from glomerular filtration. Similarly, association of miRNAs with AGO2 protein suggests that miRNA are not freely filtered at the glomerulus. The commonly accepted upper molecular mass threshold to cross the glomerular filtration barrier is around 67kDa. This

corresponds to partial filtration of albumin, a protein commonly measured in the urine as a marker of disruption of the glomerular filtration barrier. On this basis association of miRNAs with AGO2, which has a molecular mass of 97kDa, would be expected to exclude circulating miRNAs from the glomerular ultrafiltrate.

If association with AGO2 or microvesicles such as exosomes excludes circulating miRNAs from the urine, then the miRNAs in urine are predicted to originate solely from the cells of downstream of the glomerular filtration barrier. A previous study suggested that RISC protein GW182 play a role in protecting AGO-bound miRNAs [191]. The addition of the GW182 protein to associated miR-AGO2 size would increase its molecular mass by 182kD, making trans-glomerular filtration barrier passage even less likely. However, this work was carried out in HEK293 cells, in which most miRNAs were associated with exosomes, and thus cell phenotype and context-specific considerations are also likely to be significant [191].

In summary, the results presented in this chapter show that miRNAs are stabilised in urine by association with both exosomes and AGO2. The size of the resultant protein:miRNA complex or miRNA incorporation in exosome makes it possible to predict that miRNAs do not freely cross the glomerular filtration barrier and this has important implications for the use of urinary miRNAs as biomarkers.

The time available to conduct this study was sufficient to analyse association of miR-16 and miR-192 with exosomes or AGO2 protein in control urine samples. However the selected miRNAs do not represent the whole miRNA population, and profiling of urinary exosome miRNAs would be a more complete approach. In addition isolation and characterisation of urinary exosomal miRNAs from DN patients, as well as their association with AGO2 proteins, might have important implications for the development of biomarker and functional studies.

A reliable miRNA isolation technique to obtain sufficient quantity and quality urinary RNA and the stability of stored miRNA samples isolated by this method of needed to be established. Reliable detection of these transcripts provides a novel method for understanding kidney disease with the potential to identify new diagnostic biomarkers.

Chapter 4 – miRNA Profiling in diabetic nephropathy patients

4.1 Introduction

CKD is a leading cause of death worldwide and diabetic nephropathy (DN) is a progressive kidney disease secondary to diabetes. Patients with either type 1 or type 2 diabetes are at risk of DN and the disease eventually effects approximately 50% of diabetics. Diabetic nephropathy is the leading cause of End Stage Renal Disease in the western world, and remains a major contributor to increased morbidity and mortality among individuals with diabetes [228,229]. CKD is typically diagnosed by the presence of a reduced creatinine-based estimated GFR, together with typical clinical correlates including increased levels of urinary albumin, and presence of other complications such as retinopathy, although these factors are not able to indicate the type of renal injury with certainty [230]. In addition, significant renal disease can occur with minimal or no change in creatinine [230] or albumin level [231]. Renal biopsy will provide detailed diagnostic and prognostic information in the patient with CKD, but is an invasive test, with significant risk of complications, and repeated kidney biopsy to monitor progression is not practicable or desirable in the majority of CKD patients.

Uncontrolled high blood sugar along with high blood pressure can induce kidney damage; however the exact molecular pathways leading to diabetic nephropathy are still not fully characterised. The molecular pathophysiology of diabetic nephropathy is multifactorial, involving hemodynamic factors (Vascular Endothelial Growth Factor, Renin-angiotensin-aldosterone and Endothelin systems), proinflammatory (e.g. Interleukin IL-1, 6, 18) and profibrotic cytokines (such as TGF-ß) [232]. Therefore a reliable non invasive biomarker reflecting disease severity is urgently needed in the clinical management of patients with CKD [233].

Having developed a protocol for miRNA extraction from urine (see Chapter 3), it was then possible to examine differences in miRNA expression patterns within groups, and between cases and controls.

Ideally, miRNA profiling will allow early detection of kidney injury and the prediction of disease progression in CKD as well as predisposing conditions such as diabetes and hypertension. miRNA profiles offer some potential advantages over mRNA or protein-based urinary profiles, and appear to be very stable in tissues and biological fluids, even under adverse conditions such as extreme pH,

long-term room temperature storage, multiple freeze-thaw cycles and RNase activity [166,234].

Results in Chapter 3 showed that urinary miRNAs, via association with exosomes or with AGO2 protein, are resistant to RNase digestion, underlining their potential as attractive, non-invasive biomarkers. Continuing progress in miRNA research presents opportunities not only for better understanding of the pathophysiological mechanisms in kidney disease, but also for the identification of new diagnostic biomarkers. Several studies on renal diseases of varying origins have shown differences in miRNA expression between diabetic, and it is therefore possible that a 'molecular signature profile' could be developed to provide insights into diagnosis and progression of renal disease [235-238].

This considerable potential of miRNAs as biomarkers for renal injury is exemplified by the discovery of statistically significant correlation between circulating miRNA levels and various clinic-pathological endpoints [235,239,240]. Urine is an ideal source of biomarkers for disease of the kidney and urinary tract, since it can be conveniently collected in large amounts without risk to the patient [129,160,241].

The goal of the work described in this chapter was to investigate differences in urinary miRNA expression between patients with diabetic nephropathy and healthy individuals, and thereby identify potential disease biomarkers.

4.2 Results

4.2.1 Diabetic Nephropathy patients and healthy controls

Twenty urine samples from diabetic nephropathy patients and twenty from unaffected people were obtained by Dr. Alexa Wonnacott at the University Hospital of Wales. The group included patients from CKD stage 3 and eGFR of 43.3 ml/min to patients with CKD stage 4/5 and eGFR of 12.9 ml/min. Urine samples from healthy individuals were collected and the urine protein value was assessed. Patients and controls data are summarised in Table 4.1.

	CKD Patients	Controls
Sex (Number of male)	17	10
Age (year) ± SEM	73.97 ± 2.10	47.70 ± 2.46
eGFR(min/ml) ± SEM	28.96 ± 1.90	/
Urine Protein (g/l) ± SEM	0.6 ± 0.17	0.07 ± 0.003
Protein Creatinine ratio (mg/mmol) ± SEM	115 ± 33.89	9.2 ± 1.293
Blood Glucose (mM) ± SEM	9.99 ± 1.16	/

Table 4.1 CKD Patients and control data.

Urine samples from CKD patients and controls used in miRNA profiling. eGFR-estimated glomerular filtration rate.

miRNAs were isolated using the technique developed as part of the work for this thesis and described in Methods (see 2.2.1). Expression of the ubiquitously higly-expressed miR-16 was then examined by TaqMan stem-loop RT-qPCR in those samples to confirm efficient miRNA extraction. The miRNA yield could not be analysed due to the use of carrier RNA in the extraction process. A constant volume of RNA extract was therefore added to each reaction, as opposed to a constant amount of RNA. The difference in quantity of miR-16 detected in patients and controls was not large and the signal was of good quality (Table 4.2). Those samples were therefore used to study for miRNA profiling using the TaqMan Array Human microRNA Cards A and B (see 4.2.2).

PATIENT ID	miR-16	Control ID	miR-16
P12-001	30.805451	**C11-001**	28.7321695
P12-002	32.36779	**C11-004**	30.291439
P12-003	30.5314245	**C11-005**	29.6346905
P12-004	24.506028	**C11-006**	28.6871605
P12-005	31.8052535	**C11-007**	30.83218
P12-006	33.0815065	**C11-008**	32.1867215
P12-007	29.196855	**C11-010**	31.8608955
P12-012	29.694537	**C11-011**	27.6741025
P12-013	30.8973805	**C11-012**	29.155841
P12-015	25.310432	**C11-013**	31.8025055
P12-016	31.8492775	**C11-014**	29.500789
P12-017	26.411887	**C11-015**	28.340759
P12-018	33.2512475	**C11-016**	29.8473185
P12-019	32.0732385	**C11-017**	31.506639
P12-020	29.6275905	**C11-018**	29.628817
P12-022	31.978774	**C11-019**	33.280744
P12-024	31.6938305	**C11-020**	31.5154165
P12-025	32.470422	**C11-021**	37.345173
P12-026	31.5945915	**C11-022**	28.6830085
P12-027	30.233753	**C11-023**	29.6868515
Patient Mean ± SEM	30.46 ± 0.55	**Control Mean ± SEM**	30.51 ± 0.48

Table 4.2 miR-16 detection in urine samples from diabetic nephropathy patients and control urine.

miR-16 detection in urine samples from patients and controls to evaluate the possible use of those samples in future experiments.

4.2.2 Urinary miRNA profiling

For initial screening of urinary miRNA expression, TaqMan Array Human microRNA Cards A and B were used, permitting simultaneous analysis of 754 small noncoding RNAs in eight RNA extracted pooled samples. Each of four pools contained RNA from five diabetic nephropathy patients, the other four pools contained RNA from corresponding control subjects (see 2.2.2.4). Pearson correlation coefficient (R^2) was calculated to determine the linear dependence between each miRNA Ct obtained in all patient and control groups analysed. The data in Figure 4.1 and 4.2 show evidence for positive correlation between two variables for each group, increasing together with a R^2 between 0.83 and 0.94 for the Card A in patients, and between 0.83 and 0.91 in controls (Figure 4.1A and 4.1B). For Card B, R^2 was between 0.92 and 0.96 in patients and between 0.86 and 0.93 in controls (Figure 4.2A and 4.2B). The p-values below 0.0001 obtained from all data sets showed the statistical significance of the correlations, rejecting the hypothesis that these similarities were due to random sampling. A positive Pearson correlation supported by statistically significant p-values was also found for comparisons between controls and patient groups with CKD stage 3 (R^2=0.85), or CKD stage 4 and 5 (R^2=0.8477) or the whole patient group (R^2=0.8571) for Card A (Figure 4.1C). Positive correlations were also observed for corresponding analyses for Card B miRNAs (controls versus CKD stage 3 R^2=0.91, controls versus CKD stage 4 and 5 R^2=0.9222 or the whole patient group R^2=0.9202) (Figure 4.2C). The Pearson correlation values for all samples is summarised in Table 4.3 for Card A and Table 4.4 for Card B.

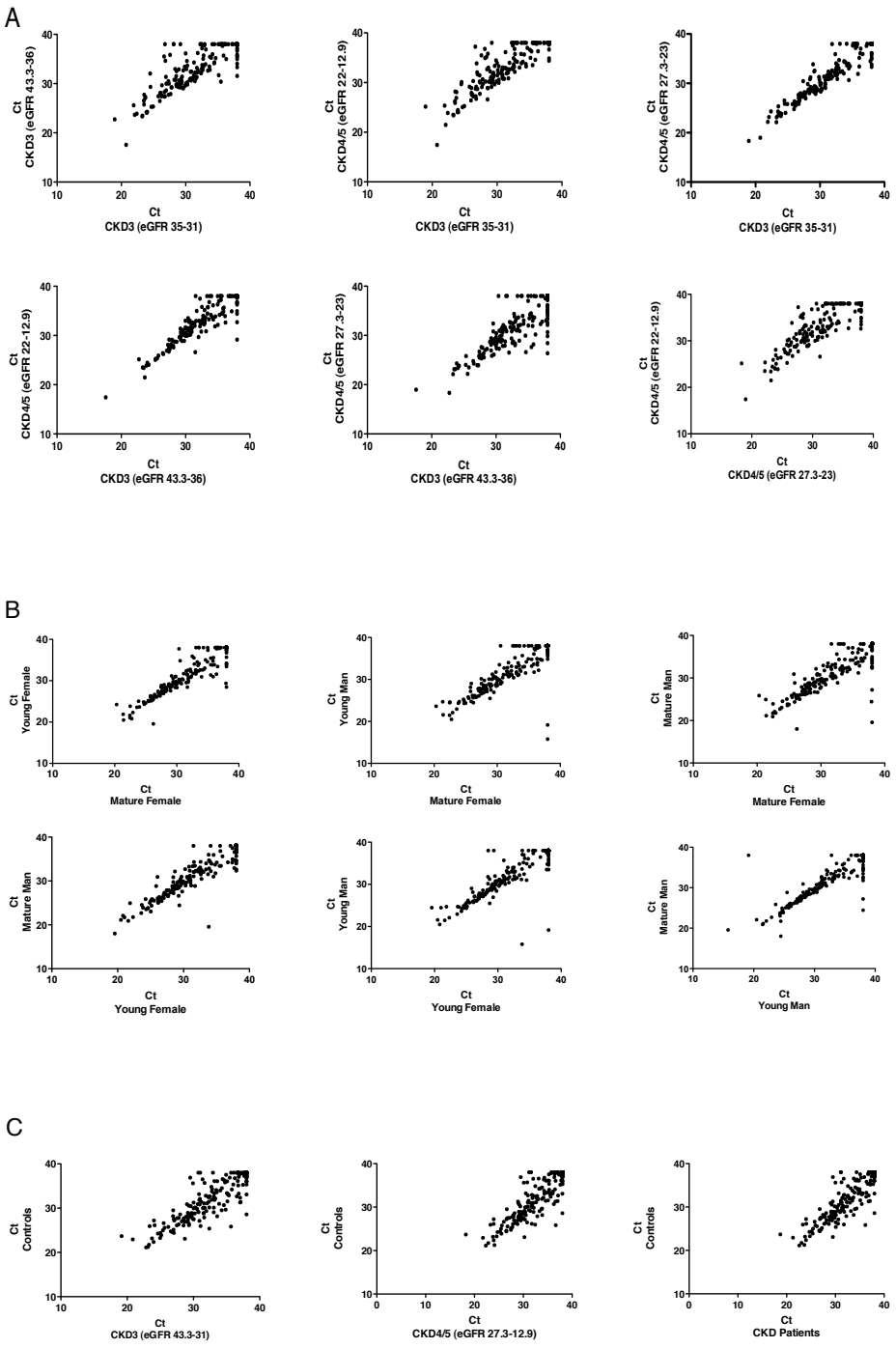

Figure 4.1. Histogram Plot relative to the Pearson correlation in Array A.

Pearson correlation was calculated using the Ct obtained in each pooled urine group used to run the TaqMan Array Human microRNA Cards A. Patients were divided in 4 groups on the basis of the CKD stage and eGFR **(A)**, controls on the basis of age and gender **(B)**. **(C)** Pearson correlation was calculated comparing controls and patients with stage 3 CKD, controls and patients with stage 4/5, and controls versus the whole CKD patients.

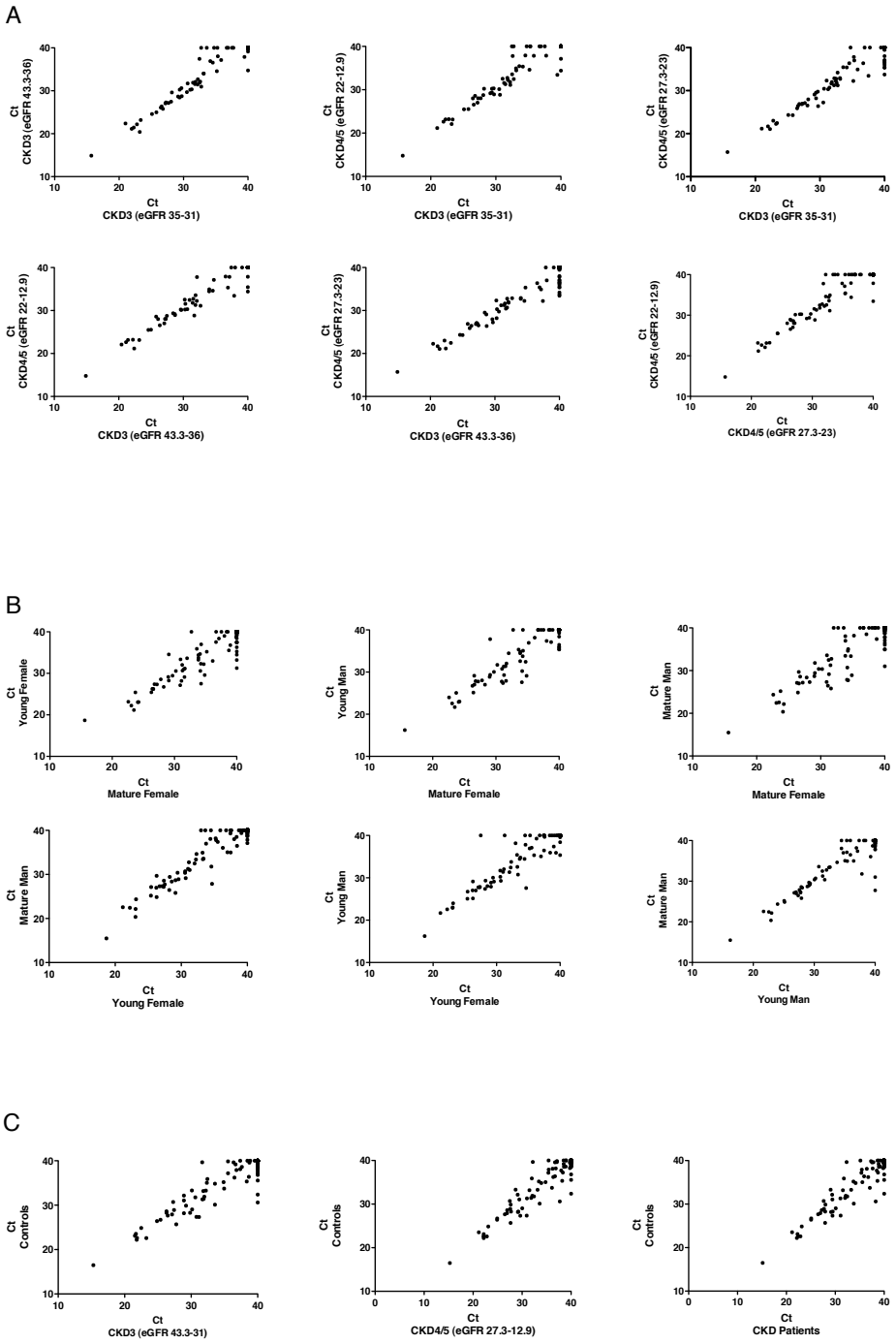

Figure 4.2. Histogram Plot relative to the Pearson correlation in Array B.

Pearson Correlation among Ct level was calculated using the Ct obtained in each pooled urine groups used to run the TaqMan Array Human microRNA Cards B. Patients were divided in 4 groups on the basis of the CKD stage and eGFR **(A)** while the controls on the basis of age and sex **(B)**. On **(C)** Pearson correlation was calculated comparing controls and patients with stage 3 CKD; controls and patients with stage 4/5 CKD and controls versus the whole CKD patients.

	CKD3 (eGFR 35-31)	**CKD3 (eGFR 43.3-36)**	**CKD 4,5 (eGFR27.3-23)**
CKD3 (eGFR 35-31)	R^2=0.8322 (p<0.0001)	R^2=0.9488 (p<0.0001)	R^2=0.8590 (p<0.0001)
CKD3 (eGFR 43.3-36)	/	R^2=0.9494 (p<0.0001)	R^2=0.9135 (p<0.0001)
CKD 4,5 (eGFR27.3-23)	/	/	R^2=0.8441 (p<0.0001)
	Young Female	**Young Male**	**Mature Male**
Mature Female	R^2=0.9180 (p<0.0001)	R^2=0.8389 (p<0.0001)	R^2=0.8470 (p<0.0001)
Young Female	/	R^2=0.8625 (p<0.0001)	R^2=0.9237 (p<0.0001)
Young Male	/	/	R^2=0.8805 (p<0.0001)
	CKD3 (eGFR 43.3-31)	**CKD4/5 (eGFR 27.3-12.9)**	**CKD Patients**
Controls	R^2=0.8531 (p<0.0001)	R^2=0.8477 (p<0.0001)	R^2=0.8571 (p<0.0001)

Table 4.3 Pearson Correlation value Array A

Pearson Correlation coefficients and p-values for patient and control groups for Card A analysis

	CKD3 (eGFR 35-31)	**CKD3 (eGFR 43.3-36)**	**CKD 4,5 (eGFR27.3-23)**
CKD3 (eGFR 35-31)	R^2=0.9494 (p<0.0001)	R^2=0.9542 (p<0.0001)	R^2=0.9338 (p<0.0001)
CKD3 (eGFR 43.3-36)	/	R^2=0.9463 (p<0.0001)	R^2=0.9675 (p<0.0001)
CKD 4,5 (eGFR27.3-23)	/	/	R^2=0.9280 (p<0.0001)
	Young Female	**Young Male**	**Mature Male**
Mature Female	R^2=0.9000 (p<0.0001)	R^2=0.9051 (p<0.0001)	R^2=0.8684 (p<0.0001)
Young Female	/	R^2=0.9020 (p<0.0001)	R^2=0.9305 (p<0.0001)
Young Male	/	/	R^2=0.9186 (p<0.0001)
	CKD3 (eGFR 43.3-31)	**CKD4/5 (eGFR 27.3-12.9)**	**CKD Patients**
Controls	R^2=0.9103 (p<0.0001)	R^2=0.9222 (p<0.0001)	R^2=0.9202 (p<0.0001)

Table 4.4 Pearson Correlation value Array B

Pearson Correlation coefficients and p-values of patients and control groups used to run Card B.

4.2.2 Identification of suitable endogenous control genes for miRNA gene expression analysis

The goal of this miRNA RT-qPCR expression profile analysis was to identify differences between controls and diabetic nephropathy patients. Data normalization is used to minimise detection of variation between groups and therefore assist identification of genuine disease-related differences. Accurate normalization is therefore a critical factor in quantitative gene expression analysis.

Criteria used to identify suitable miRNAs to normalize the array data were:

- The miRNA must be highly expressed in most, if not all, pooled samples
- The miRNA must be expressed consistently in all pools
- The miRNA must be detectable by commercially available RT-qPCR assay.

Preference was given to miRNAs identified independently as suitable reference miRNAs.

On the basis of these criteria, data from Card A and B, each representing 377 miRNAs, were inspected using the NormFinder algorithm to assess the variance in expression levels [242]. NormFinder analyses expression data, identifying transcripts that are expressed consistently across different test groups, and are therefore potential reference genes for normalization of that set of expression data. It calculates both intragroup variance, describing the stability of gene expression within each group, and intergroup variance, which describes the stability of the gene expression between the groups. Genes that have the least inter and intragroup variation and lowest slope value are considered the most stable. This toll was used in previous studies to identify the stability candidate miRNA and small RNA reference gene experiments. A slope value of 0.176 for

miR-23a was identified in a microarray study performed on uterine cervical tissues [243], 0.312 for let-7a in a gene expression analysis in human breast cancer [244] and 0.192 for miR-191 in a study conducted in normal and cancerous human solid tissues [245].

Table 4.5 shows the top 8 miRNAs identified by NormFinder as potential reference miRNAs, together with the 3 most used Card A housekeeping miRNAs, each with its corresponding slope value.

Figure 4.3 shows a plot of Ct values of the candidate miRNAs in the 8 RNA pools. NormFinder ranked miR-422a, miR-342-3p, miR-454 and miR-191 as the

most stably expressed miRNAs across the all groups; and miR-191 had the lowest Ct values. Two published studies have also suggested the use of miR-191 as optimal reference miRNA for normalization in profiling data from analysis of human uterine cervical cancer [243] and in normal and cancerous human solid tissues [245]. As a result of the above, microarray RT-qPCR data were normalised against miR-191 expression.

	NormFinder Slope value
has-miR-422a-4395408	0.013
has-miR-342-3p-4395371	0.013
has-miR-454-4395434	0.015
has-miR-191-4395410	0.016
has-miR-323-3p-4395338	0.017
has-miR-548a-3p-4380948	0.017
has-miR-628-5p-4395544	0.018
has-miR-106b-4373155	0.018
RNU48-4373383	0.035
MammU6-4395470	0.046
has-miR-16-4373121	0.053

Table 4.5. NormFinder slope value data for analysis of miRNAs in Array A

The top 8 miRNAs identified by NormFinder as suitable reference genes, and the 3 most common miRNAs currently used to normalize RT-qPCR data: miR-16, RNU48 and MammU6.

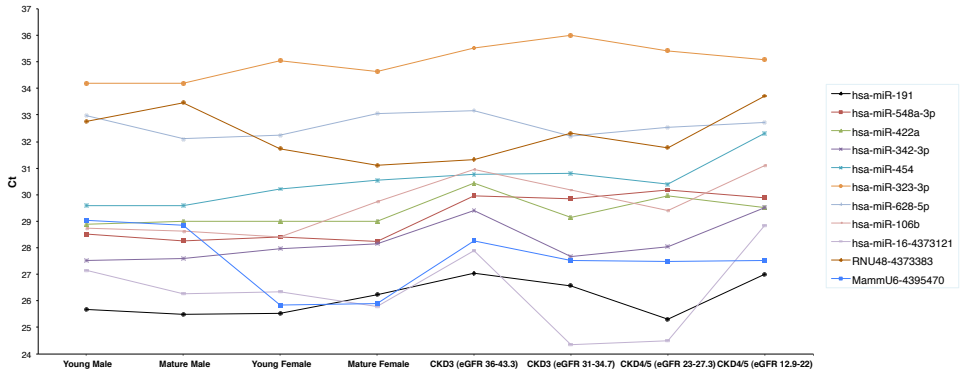

Figure 4.3. Representation of possible housekeeping gene for Array A

The top 8 miRNAs identified by NormFinder as suitable reference genes, and the 3 most common miRNAs currently used to normalise RT-qPCR data: has-miR-16, RNU48 and MannU6.

Table 4.6 shows data for Normfinder analysis of the TaqMan Array Human microRNA Cards B, featuring the top 9 miRNAs selected on the basis of slope value data and the two miRNAs suggested by the microarray manufactures as endogenous controls. Figure 4.4 shows the Ct values of Card B miRNA expression. Normfinder identified miR-1276 with the lowest slope value. miR-30a-5p had the lowest Ct value and a low slope value, however the expression of this miRNA was know to be increased in serum and urine in children with idiopathic nephrotic syndrome [165] and its use as reference gene has not been reported. By contrast, there was no evidence suggesting variation of miR-1276 expression in nephropathy, and this miRNA was therefore used to normalize RT-qPCR data for Card B.

	NormFinder Slope value
has-miR-1276-002843	0.014
has-miR-30a-5p-000417	0.018
has-miR-19b-1*-002425	0.019
has-miR-520c-3p-002400	0.019
has-miR-151-3p-002254	0.024
has-miR-1305-002867	0.027
has-miR-432-001026	0.028
has-miR-625*-002432	0.029
has-miR-572-001614	0.033
U6 snRNA-001973	0.044
RNU48-001006	0.084

Table 4.6. NormFinder slope value Array B

The top 9 miRNAs identified by NormFinder as suitable reference genes, and the 2 most common currently used at the moment to normalize the RT-qPCR data: U6 and RNU48.

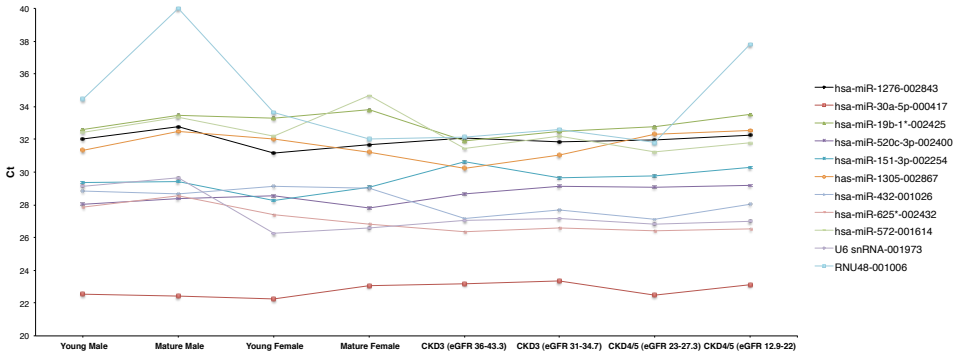

Figure 4.3 Candidate reference genes for Array B

The top 9 miRNAs identify by NormFinder as suitable reference genes, and the 2 most common small-nucleolar RNAs currently used: RNU48 and U6

4.2.3 Urinary miRNA expression from patients with diabetic nephropathy

miRNA expression data generated using the TaqMan Array Human microRNA Cards A and B were normalized to the corresponding endogenous controls using DataAssist software. Figures 4.4 and 4.5 are presented as volcano plots and show log_2-fold changes between DN patients and controls (y-axis) and –log10p-value (x-axis). This plot provides a means of rapid identification of miRNAs with the largest changes in expression between patients and controls that are statistically significant.

Candidate miRNAs were excluded if:

- They showed a large fold change but failed to reach statistical significance since this may be the result of one or more outliers with large fold-change values in one group. These miRNAs are seen below the blue line.
- Statistically significant test data resulted from a low fold change in expression. These data are shown as black points.

On Card A, a total of 47 miRNAs were significantly differentially expressed when comparing diabetic nephropathy patients to the controls, with 35 urinary miRNAs downregulated and 12 upregulated (Figure 4.4 B). On Card B, 12 miRNAs showed significantly different expression; expression of 10 of these 12 transcripts was upregulated in DN (Figure 4.5 B). The most highly characterised miRNAs were analysed on Card A, while Card B contained many more recently discovered miRNAs along with miRNA* sequences.

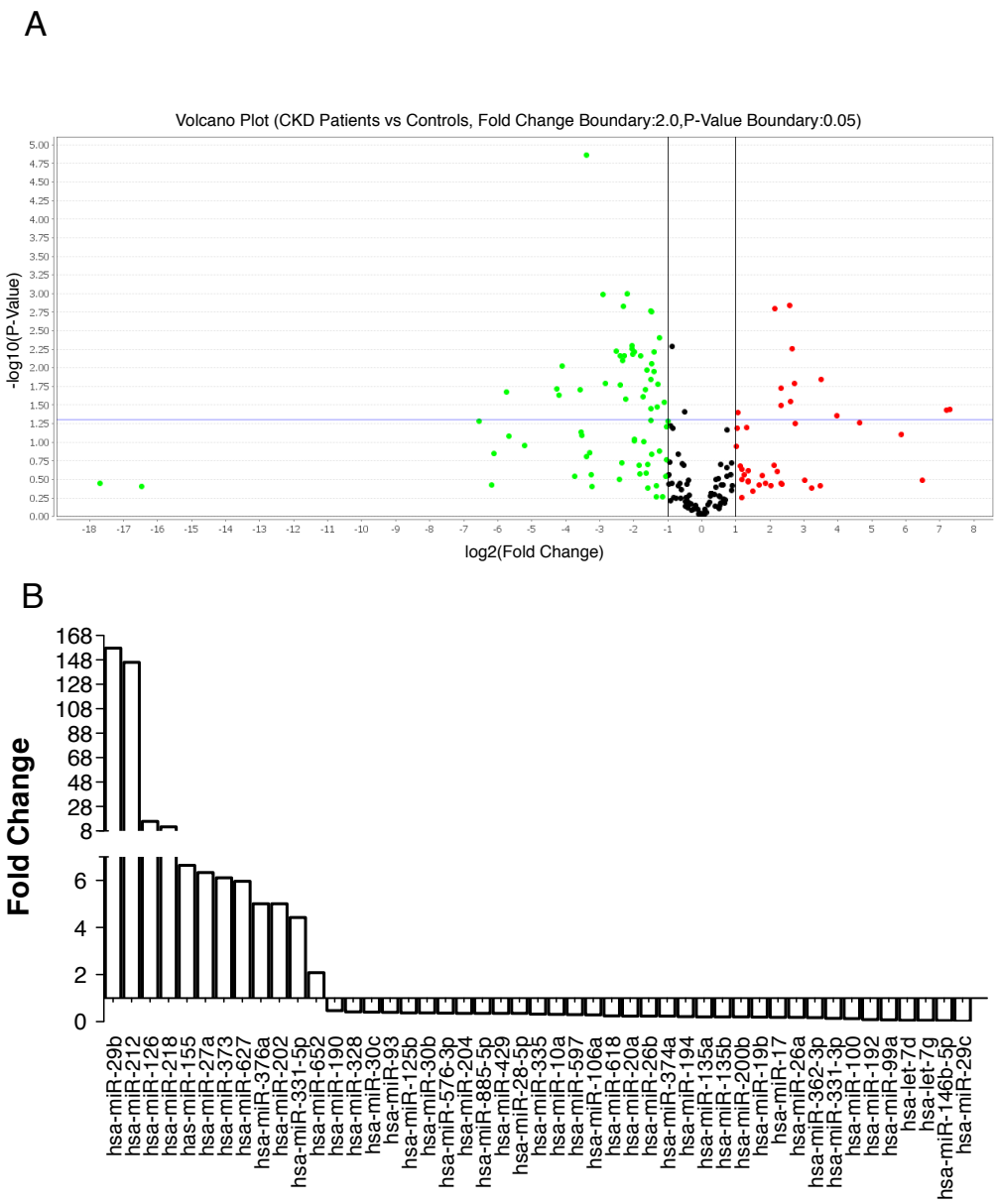

Figure 4.4. miRNA profiling of TaqMan Array Human microRNA Card A in diabetic nephropathy patients.

(**A**)Volcano Plot of fold-change and statistical significance for miRNA expression between compared urine of diabetic nephropathy patients (n=20) and urine of unaffected individuals (n=20). The y-axis is the negative log10 of p-values (a higher value means greater significance) and the x-axis is $\log_2$ of the difference in expression between the two experimental groups. The horizontal blue line represents a p-values boundary of 0.05. (**B**) Fold change of miRNAs with statistically significant differential expression between patients and controls.

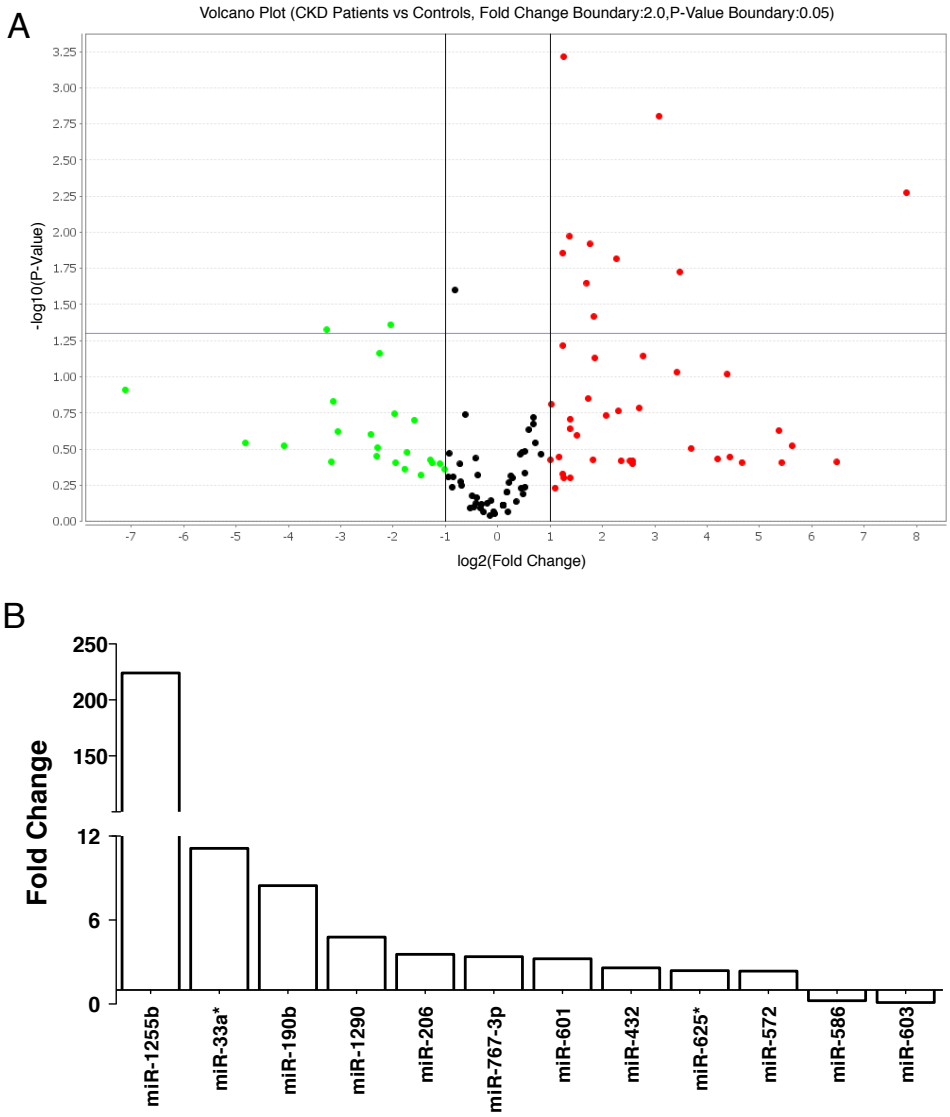

Figure 4.5. miRNA profiling TaqMan Array Human microRNA Card B in diabetic nephropathy patients.

(**A**)The Volcano Plot of fold-change and statistical significance of miRNA expression compared between urine of diabetic nephropathy patients (n=20) and urine of unaffected individuals (n=20). The y-axis is the negative log10 of *P* values (a higher value means greater significance) and the x-axis is $\log_2$ difference in expression between the two experimental groups. The horizontal blue line represents a p value boundary of 0.05. (**B**) Fold change of miRNAs with statistically significant differential expression between patients and controls.

4.2.4 Validation TaqMan Array Human microRNA Cards A by qPCR

For further analysis the first 5 miRNAs that showed the greatest statistically significant difference in expression between diabetic nephropathy patients and control urine samples (miR-29b, miR-212, miR-126, miR-218 and miR-155) and two miRNAs whose expression was down-regulated in patients (miR-200b and miR-192) were selected, the latter two have being previously studied in our laboratory as miRNA correlated with tubulointerstistial fibrosis [220]. To replicate the array data, these 7 miRNAs were quantified in all 40 individual urine samples with stem-loop RT-qPCR assay and using miR-191 as reference gene to normalize the RT-qPCR data.

Six out of these seven miRNAs showed significant differences between patients and controls, confirming the previous array data (Figure 4.6 – 4.11). In each case the findings from array data were replicated in individual assay with the exception of miR-218. Due to technical difficulties, this miRNA was not analysed further.

Determining a threshold value for a diagnostic laboratory test separating a diagnosis of affected from one of unaffected is not straightforward. Plotting a receiver-operator characteristic (ROC) curve helps to visualize and understand the relationship between sensitivity and specificity when discriminating between clinically normal and abnormal diagnostic test values. Sensitivity can be defined as the fraction of people with disease that the test identifies correctly (true positives), specificity as the fraction of people without the disease that the test identifies correctly (true negatives). The area under the ROC curve (AUC) quantifies the overall ability of the test to discriminate between affected and unaffected individuals. An undiscriminatory test has an area of 0.5, while a perfect test has an area of 1. ROC curves were plotted to assess the diagnostic potential of the six candidate miRNAs.

Figures 4.6 – 4.11 shows that the AUC was 0.77 or greater for each miRNA, suggesting that they had potential as diabetic nephropathy biomarkers. The p-values obtained confirmed the statistical significance of the discrimination between patients and controls.

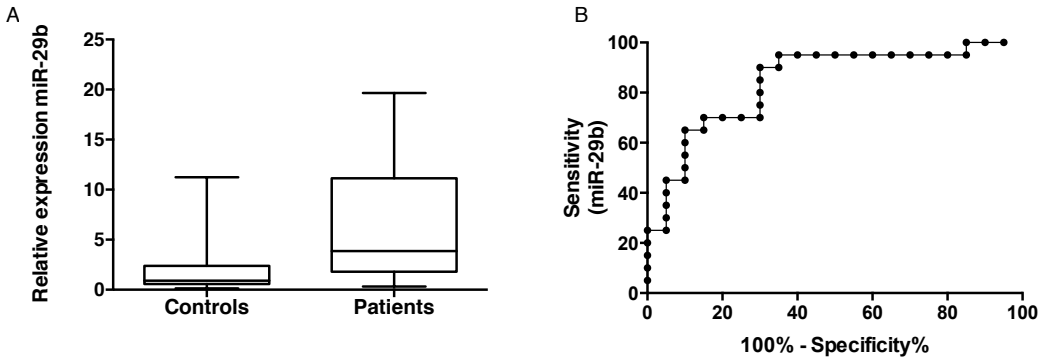

Figure 4.6. Confirmation of statistically significant miR-29b expression microarray data using stem-loop RT-qPCR and ROC curve analysis

miR-29b expression **(A)** was examined in individual urine samples that were pooled for use in miRNA profiling (20 controls and 20 DN patients) by stem-loop RT-qPCR, using miR-191 as endogenous control. Data are presented using a box-and-whiskers plot with minimum and maximum of all the values. RT-qPCR data for all miRNAs showed significant difference between diabetic nephropathy patients and controls (p-value =0.0024). Receiver operating characteristic curves analysis displays the diagnostic power to predict diabetic nephropathy of miRNAs miR-29b **(B)** with an AUC= 0.84 and a p-value =0.0002. AUC= Area under the curve. Unpaired t-test with Welch's correction.

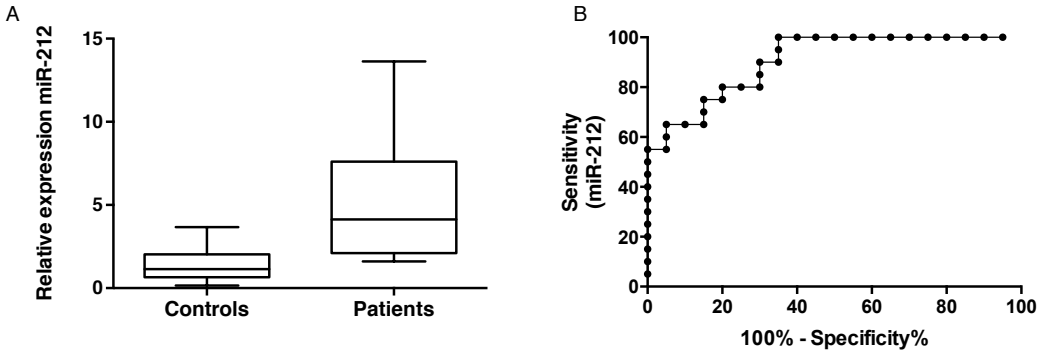

Figure 4.7. Confirmation of statistically significant miR-212 expression microarray data using stem-loop RT-qPCR and ROC curve analysis

miR-212 expression **(A)** was examined in individual urine samples that were pooled for use in miRNA profiling (20 controls and 20 DN patients) by stem-loop RT-qPCR, using miR-191 as endogenous control. Data are presented using a box-and-whiskers plot with minimum and maximum of all the values. RT-qPCR data for all miRNAs showed significant difference between diabetic nephropathy patients and controls (p-value *s*=0.0002). Receiver operating characteristic curves analysis displays the diagnostic power to predict diabetic nephropathy of miRNAs miR-212 **(B)** with an AUC= 0.90 and a p-value <0.0001. AUC= Area under the curve. Unpaired t-test with Welch's correction.

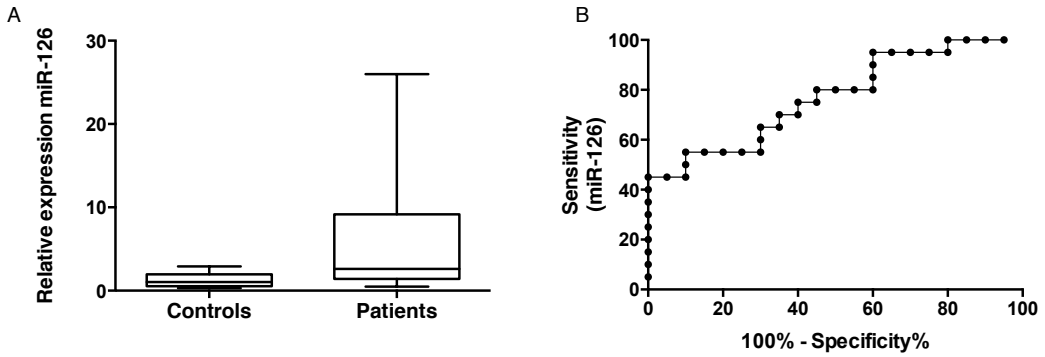

Figure 4.8. Confirmation of statistically significant miR-126 expression microarray data using stem-loop RT-qPCR and ROC curve analysis

miR-126 expression **(A)** was examined in individual urine samples that were pooled for use in miRNA profiling (20 controls and 20 DN patients) by stem-loop RT-qPCR, using miR-191 as endogenous control. Data are presented using a box-and-whiskers plot with minimum and maximum of all the values. RT-qPCR data for all miRNAs showed significant difference between diabetic nephropathy patients and controls p-value *s*=0.0087). Receiver operating characteristic curves analysis displays the diagnostic power to predict diabetic nephropathy of miRNAs miR-126 **(B)** with an AUC= 0.77 and a p-value =0.003. AUC= Area under the curve. Unpaired t-test with Welch's correction.

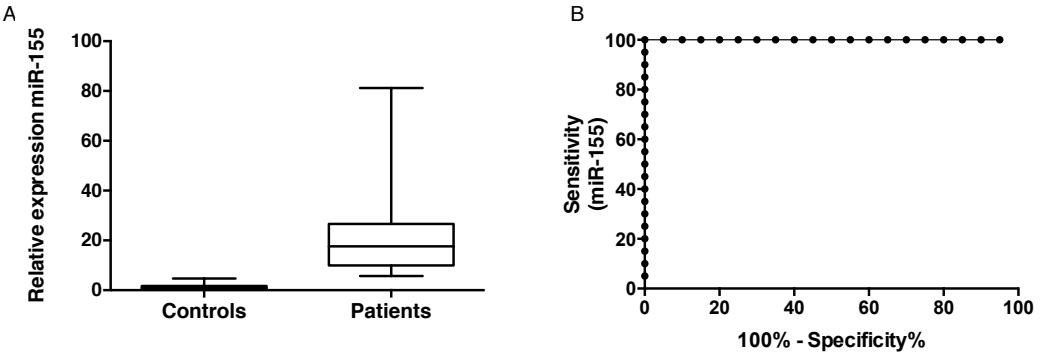

Figure 4.9. Confirmation of statistically significant miR-155 expression microarray data using stem-loop RT-qPCR and ROC curve analysis

miR-155 expression **(A)** was examined in individual urine samples that were pooled for use in miRNA profiling (20 controls and 20 DN patients) by stem-loop RT-qPCR, using miR-191 as endogenous control. Data are presented using a box-and-whiskers plot with minimum and maximum of all the values. RT-qPCR data for all miRNAs showed significant difference between diabetic nephropathy patients and controls (p-value =0.0002). Receiver operating characteristic curves analysis displays the diagnostic power to predict diabetic nephropathy of miRNAs miR-155 **(B)** with an AUC= 1 and a p-value <0.0001. AUC= Area under the curve. Unpaired t-test with Welch's correction.

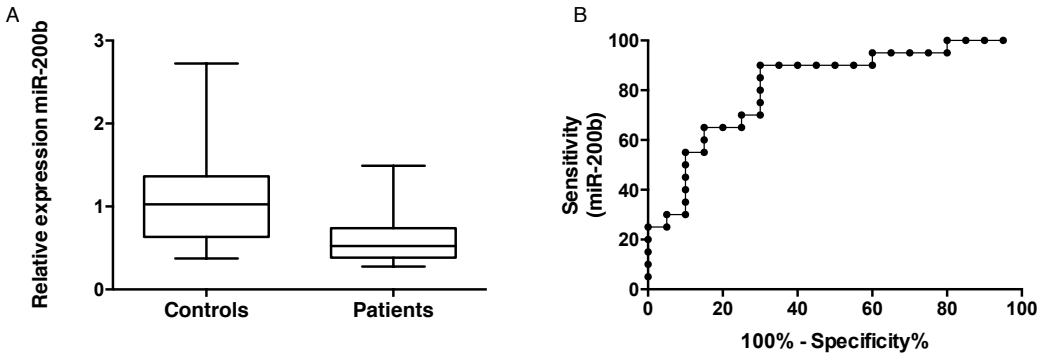

Figure 4.10. Confirmation of statistically significant miR-200b expression microarray data using stem-loop RT-qPCR and ROC curve analysis

miR-200b expression **(A)** was examined in individual urine samples that were pooled for use in miRNA profiling (20 controls and 20 DN patients) by stem-loop RT-qPCR, using miR-191 as endogenous control. Data are presented using a box-and-whiskers plot with minimum and maximum of all the values. RT-qPCR data for all miRNAs showed significant difference between diabetic nephropathy patients and controls (p-value =0.0012). Receiver operating characteristic curves analysis displays the diagnostic power to predict diabetic nephropathy of miRNAs miR-200b **(B)** with an AUC= 0.81 and a p-value =0.0006. AUC= Area under the curve. Unpaired t-test with Welch's correction.

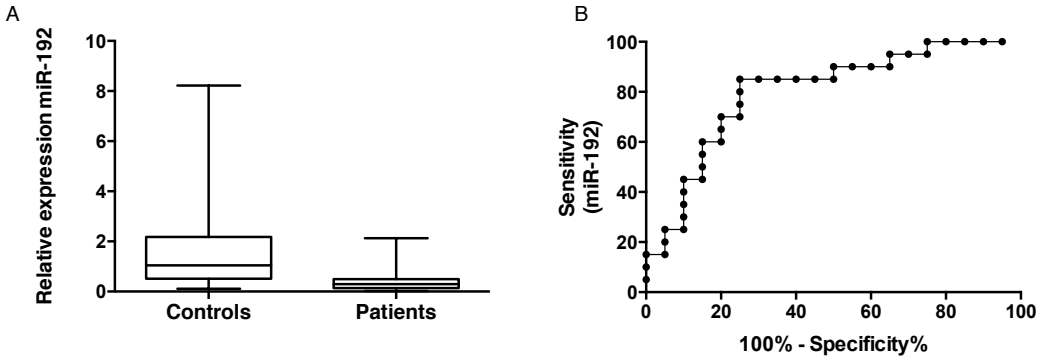

Figure 4.11. Confirmation of statistically significant miR-192 expression microarray data using stem-loop RT-qPCR and ROC curve analysis

miR-192 expression **(A)** was examined in individual urine samples that were pooled for use in miRNA profiling (20 controls and 20 DN patients) by stem-loop RT-qPCR, using miR-191 as endogenous control. Data are presented using a box-and-whiskers plot with minimum and maximum of all the values. RT-qPCR data for all miRNAs showed significant difference between diabetic nephropathy patients and controls (p-value =0.011). Receiver operating characteristic curves analysis displays the diagnostic power to predict diabetic nephropathy of miRNAs miR-192 **(B)** with an AUC= 0.8 and a p-value =0.001. AUC= Area under the curve. Unpaired t-test with Welch's correction.

Subsequently, the relationship between the expression of each miRNA and urine protein/creatine ratio (PCR) or eGFR was investigated. Correlations between PCR and miR-212, miR-126, miR-155 and miR-200b (Figure 4.12) were found to be significant. Moreover statistical correlations were observed between eGFR and the selected miRNAs (Figure 4.13).

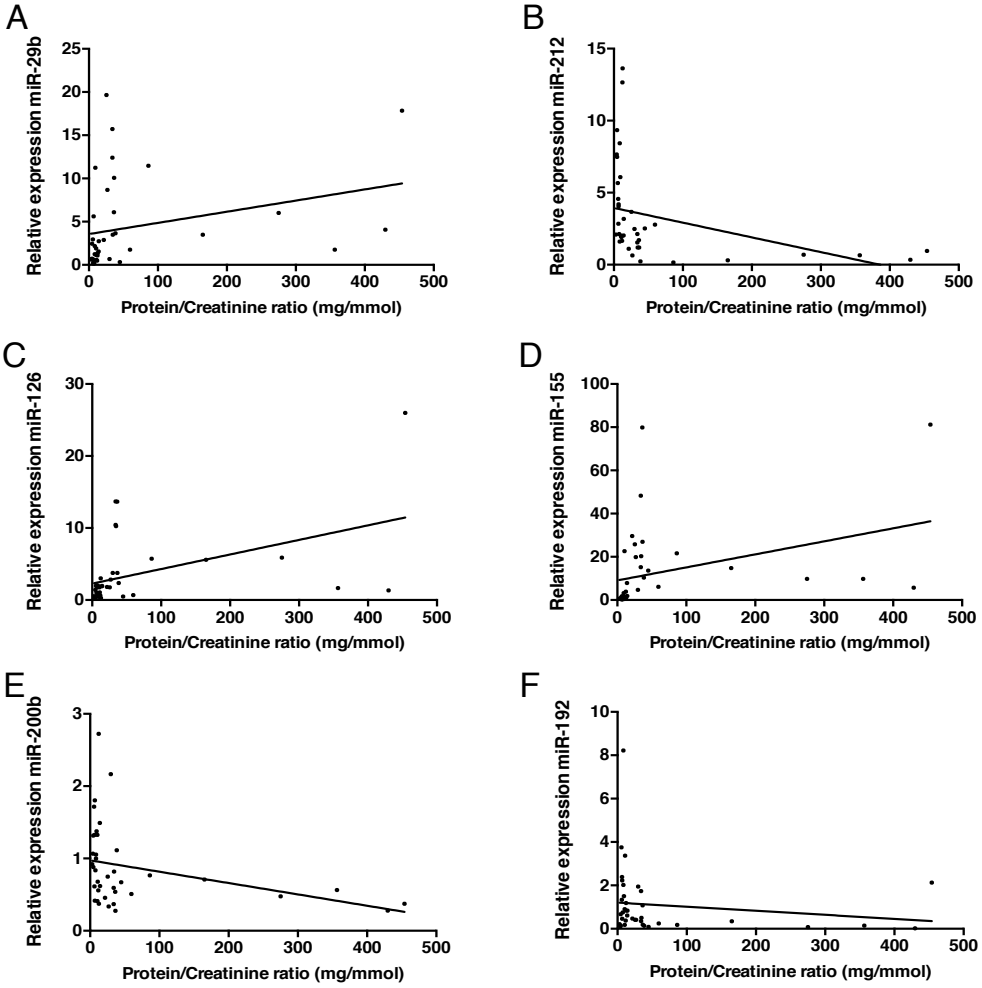

Figure 4.12. Correlation of miRNA expression with protein/creatinine ratio

Relationship between protein/creatinine ratio and miRNAs expression in diabetic nephropathy patients and controls. Significant correlations were found for **(B)** miR-212 (r^2=0.13; p-value 0.02), **(C)** miR-126 (r^2=0.2; p-value =0.003), **(D)** miR-155 (r^2=0.13; p-value 0.02) and **(E)** miR-200b (r^2=0.11; p-value =0.04).

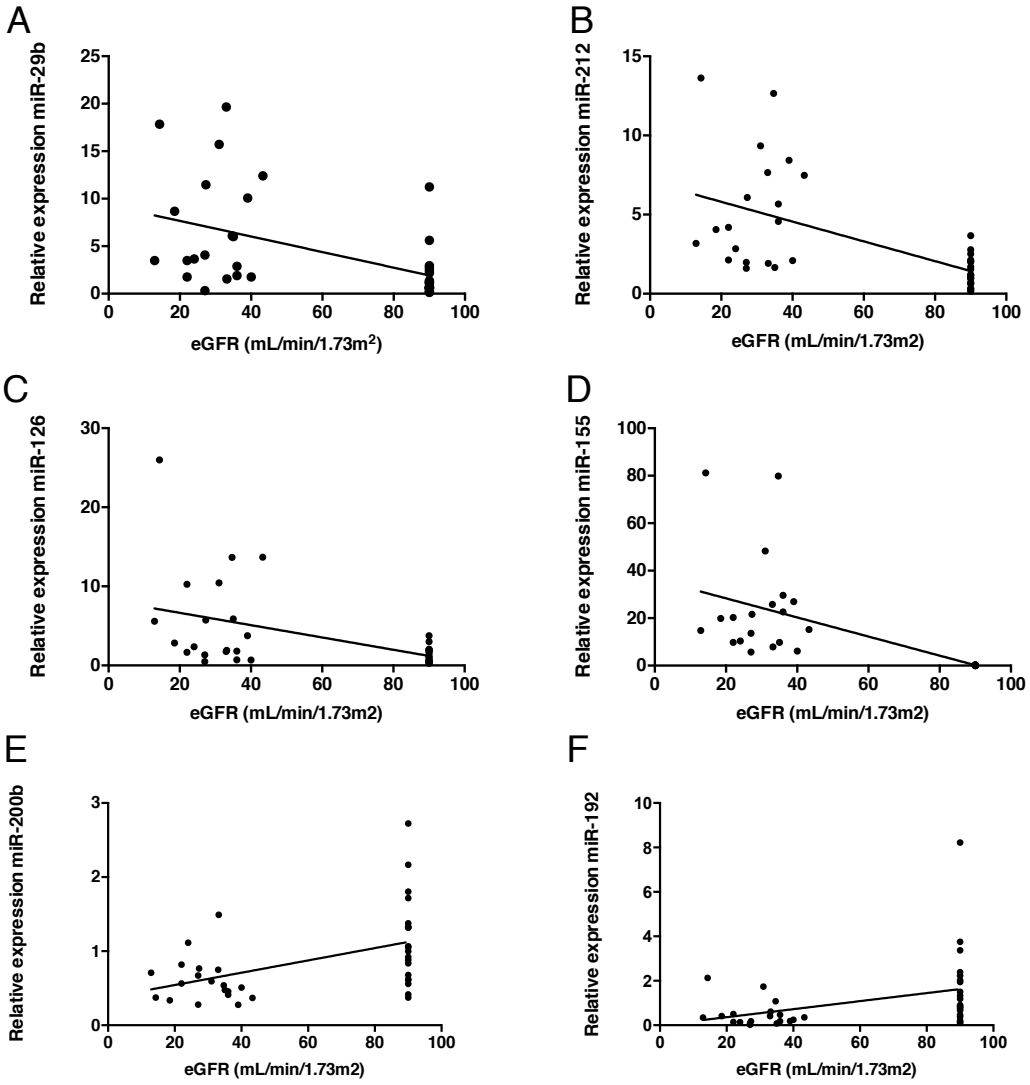

Figure 4.13. Correlation of miRNA expression with eGFR

Relationship between eGFR and miRNAs expression in diabetic nephropathy patients and controls. Significant correlations were found for **(A)** miR-29a (r^2=0.24; p-value =0.001), **(B)** miR-212 (r^2=0.34; p-value <0.0001), **(C)** miR-126 (r^2=0.23; p-value =0.02), **(D)** miR-155 (r^2=0.4; p-value <0.0001), **(E)** miR-200b (r^2=0.22; p-value =0.002) and **(F)** miR-192 (r^2=0.14; p-value =0.01).

4.3 Discussion

The experiments described in this chapter were designed to identify urinary miRNAs with the potential to act as non-invasive and robust biomarkers in diabetic nephropathy. Expression profiles of urinary miRNAs were compared between diabetic nephropathy patients and controls.

As discussed in Chapter 3, analysis of miRNA expression has some methodological advantages over mRNA expression analysis, particularly in the clinical setting. Obtaining high yields of intact, long mRNA transcripts from urine samples is difficult due to the high RNase concentrations that lead to RNA degradation. By contrast, short mature miRNAs are more stable against nuclease degradation as described in chapter 3.

Between the miRNAs statistically differentially expressed and detected using TaqMan Array Human microRNA Cards A, there is a trend showing a reduction of miRNA expression with 35 miRNAs down-regulated from a total of 47. Nevertheless, we identified a group of miRNAs that were differentially expressed in controls in comparison to patients. Some of these miRNAs (miR-29b, miR-212, miR-126 and miR-155) presented higher differences in fold change in the over-expressed and two miRNAs (miR-192 and miR-200b) down-regulated were selected for further investigation. Statistically different expression of these miRNAs was replicated by RT-qPCR using single assay.

Protein creatinine ratio was found to be associated with an increase level of miR-212, miR-126, miR-155 and decreased expression of miR-200b. In addition increase of miR-29b, miR-212, miR-126, miR-155 and reduction of miR-200b and miR-192 expression correlates with reduction in eGFR from patients with DN. However, the data show a weak correlation, with r^2 not exceeding 0.4, between miRNA expression and both P:Cr ratio and eGFR. Therefore, studies of larger patient groups are needed to clarify the association of these variables. ROC curve analysis supports the possibility of using those miRNA as new biomarkers for the diagnosis of DN.

Expression levels of miRNAs in body fluids may reflect tissue-specific injury or expression, making them strong candidates for use as disease biomarkers [167]. Profiling of urinary miRNA expression by TaqMan®Array Human MicroRNA Cards has detected specific organ and tissue miRNAs such as liver-specific miR-122 [246,247] in plasma samples [170,248,249]. However, miR-122 was not detected in our urine samples from controls or CKD patients. Similarly, miR-208, a heart-specific miRNA [250], has been detected in plasma but was not found in urine samples in our laboratory or elsewhere [227].

The absence of detectable levels of systemic miRNAs in the urine supports the idea of miRNA being unable to freely cross the intact glomerular filtration barrier. If the systemic and urinary miRNA populations exist in isolation, specific cell types throughout the nephron would form the source of urinary miRNAs, and their expression might therefore be associated with biological function.

An example is miR-126, that has been detected in plasma and serum of healthy individuals [170], and is known as an endothelial-specific miRNA [251]. Loss of miR-126 expression was found in plasma samples of DM patients [154]. In the present study, miR-126 was detected at low level in control urine samples and much higher level in the patients' urine. A similar profile of miRNA expression was demonstrated for miR-29b. A number of reports have implicated members of the miR-29a/b/c family in the pathogenesis of renal fibrosis. It was demonstrated that under high glucose condition, TGF-ß1 decreases the expression of miR-29a/b/c in tubular epithelium-like cells and podocytes, and that this was associated with increased expression of collagens I, III and IV [141,143]. Both of these miRNAs are particularly promising as possible biomarkers for the diagnosis of DN and will be the focus of Chapter 5.

miR-212 is mainly known, until now, for its regulation and functions in the neuronal context [252] even if lately some studies have recognized a role in hypertension [253] and cardiac hypertrophy and autophagy [254]. It has similar mature sequences to miR-132, with which it shares a seed region, and is therefore predicted to largely overlap in terms of targets [252]. Both of these miRNAs, targeting the AMP-response element binding (CREB), were found to have a key role in the development and function of neuronal cells [255-258]. In

addition, loss of miR-212 expression was linked to disorders related to the brain such as anencephaly, Huntington's disease and Alzheimer's disease [259-261]. Up or down-regulation of miR-212 was also found in relation to different cancer types but also to cancer treatments [262-264]. In addition, work conducted by Ucar showed that both miR-212 and miR-132 were necessary for mammary growth in mice and highly expressed in the stroma, where they were targeting matrix metalloproteinase 9 (MMP-9) regulating therefore the epithelial-stromal interaction [258]. A recent paper demonstrated that miR-212/miR-132 were highly expressed in a mouse model of cardiac stress and in an *in vitro* model of cardiac hypertrophy suggesting that these play a key role in cardiac hypertrophy and heart failure [254].

miR-155 is mainly known as an "inflammatory" miRNA since it was first found within the exon of the B cell integration cluster (BIC) [265] and several papers found that this non coding RNA was involved in innate and adaptive immunity, inflammation and tumorigenesis [266,267]. miR-155 is up-regulated in macrophages and other immune cells by inflammatory cytokines, such as IL-1-ß via TNF-α, NK-kB or other Toll-like receptors (TRL) [268,269]. In addition, it was found that activation of miR-155 by pro-inflammatory signalling can also intensify macrophage activation [268]. Work conducted by Chenhe and colleagues showed that miR-155 has an anti-HBV effect by targeting suppressor of cytokine signaling 1 (SOCS1) and increasing innate antiviral immunity by promoting JAK/STAT signalling pathway [270]. miR-155 has also a role in the regulation of the inflammatory response in endothelial cells via angiotensin-II [271] and an increase of miR-155 was observed in human umbilical vein endothelial cells (HUVECs) treated with TNF-α [272]. Reduction of miR-155 expression was found in plasma samples of patients with ESRD in comparison to healthy controls [273].

miR-200b, belongs to miR-200 family, is known to both have an high expression in kidney samples from patients with hypertensive glomerusclerosis and plays a role in DN and also in regulating the EMT by targeting ZEB1 and ZEB2, transcriptional repressors of E-cadherin [123]. miR-200b reduction was also detected in a renal fibrosis model of unilateral ureteral obstruction (UUO) [274] and confirmed in another study where proximal tubule cells where treated with TGF-β [275]. Opposite results were obtained by Kato in a study conducted in

glomeruli from type 1 and type 2 diabetic mice as well as in mouse mesangial cells (MMC) treated with TGF-β [147]. The same authors found also an increase of type IV collagen mRNA in MMC by miR-200b and TGF-β [147]. An additional role of miR-200b is the induction of hypertrophy and fibrosis in diabetic kidney via phosphatidylinositol-3-kinase (PI3K) activation by targeting Fog2, PI3K inhibitor [276].

miR-192 was shown to be detectable in serum samples [170], and this study and also previous publications from our laboratory showed that this miRNA is down-regulated in diabetic nephropathy [220]. More specifically, these data have shown that miR-192 is down-regulated by key fibrotic mediator TGF-β1 in renal proximal tubular epithelial cell [277] and exhibits pleiotropy in the kidney [278]. The pleiotropic role of miR-192 in renal homoeostasis and in the fibrotic kidney has been studied extensively [278]. Urinary levels of miR-192 were found to be down regulated in patients with IgG nephropathy [215]. Krupa et al. previously demonstrated a down-regulation of miR-192 in renal biopsies from advanced diabetic nephropathy patients and a correlation between low miR-192 expression and tubulointerstitial fibrosis and reduced estimated glomerular filtration rate [220]. Incubation of human renal PTCs with TGF-β1 *in vitro* decreased miR-192 expression [20]. Enforced ZEB1 and ZEB2 (zinc finger E-box-binding homeobox proteins 1 and 2) are down regulated by miR-192 expression in PTCs and thus opposed TGF-β1-mediated suppression of E-cadherin expression, an early key step in TGF-β1-mediated renal fibrogenesis [220].

Down-regulation of miR-192 by TGF-β1 in PTCs and in kidneys from diabetic apoE (apolipoprotein E)-deficient mice and rat PTCs has also been reported by Wang et al., and linked to TGF-β1-mediated repression of E-cadherin [137]. However, the opposite was found by Kato et al. in mouse mesangial cells. This group showed that TGF-β1 increases miR-192 expression, and that repression of ZEB1 and ZEB2 expression by miR-192 facilitates collagen synthesis, enhancing matrix deposition and glomerulosclerosis [134].

Changes in urinary miRNAs levels may be reflective of pathologies in the kidney or urinary tract. Hanke et al. explored the possible use of urinary miRNAs

as a novel and robust technique to analyse small RNAs to detect urothelial bladder cancer [32]. They found that the RNA ratio of miR126:miR152 was a sensitive method of detecting this tumour [213]. Similarly, Snowdon et al. have found a decrease of miR-125 and an increase of miR-126 in urine samples from patients with low- and high-grade urothelial cancer [279]. The use of miRNAs as novel sensitive biomarkers was investigated in other pathologies such as myocardial injury [280], prostatic cancer [281], systemic lupus erythematosus [282] or hepatocellular carcinoma [283].

Many studies have reported that miRNAs play an important role in regulating glucose and lipid metabolism in diabetes, and their level in blood or urine reflects the disease process and predicts clinical course [284]. Argyropoulos et al. found that micro-albuminuria is associated with decreased levels of miR-323b-5p and increased urine concentration of miR-429 in patients with long standing type 1 diabetes [164]. Interestingly, in another study, it was shown that miR-429 correlates with the level of proteinuria and renal function in renal disease such as IgA nephropathy [215,285]. Analysing serum and urinary miRNAs from nephrotic syndrome children, Luo et al. found that miR-30a-5p, miR-151-3p, miR-150, miR-191 and miR-19b were highly increased in the serum of patients compared with controls while in urine only miR-30a-5p was increased [19]. The concentration of these serum and urinary miRNAs decreased with the clinical improvement of the patients and they concluded that these miRNAs could represent potential diagnostic and prognostic biomarkers for idiopathic paediatric nephrotic syndrome [165].

Hitherto, published studies have only sporadically focused their attention on the use of urinary miRNA detection for the diagnosis of CKD, and in each case detected miRNAs that had already been reported as being involved in renal fibrosis and CKD progression. For example, Szeto et al. studied patients who underwent kidney biopsy, excluding those with acute renal failure or active glomerulonephritis; and studied the urine pellet obtained after centrifugation at 13,000 g [42]. These authors found that urinary miR-21 and miR-216a expression correlated with the rate of decline in renal function and risk of progression to dialysis-dependent renal failure and, more generally, the miRNA analysed had

different expression in the different diagnosis group analysed (IgA nephropathy, diabetic nephrosclerosis and hypertensive nephrosclerosis) [140].

microRNA expression in mesangial cells exposed to high glucose rather than TGF-ß was investigated by Wang et al. [43]. miR-377 expression was upregulated in human mesangial cells under those conditions, as well as in mouse diabetic nephropathy models *in vivo*. This miRNA was associated with increased expression of matrix proteins such as fibronectin and led to reduced expression of p21-activated kinase and superoxide dismutase, which enhanced fibronectin protein production [286]. Another study on mesangial cells showed that TGF-ß activates Akt by inducing the miR-216 and miR-217, both of which target phosphatase and tensin homolog (PTEN), an inhibitor of Akt activation [287].

To investigate renal expression profiles of microRNAs and their potential involvement in early diabetic nephropathy, Chen and colleagues induced a diabetic model in Dilute Brown Non-Agouti (DBA/2) mice [45]. Nine miRNAs (miR-1187, miR-320, miR-214, miR-34a, miR-762, miR-466f, miR-720, miR-744 and miR-1937b) were increased significantly. While other 9 miRNAs (miR-1907, miR-195, miR-568, miR-26b, miR-703, miR-1196, miR-194, miR-805 and miR-192) were decreased markedly in these diabetic mice [45]. These workers also found that miRNA-195 expression was negatively related to glomeruli diameter, mesangial score and extracellular matrix (ECM) accumulation, plus its inhibition protected mesangial cells from apoptosis and promoted the cellular proliferation *in vitro*. [288].

Wang et at. found that miR-10a and miR-30d, as well as other miRNAs in miR-1 and miR-30 families, were relatively enriched in kidney tissue in comparison to other mouse organs analysed such as, heart, spleen, kidney, colon and lung [49]. Importantly, using both ischemia reperfusion-induced acute kidney injury and Streptozotocin (STZ)-induced kidney damage, animal models were able to show that changes in the levels of urinary miR-10a and miR- 30d occurred as a result of renal damage [49]. Furthermore, the substantial elevation of the urinary miR-10a and miR-30d levels was also observed in focal segmental glomerulosclerosis (FSGS) patients compared to healthy donors [163]. Strong up-regulation of miR-

21 in kidneys of mice with unilateral ureteral obstruction, and also in the kidneys of patients with severe kidney fibrosis, was established by Glowacki and colleagues [129].

The above suggests that miRNAs play an important role in the pathogenesis of diabetic nephropathy and in the initiation of renal glomerular mesangial cell dysfunction, and therefore miRNA can modulate the pathogenesis of diabetic nephropathy by affecting various different pathways. Most of the work described above was conducted in different cell lines and animal models, focusing the attention on miRNAs previously associated with disease. The approach taken in this study for the identification of a cohort of miRNAs that are up-regulated or down-regulated in the diabetic nephropathy takes into consideration the analysis of this noncoding RNA family in the urine of DN patients in comparison with those expressed in urine from healthy people.

Preliminary analyses on control and patient urine samples confirmed that the miRNA could be readily detected by RT-qPCR. The final miRNA profiling experiment using RT-qPCR-based array, in addition to demonstrating that global miRNA expression can be analysed in urine samples, revealed multiple differences in miRNA expression in the CKD stage and eGFR levels.

The results presented in this chapter identified miRNA for further study, and suggest that miRNA quantification might provide useful prognostic information for patients with diabetic nephropathy. The major finding was that expression of miR-29b, miR-212, miR-126 and miR-155 was upregulated, and expression of miR-200b and miR-192 was down-regulated in urinary DN samples.

This work arrives at a different conclusion in comparison to all the work previously mentioned with exception of miR-192 down-regulation, as also reported by Krupa [220]. The data also imply that these changes in miRNA expression found in the experiment are very likely to be meaningful and will be fruitful for further investigations. Sadly, limitations in time and materials permitted only a detailed characterization of some miRNAs potentially important in this disease and unfortunately, it was not possible to validate any of the miRNAs identified in the array B.

In addition the relatively small sample size and the advanced CKD stage of the patients (Stage 3, 4 and 5) meant that the prognostic value of the data was limited. Larger validation analyses, including DN patients with CKD Stage 1 and 2 will be required to evaluate the utility of urinary miRNAs in this context. Moreover, it will be useful to investigate the miRNAs expression in patients suffering from diabetes (T1DM, T2DM) and also other types of renal disease (IgA nephropathy, polycystic kidney disease, glomerusclerosis, acute kidney disease) to investigate the specificity of those miRNAs as biomarkers for DN.

Investigation of the origin and function of these miRNAs will be the focus of Chapter 5.

Chapter 5 – Source and possible cause of miRNAs secretion in urine

5.1 Introduction

Defining miRNA expression pattern by specific cell-type will help to clarify their function and involvement in the regulation or maintenance of physiological characteristics of various tissues. Thanks to Landgraf et al. it is possible to know cellular expression pattern for 51 miRNAs. Surprisingly only a few of them were expressed in individual cell types [289]. Comparing those data with the results obtained in Chapter 4 made it possible to have a general idea of miRNAs tissue localization. For example, an increase of miR-126 was identified in the cardiovascular system, miR-192 in the respiratory system and liver, and miR-155 in the hematopoietic system, connective tissue and kidney. A limitation of this work is its reliance on cell lines rather then tissue. Unfortunately, results obtained from the mentioned work and also after a detailed literature search, were not able to clarify the tissue/cell line source for miR-29b, miR-212, miR-126, miR-155, miR-200b and miR-212 in the kidney. The first goal of this chapter was therefore to identify in which nephron tissue region and more precisely from which kidney cell type, those miRNAs were highly expressed.

Because the pathogenesis of diabetic nephropathy (DN) is a multifactorial event that involves hyperglycaemia, hyperlipidaemia and hypertension [290], mechanisms responsible for the development and progression of this disease are not yet fully known. Inflammatory cytokines like TNF-α, INFγ, IL-6 may have a critical role in development of this disease [88]. Also haemodynamic and metabolic factors [291] such as vasoactive hormone pathways including the renin angiotensin system [292] or fibrotic cytokines such as TGF-ß or various growth factors including VEGF could be involved with diabetes nephropathy's evolution.

The second goal of this chapter was to incubate cells with different stimuli implicated in initiation of DN, and then analyse the expression of selected miRNAs in cell lines from various nephron segments and miRNA content in conditioned media.

5.2 Results

5.2.1 miRNAs expression in different nephron sub-compartments by LCM

LCM (laser capture microdissection) is a method for isolating target cells from multicellular tissue samples [293]. Using this technology, the cells of interest are visualised by microscopy while a thermoplastic transfer film is attached to a plastic cap lying on top of the cells. Laser energy is then transferred to the film, a polymer-cell complex is formed, and the cells of interest are removed from the sample section. The cells isolated by LCM maintain their morphology and their DNA, RNA and proteins remain intact.

LCM was used to identify the sources of 4 target miRNAs found to be highly expressed in urine samples from diabetic nephropathy patients plus 2 miRNAs with significantly down-regulated expression in patients when compared to unaffected individuals.

CD10 antigen is expressed at the surface of glomerular and proximal tubular cells, but not distal tubular cells (Figure 5.1.). Duplicate 6 µm sections were used to isolate glomeruli, proximal tubular and distal tubular cells from five renal biopsies by LCM. Cells of interest were identified on the basis of morphological characteristics. The staining process can result in tissue cross-linking between nucleic acid and protein that could interfere with RNA analysis. Therefore, two consecutive biopsy sections were cut from each sample, one of which was stained with anti-CD10 antibody while the other one was used to isolate the above-mentioned sub compartment's nephron. Subsequent RNA isolation was carried out using a dedicated extraction kit as describe in 2.2.1.2.

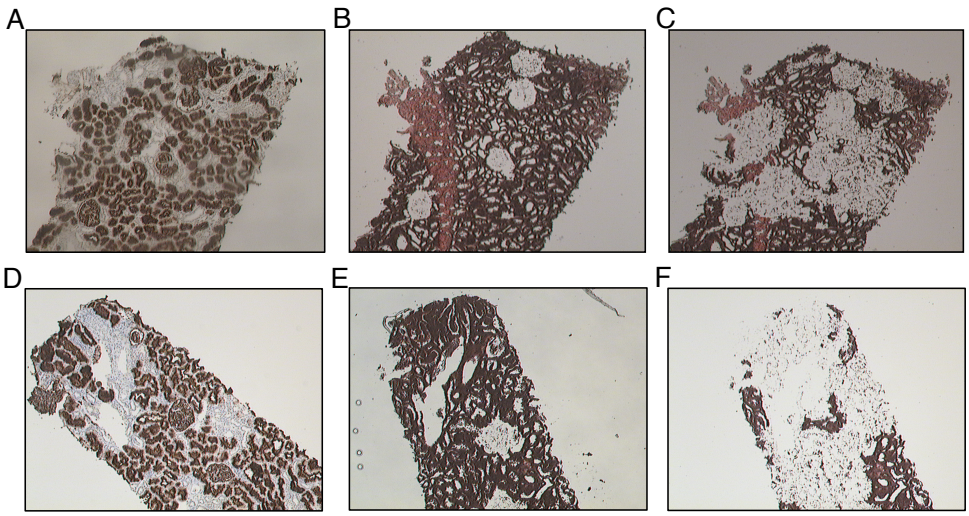

Figure 5.1. Isolation of nephron sub-compartments using LCM

Images captured using the Arcturus Pixcell IIe system on two renal biopsy tissues. **A** and **D:** The 6µm renal sections were stained with antigen anti-CD10 to easily identify the glomeruli and proximal tubular cells. For downstream analyses, glomeruli, proximal and distal tubules were isolated from a contiguous, unstained section using the sections outlined by staining as a guide. The remains of renal biopsy tissue following **B** and **E:** glomerular extraction, **C:** proximal tubular extraction and **F:** proximal and distal tubular cells.

Expression of putative disease-associated miRNAs (see Chapter 4) was then analysed in glomerular, proximal and distal tubular RNA extracts. As seen in Figure 5.2, expression of miRNAs -29b, -212 and -126 was greatest in the glomerulus, with 30-fold greater glomerular expression of miR-126. Expression of miRNA-155 was approximately equally expressed in each nephron sub-compartment, miR-200b was significantly greater in the distal tubule section and miR-192 expression was highest in the proximal tubule (Figure 5.2).

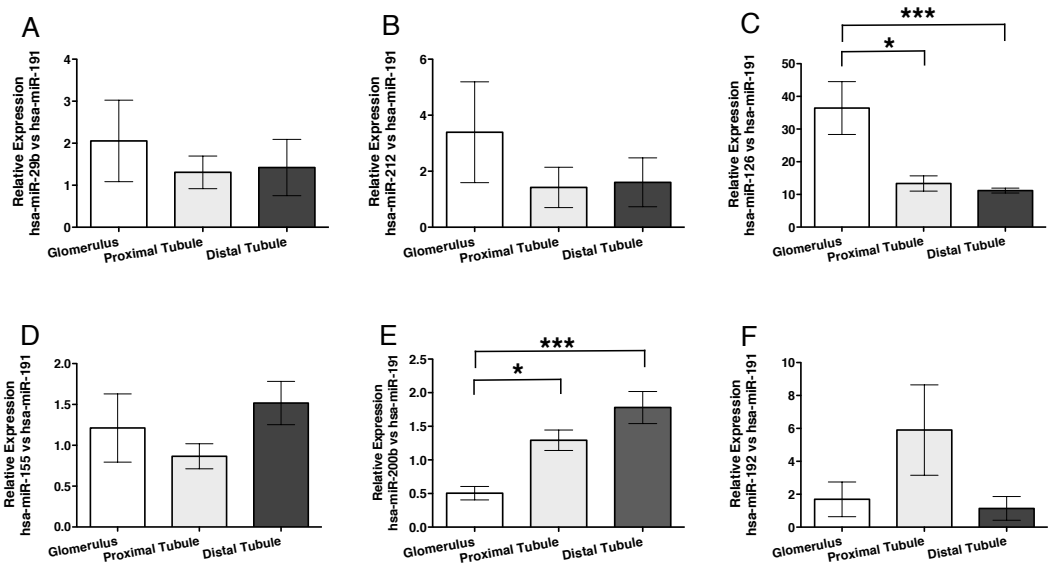

Figure 5.2. miRNA expression in nephron sub-compartments

A-**C:** Greater levels of miR-29b, -212 and -126 expressions were detected in glomerular extracts, for miR-126 this reached statistical significance ($p = 0.0056$). **D:** miR-155 was equally expressed in all nephron regions. **E:** miR-200b expression was statistically higher in distal tubular samples ($p = 0.0008$). **F:** miR-192 was expressed principally in the proximal tubule. Glomerular, proximal tubular and distal tubular subcompartments were isolated from 5 renal biopsies of healthy individuals and miRNA expression analysed by RT-qPCR. One-way ANOVA analysis was carried out with Tukey's multiple comparison. * $p \leq 0.05$, *** $p \leq 0.001$.

5.2.2 miRNA cell line expression

The architecture of the nephron is complex and the nephron is composed of a variety of cell types with specific functions. The Bowman's capsule contains parietal epithelial cells, podocytes that cover the outer aspect of the glomerular filtration barrier, fenestrated endothelial cells that are in direct contact with blood, and mesangial cells that sit between the capillary loops. The renal tubule is made up of the proximal convoluted tubule (proximal tubular cells), loop of Henle (simple squamous epithelial cells) and distal convoluted tubule (distal tubular cells). In addition the renal interstitium is composed of renal support cells, and fibroblasts are the most abundant [294].

Glomerular, proximal tubular and distal tubular nephron subcompartments were isolated by LCM, but isolation of 3-dimensional structures from sections cannot be absolutely precise. Therefore cell-specific miRNA expression was investigated in renal cell lines HK-2 (immortalized proximal tubule epithelial cell line from normal adult human kidney), conditionally immortalized podocytes and glomerular endothelial cells (CiGEnCs), and fibroblasts.

Unfortunately, I did not have the possibility to analyse miRNAs expression in other cell type such as mesangial cells, parietal epithelial cells or distal tubule cells.

As shown in Figure 5.3, cell line miRNA expression data supported the observations from LCM-isolated nephron regions (Figure 5.2). miR-29b and miR-126 was significantly increased in CiGEnC, while miR-212 expression in fibroblasts increased significantly in comparison with other cells. The magnitude of miR-155 expression was similar in each cell line. miR-200b was most highly expressed in HK-2 cells and podocytes, while miR-192 was expressed primarily in HK-2 PTCs (Figure 5.3).

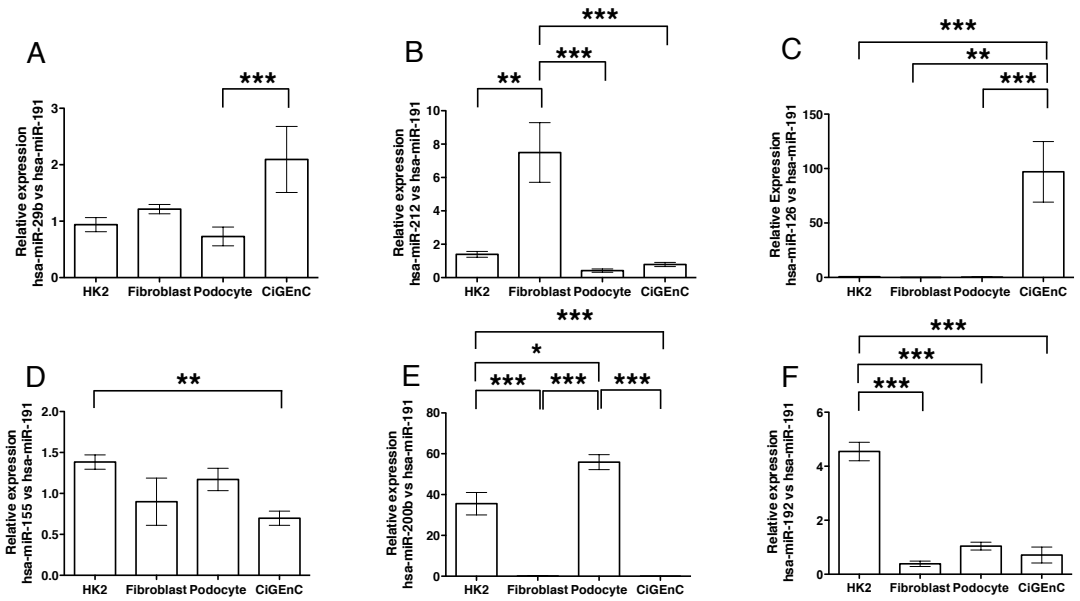

Figure 5.3. miRNA cell line expression

Expression of 6 putative disease-associated miRNAs was analysed by RT-qPCR in HK-2, fibroblast, podocyte and CiGEnC cells. **(A)** Elevated miR-29b expression in CiGEnC in comparison to podocytes ($p = 0.03$). (**B**) Abundance of miR-212 was found in fibroblast cell line (p-value < 0.001). (**C**) Statistical increase of miR-126 expression was detected in CiGEnC in comparison to the other cell lines (p-value= 0.0002). (**D**) Similar expression of miR-155 across the different cell lines. (**E**) Increase of miR-200b in HK-2 and podocyte cell lines (p-value < 0.001). (**F**) miR-192 was mainly expressed in HK-2 cells (p-value < 0.001). One-way ANOVA with Tukey's multiple comparison test. Stars are representative of the Tukey's multiple comparison test value; $* \ p \leq 0.05$, $** \ p \leq 0.01$, $*** \ p \leq 0.001$.

5.2.3 Glucose-dependent expression of miR-29b and miR-126

The data generated to this point describe a cohort of miRNAs that are differentially expressed in urine samples from diabetic nephropathy patients and show varied nephron sub-compartment localization. miR-126 and miR-29b were both highly expressed in urine samples from diabetic nephropathy patients, microdissected glomeruli and CiGEnC. Further analyses were then carried out to analyse if these expression changes were dependent on glucose concentration.

miR-29b and miR-126 expression was analysed in CiGEnC treated with 5.5 mM glucose (homeostatic glucose), 20 mM L-glucose (osmotic control) or 20 mM D-glucose concentration (hyperglycaemic glucose). No statistically significant difference was observed (Figure 5.4).

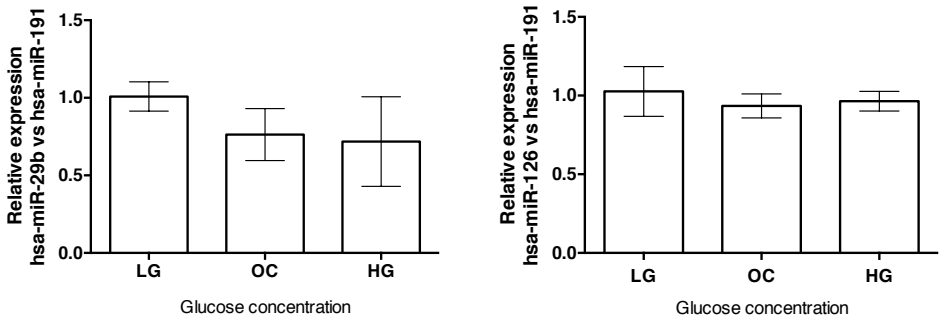

Figure 5.4. CiGEnC treated with different glucose concentrations

CiGEnC were treated with 5 mM glucose (LG), 20 mM L-glucose (OC) or 20 mM D-glucose (HG) for 4 h, following by RT-qPCR to detect miR-29b and miR-126. Average values from three samples ± SEM are shown. No statistically difference was observed.

The effects of glucose on miR-29b and miR-126 expression was also investigated in the kidney of non-obese diabetic (NOD) mice that have a susceptibility to develop type 1 diabetes following spontaneous autoimmune destruction of β cells. After the beginning of the hyperglycemia, the survival of these animals is dependent on insulin treatment. A summary of the detail of the 6 diabetic and 6 non-diabetic NOD mice analysed are shown in Table 5.1.

	Diabetic NOD	Non-diabetic NOD	p-value
Sex (Number of female)	5	4	
Age (weeks) ± SEM	16.47 ± 2.83	13.12 ± 2.41	
Blood Glucose (mmol/l) ± SEM	30.07 ± 9.87	5.6 ± 0.57	0.03

Table 5.1 Data for NOD mice analysed

As shown in figure 5.5, no significant differences in expression of either miR-29b or miR-126 were observed between diabetic and non-diabetic mice.

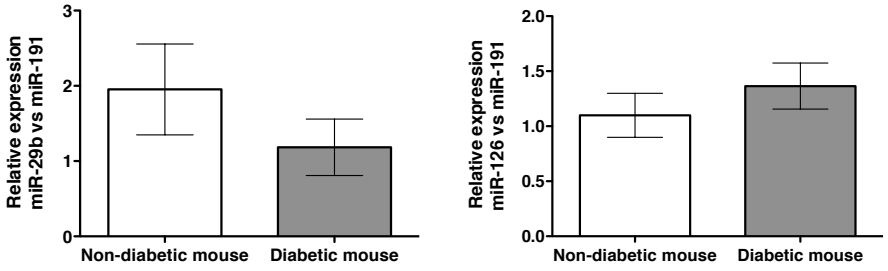

Figure 5.5. Expression of miR-29b and miR-126 in diabetic and non-diabetic NOD mice.

6 RNA samples from diabetic NOD mice and 6 from non-diabetic NOD mice were used to evaluate miR-29b and miR-126 expression by RT-qPCR. No statistical difference was observed.

To further study the possible mechanisms underlying the increase in specific microRNAs that I had detected in urine from DN patients, I examined miRNA expression in a cohort of patients with polycystic ovarian syndrome. These samples were obtained as part of a collaboration with Dr Aled Rees, Consultant Endocrinologist, and are part of an on-going study of endocrine and metabolic parameters in patients with polycystic ovarian syndrome in whom insulin resistance has been confirmed by laboratory studies of glucose and insulin metabolism (Dr Aled Rees, personal communication). Baseline characteristics of these patients are summarised in Table 5.2.

	PCOS	Control
Number	17	15
Age (year) ± SEM	30.76 ± 1.48	29.33 ± 1.60
BMI ± SEM	29.77 ± 1.53	28.35 ± 1.71
Waist ± SEM	91.29 ± 3.6	85.47 ± 3.7
WHR ± SEM	0.81 ± 0.01	0.82± 0.03
Hip ± SEM	111.3 ± 3.97	103.7 ± 3.08
Glucose ± SEM	4.7 ± 0.10	4.68 ± 0.22

Table 5.2 Control subject and patient data

Mean and SEM values for selected variables in PCOS patients and unaffected control subjects.

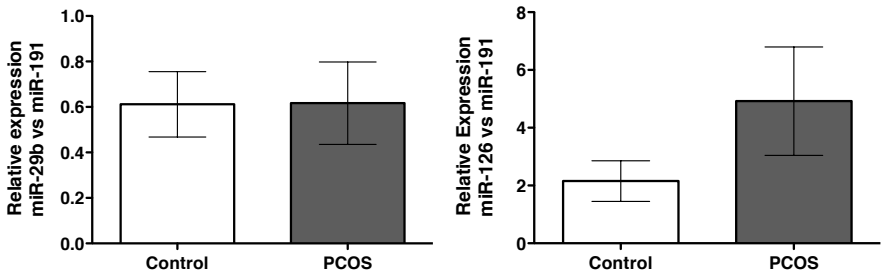

Figure 5.6. miR-29b and miR-126 expression PCOS patients and controls

Expression of miR-29b and miR-126 was analysed by RT-qPCR in urine samples from 17 PCOS patients. No statistically significant differences were observed.

No statistical significant difference was observed in miRNA expression between patients and controls (Figure 5.6).

These data suggest that the increase in miR-29b and miR-126 detected in the urine of diabetic nephropathy patients with decreased eGFR is not related to systemic insulin resistance. Having also demonstrated that in the kidney, these microRNAs are expressed almost exclusively in the glomerular endothelial cell, I next evaluated their synthesis and release by glomerular endothelial cells subjected to injurious stimuli known to be relevant to the glomerular insult that occurs in diabetic nephropathy.

5.2.4 CiGEnC characterization

The conditionally immortalised CiGEnC cell line used in this study was initially characterised by detection of endothelial cell-specific markers [196]. To ensure these characteristics had been maintained through long-term storage, CiGEnCs were analysed following culture at the non-permissive temperature of 37°C for 5 days for selected endothelium-specific and matrix-related genes. RT-qPCR was used to quantify expression of platelet endothelial cell adhesion molecule-1 (PECAM1), vascular endothelial growth factor receptor-2 (VEGFR2), Von Willebrand factor (vWF) and plasminogen activator inhibitor (PAI-1). As shown in Figure 5.7, CiGEnC expressed these specific endothelium markers, while HK-2 and podocytes did not.

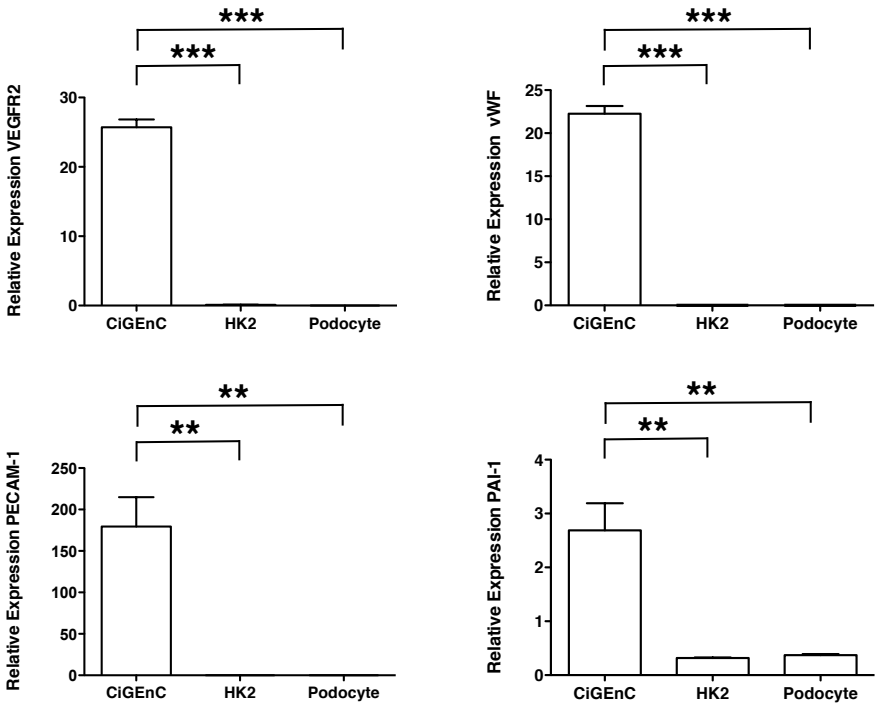

Figure 5.7 Expression of endothelium-specific and matrix-related genes in podocytes, CiGEnC and HK-2 cells.

Expression of endothelial specific markers VEGFR2, vWF, and PECAM-1and matrix related gene (PAI-1) were analysed by RT-qPCR using SYBR green chemistry. Upregulated expression of each gene was seen in CiGEnC compared to HK-2 cells or podocytes. One-way ANOVA with Tukey's multiple comparison test was used. VEGFR2 p-value < 0.0001, vWF p-value < 0.0001, PECAM-1 p-value = 0.0012 and PAI-1 p-value = 0.0018. Asterisks are representative of the Tukey's multiple comparison test value; ** p ≤ 0.01, *** p ≤ 0.001. Expression data were normalised to expression of the reference gene glyceraldehyde-3-phosphate dehydrogenase (GAPDH).

5.2.5 CiGEnC treatment with different cytokines stimuli

While persistent elevation of systemic glucose concentration underlies the pathophysiology of DN, the exact molecular and/or cellular mechanisms have not yet been characterised. Cytokines have also been strongly implicated in the development of diabetes, playing a significant role in the progression of neuropathy, retinopathy and nephropathy [88,295,296]. Pro-inflammatory cytokines implicated in the pathogenesis of diabetic nephropathy include interleukin-1 (IL-1), interleukin-6 (IL-6), and tumour necrosis factor-alpha (TNF-α). Others disease-related cytokines include the fibrotic mediator transforming growth factor (TGF-ß), and the potent inducer of vasopermeability and angiogenesis, vascular endothelial growth factor (VEGF).

To investigate these stimuli, CiGEnC were maintained at a non-permissive temperature of 37°C for 5 days, growth-arrested for then cultured in 5mM or 25mM of glucose in the presence or absence of VEGF (20ng/ml), TNF-α (10ng/ml), TGF-ß1 (1ng/ml) or IL-6 (1ng/ml) for 24h. Total RNA was isolated from cells and conditioned culture medium, then expression of miR-29b, miR-126 and miR-191 (used as reference gene) was detected by RT-qPCR.

Figure 5.8 shows that statistically significant down-regulation of miR-29b expression was observed following incubation with 25 mM glucose plus VEGF, TNF-α and TGF-ß1, but no change was seen in the presence of IL-6. Similarly, miR-126 expression decreased in all cases except following IL-6 addition.

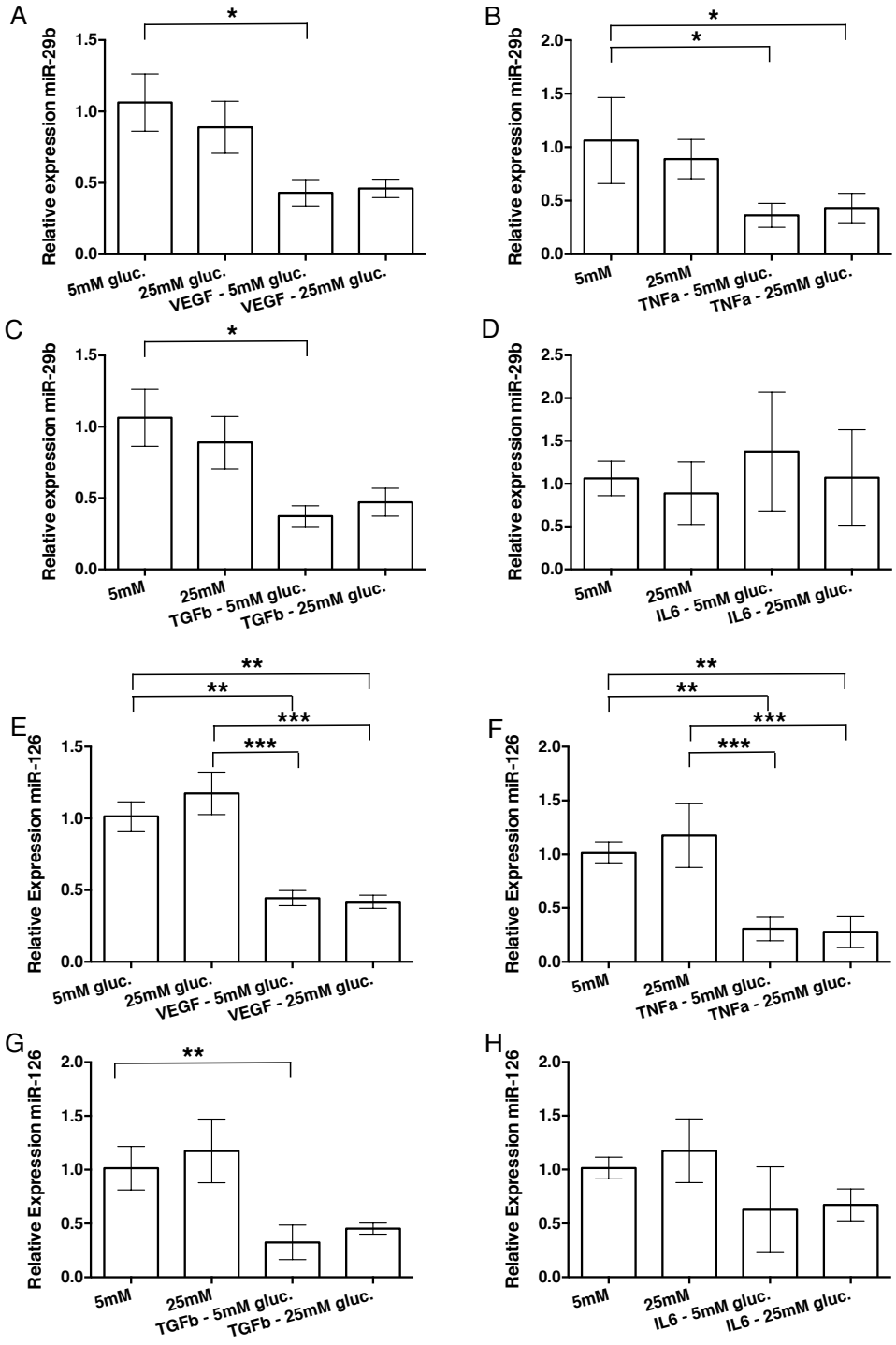

Figure 5.8. Relative expressions of miR-29b and miR-126 in CiGEnC cultured in high glucose +/- selected cytokines.

Confluent CiGEnC were cultured for 24 h in control medium with 5 mM glucose, or in 25 mM glucose, together with: VEGF (**A** and **E**), TNF-α (**B** and **F**), TGF-ß1 (**C** and **G**) and IL-6 (**D** and **H**). Downregulated expression of both miR-29b (**A**-**D**) and miR-126 (**E**-**H**) was shown by RT-qPCR analysis with all cytokines except IL-6. miR-191 was used as reference gene. One-way ANOVA analysis with Tukey's multiple comparison test was used, miR-29b: VEGF, $p = 0.02$; TNF-α, p-value $p < 0.0001$, TGF-ß1, $p = 0.018$; miR-

126: VEGF p = 0.0002, TNF-α p = 0.01 and TGF-ß1 p = 0.01. ∗ p ≤ 0.05, ∗∗ p ≤ 0.01, ∗∗∗ p ≤ 0.001. Error bars represent SEM, n=4.

Figure 5.9 shows a significant increase in miR-29b expression in the conditioned medium of TGF-ß1 -treated CiGEnC at both glucose concentrations. Statistically significant up-regulation of miR-126 was also seen in 5 mM glucose medium in cells cultured with 10 ng/ml TNF-α. By contrast, miR-126 expression was significantly downregulated in the presence of IL-6 and 25 mM glucose.

The above data allowed direct comparison between miR-29b and miR-126 expression in cytokine-treated cells cultured in homeostatic and elevated glucose and the conditioned CiGEnC medium from these experiments. Expression of miR-29b following TGF-ß1 treatment, and miR-126 in the presence of TNF-α, was significantly decreased in CiGEnC and significantly increased in conditioned culture medium (Figures 5.8C and 5.9C and Figures 5.8F and 5.9F). Significant down-regulation of miR-126 expression was observed in conditioned medium in the presence of IL-6 (Figure 5.9H).

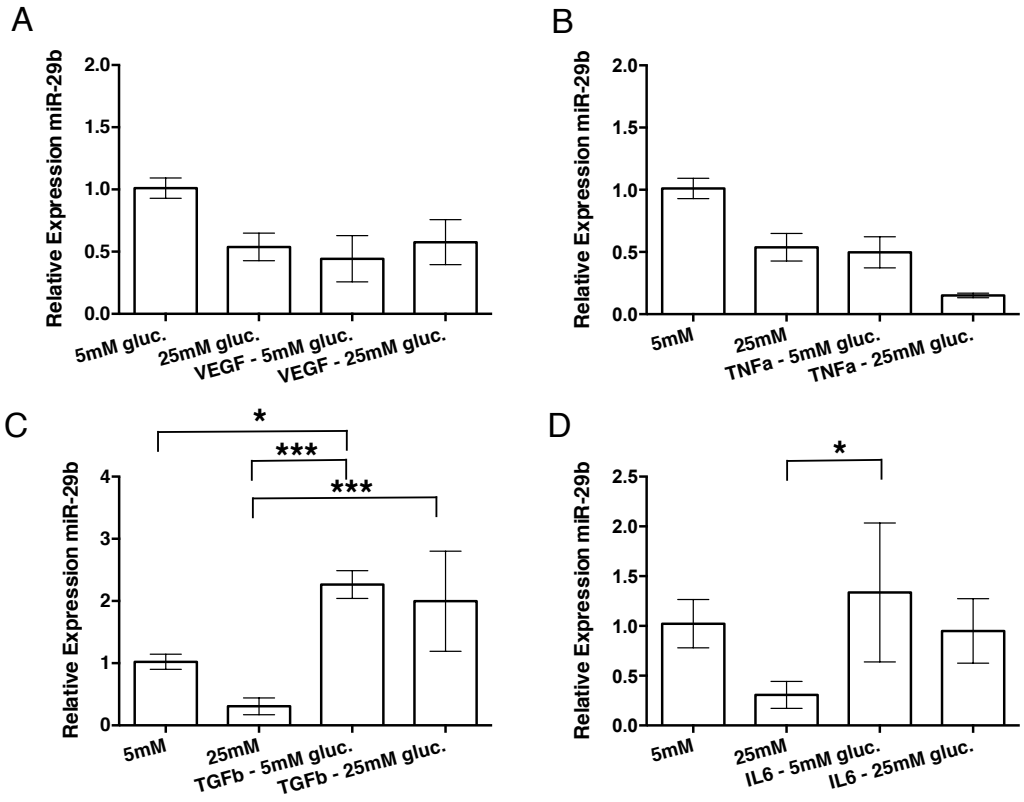

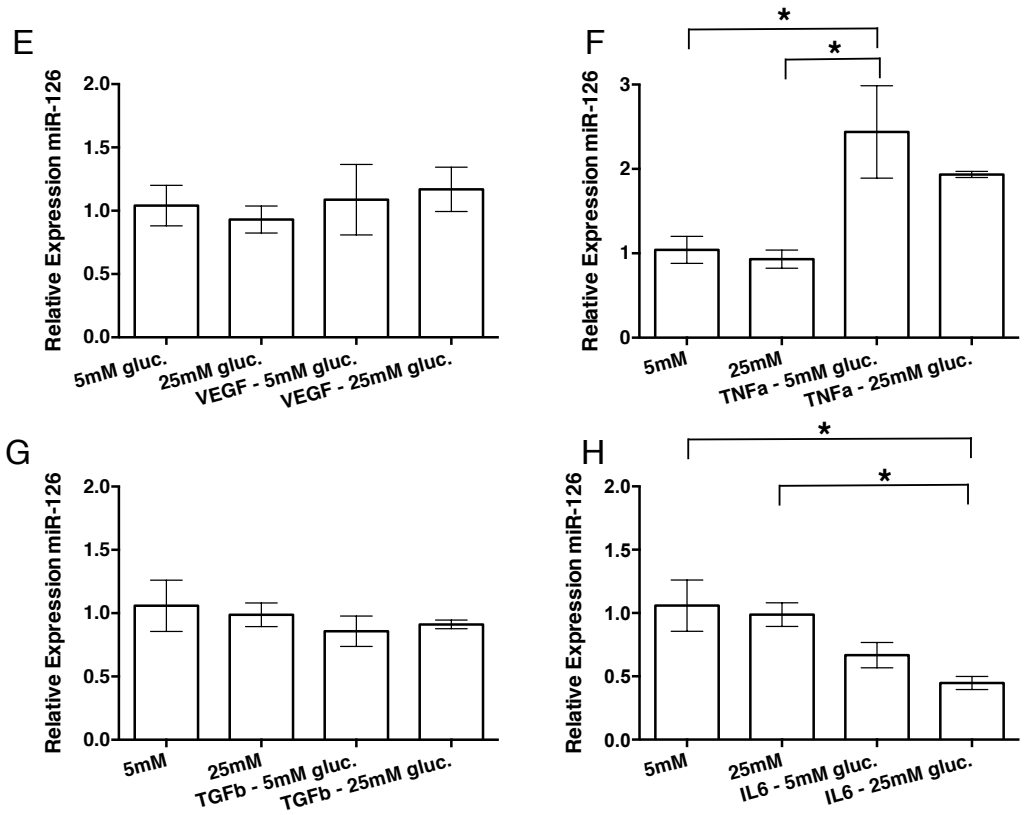

Figure 5.9. Relative expressions of miR-29b and miR-126 in CiGEnC conditioned medium with high glucose +/- selected cytokines.

Confluent CiGEnC were cultured for 24 h in control medium with 5 mM glucose, or in 25 mM glucose, together with: VEGF (**A** and **E**), TNF-α (**B** and **F**), TGF-ß1 (**C** and **G**) and IL-6 (**D** and **H**) for 24h. Expression in conditioned culture medium was analysed by RT-qPCR for miR-29b (**A**-**D**) and miR-126 (**E**-**H**). miR-29b expression was upregulated significantly in TGF-ß1 -treated CiGEnC medium (**C**; $p = 0.0003$). Upregulated expression of miR-126 was detected in medium containing TNF-α (**F**; $p = 0.008$), while miR-126 expression in medium containing IL-6 was downregulated (**H**; $p = 0.02$). ANOVA with Tukey's multiple comparison test was used: $* p \leq 0.05$, $** p \leq 0.01$, $*** p \leq 0.001$. The error bars represent SEM, n=4.

5.2.6 miR-29b and miR-126 association with exosomes and AGO2

Data from chapter 3 showed that both miR-16 and miR-192 were associated with both AGO2 protein and exosomes. Detection of miR-29b and miR-126 was carried out in extracellular vesicles and supernatant previously isolated (see 2.3-2.4 and 3.2.2.2-3.2.2.3).

Figure 5.10A shows that miR-126 was detected in association with exosomes a mechanism by which miRNAs can evade RNase degradation. The RT-qPCR analysis in Figure 5.10B in urine samples immunoprecipitated with anti-AGO2 antibody showed that this transcript was recovered in significantly greater abundance in the Ago2 immunoprecipitation than in the negative control mouse IgG.

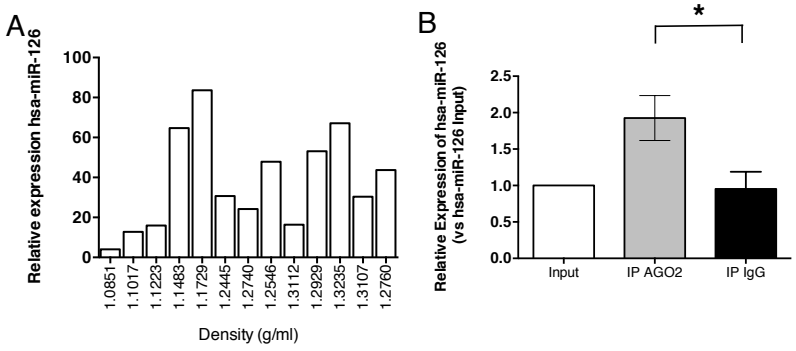

Figure 5.10. miR-126 association with exosome and AGO2 protein

miR-126 was detected using RT-qPCR from extracellular vesicles fraction obtained by ultracentrifugation. RT-qPCR analysis of miR-126 showed that it was present in the extracellular vesicles and mainly in the exosome fraction (**A**). This miRNA was then also detectable in the ultra-centrifugation supernatant (**B**). Immunoprecipitation (IP) from 10 urine samples using anti-AGO2 antibody detected AGO2, with negative normal mouse IgG. RT-qPCR detected increased miR-126 in Ago2 immunoprecipitates in comparison with untreated urine input and mouse IgG reactions with p-value=0.02 (**C**). Error bars represent mean ± SEM.

Similarly, miR-29b was also detected both in association with exosomes and with AGO2 protein. Higher expression of this miRNA was found in the exosome fractions in comparison to the other fractions containing extracellular vesicles. Surprisingly, detection of miR-29b in the supernatant obtained after ultra-centrifugation showed a Ct=38 suggesting that this miRNA is mainly expressed in the extracellular/exosome fraction. Analysis of this transcript was also carried out in the urine sample immunoprecipitated with anti-AGO2 antibody. Considerable variation in Ct was found across the 10 samples, in 6 of them miR-29b was not

detectable (Ct around 39) while in the others 4 the Ct was around 33. This difference is also observable by the large error bar for the relative expression in Figure 5.11. Similar results regarding this miRNA were found by Arroyo et al. in plasma samples [170].

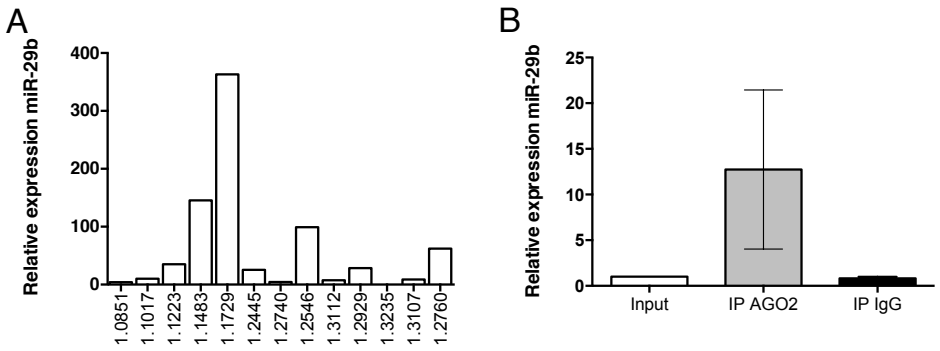

Figure 5.11. miR-29b association with exosome and AGO2 protein

Exosome and extravesicle samples were obtained after ultracentrifugation and used to detect miR-29b by RT-qPCR. Data show that miR-29b is mainly expressed in the exosome fraction in comparison to the other one (**A**). No statistical variation for miR was identified in 10 urine samples immunoprecipitated with anti-AGO2 antibody. IgG were used as negative control (**B**). Error bars represent mean ± SEM.

5.2.7 *In silico* analysis

miRNAs act as post-transcriptional regulators of gene expression by targeting mRNA targets and causing translational repression, with the potential to affect multiple biological pathways. Predicted and validated miRNA-target interactions were analysed *in silico* by Cytoscape with CyTargetLinker [205]. This software was used to visualise predicted targets for miR-29b and miR-126. Target predictions were cross-referenced with results from four databases: TargetScan, Microcosm, miRTarBase and miRecords.

In Figure 5.12, miRNAs and miRNA-targets are represented as nodes and intermolecular interactions as lines connecting these nodes. Using this software it was also possible to identify mRNAs (in orange) that could be bound by both miRNAs. Table 5.3 lists mRNAs that are potential targets of both miRNAs.

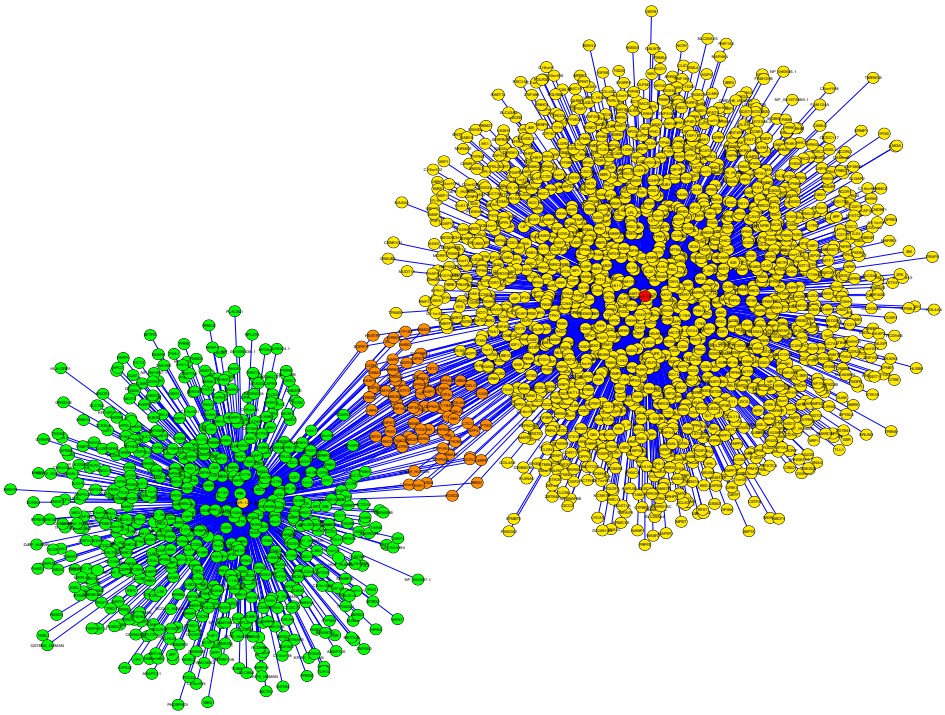

Figure 5.12. Extended miRNA networks for miR-29b and miR-126

miR-29b and miR-126 are shown, respectively, as red and yellow circles with target mRNAs represented as yellow (miR-29b) and green (miR-126). Orange circles represent mRNAs targeted by both miRNAs.

ABCE1	CR1L	IDH2	Q9NW00_HUMAN
ACPL2	CREB5	IRS1	RARRES2
ADAMTS6	DCBLD1	KDELC1	RDH12
AFF4	DENND1B	KIAA1546	RIT1
AGPAT4	DIP2C	KIF5B	RNF165
AHSG	CREB5	KPNA1	SEMA5B
AKAP13	DCBLD1	KRAS	SGK69_HUMAN
AKAP5	DENND1B	LARP6	SLC26A6
ANTXR2	DIP2C	LRP6	SLC43A1
ATF2	DNM3	MANEAL	SLITRK4
ATP1B1	DNMT1	MARK3	SMAD6
BANP	DOPEY1	METTL21D	SR140_HUMAN
BRD1	EDC3	MRPS26	STAMBPL1
C10orf68	EN1	NAPB	STK38
C11orf9	FBXO7	NFATC3	SYT9
C17orf68	FGD2	NMI	THSD4
C9orf92	FLCN	NPAS4	TIMELESS
CCR6	FOXO3A	NRSN1	TMC7
CDKN2A	FTCD	PCDHA11	TUBB2A
CEACAM1	G6PC	PDGFB	UBTD1
CHMP4B	GAP43	PEX5	USP7
CILP2	GNA13	PIR	VEGFA
COL4A5	GPR37	PPM1D	WDR18
CORT	GRHL3	PPP1R16A	ZNF524
CPEB3	GRIA3	PTX3	
CR1L	HEATR1	Q9HCM3_HUMAN	

Table 5.3. Predicted mRNA targeted by both miR-29b and miR-126

5.3 Discussion

The first aim of the present chapter was to determine the feasibility of LCM in conjunction with miRNA detection by RT-qPCR, to identify miRNA expression from defined nephron segments. Previous work has shown that this technique can be used to study alterations in mRNA abundance in an animal model of renal disease [297]. A previous study on rats demonstrated that LCM was accurate in detecting variations in miRNAs expressed in 9 specific cell types in solid organs, suggesting that miRNAs may have tissue / organ-specific roles [298].

In the present study, LCM was used to isolate glomeruli, proximal tubular and distal tubular nephronic regions from 5 control biopsies. A statistically significant increase in miR-126 expression was observed in glomeruli in comparison to proximal and distal tubular tissue extracts. Although great pains were taken to ensure clear separation of nephron segments, it is hard to definitively prove that dissection of absolutely discrete nephronic regions by the above LCM method was not partly compromised by simultaneous sampling of underlying biopsy tissue. Analysis of miRNA expression was carried out from patients biopsies that were found to be disease free. Analysis of miRNA expression in kidney biopsy samples from DN patients will provide very valuable data in disease mechanisms. However, to further refine the LCM, analysis of putative disease-associated miRNAs was carried out in podocytes and glomerular endothelial cells, HK-2 and fibroblast cell lines.

Abundant miR-126 expression in LCM-dissected glomeruli was supported by almost exclusive expression of this miRNA in glomerular endothelial cells. A previous study has demonstrated that miR-126 expression appears endothelial-specific [251]. Highly vascularised tissues such as heart and lungs have greater expression of miR-126, and it has also been shown to be vascular system-specific in zebrafish, and to be expressed in primary human umbilical vein endothelial cells (HUVECs) and other endothelial cell lines [251,299,300]. Another study showed that miR-126 expression is restricted to the glomerular endothelial cells with little expression in mesangial cells and podocytes [301].

The LCM results for miR-29b showed an abundance of this miRNA in the glomerulus. Analysis of cultured cells showed a statistically significant abundance of miR-29b expression in glomerular endothelial cells, and miR-29b was also detected in fibroblasts. The majority of previously published observations have shown miR-29b expression and function in fibroblasts from different origins [302-304]. However, a tissue specific source for miR-29b in kidney tissue has not been described.

The two miRNAs principally expressed in endothelial cell lines, miR-29b and miR-126, were further investigated to evaluate if differential expression in DN patients was glucose-dependent. Analyses were then carried out using three glucose-depend models:

- CiGEnC treated with high glucose concentration
- Diabetic NOD mice
- Urine from PCOS females with insulin resistance

Data obtained from these models suggest that the change of miR-29b and miR-126 expression is not affected by variation in glucose concentration.

Zampatetaki and colleagues analysed plasma miRNA profiles from patients with T2DM, one of the major risk factors for both cardiovascular disease and diabetic nephropathy and found a reduction of miR-29b and miR-126 [155]. Specifically, high glucose concentrations significantly decreased miR-126 levels in endothelial apoptotic bodies and in plasma [154]. Down-regulated miR-126 expression was also detected in plasma from patients affected by coronary artery disease when compared to healthy controls [155], in endothelial progenitor cells from diabetic patients [305], and in bronchial brushings from cystic fibrosis patients [306]. Snowdon and colleagues reported increased expression of miR-126 in urine samples from urothelial cancer patients [279]. The miRNAs analysed in this study were chosen on the basis of published literature on miRNA expression in solid bladder tumour and not after a profiling experiment [279].

Increased miR-126 expression has been shown in the aortas of CKD mice, along with a concomitant down-regulated expression of targets VCAM-1 and SDF-1 proteins, while miR-126 antisense treatment strongly enhanced the expression of these targets [307]. Surprisingly in light of the above findings,

induction of miR-126 expression resulted in increased abundance of the VCAM-1 and SDF-1 mRNAs, possibly a result of other factors compensating for the miR-126 inhibitory effect [307]. Using the diabetic Goto-kakizaki rat model, He and colleagues found increased miR-29a and miR-29b expression due to the hyperglycaemic and hyperinsulinemic conditions [308].

Our data presented in this thesis suggest that increased miR-126 and miR-29b expression is not conditional on high glucose concentration in the models tested. However, this effect may be due to the influence of other mechanisms that play a role in diabetic nephropathy development and progression.

The role of miRNAs in the fibrotic process during diabetic nephropathy and the involvement of inflammatory mechanisms in this disease have already been discussed in Chapter 1. Therefore, miR-29b and miR-126 expression was analysed in CiGEnC following treatment with VEGF, TNF-α, TGF-ß and IL-6 as *in vitro* models of DN. Decreased detection of both miR-29b and miR-126 was identified in cytokine-treated cells. Statistically significant increased expression of miR-126 expression was observed in conditioned media of TNF-α-treated CiGEnC and of miR-29b following TGF-ß1 treatment.

De Jong and colleagues have shown that, following treatment with 10ng/ml of TNF-α, exosomes secreted by endothelial cells showed increased protein levels of intercellular adhesion molecule 1 (ICAM-1) and TNF-α, alpha-induced protein 3 (TNFAIP3) [30]. By contrast, elevated concentrations of glucose or mannose did not lead to significant changes in mRNA level and only a few proteins are modified by these conditions [309]. These authors did not analyse changes in exosomal miRNA levels, and it is possible that the induction of miR-126 expression by TNF-α in CiGEnC condition medium observed in this study might be exosome-associated.

TNF-α treatment induces VCAM-1 protein synthesis predominantly in arteriolar and peritubular endothelial cells, where miR-126 regulates VCAM-1 expression [301]. miR-126 and VCAM-1 protein and mRNA levels were studied in the glomerular endothelium and arteriolar endothelium in the kidneys of C57BL/6 mice. Elevated miR-126 levels in the glomerular endothelium corresponded with

low VCAM-1 protein expression. In contrast, in arterioles, low miR-126 levels were associated with high VCAM-1 protein levels [301]. These data suggested that in reaction to an inflammatory stimulus, less VCAM-1 protein was produced in the glomerular compartment [301]. VCAM-1 is also responsible for mediating leukocyte adhesion on the endothelial surface [310]. Therefore, inhibition of VCAM-1 expression by miR-126 may regulate leukocyte homing in the vessel wall, suggesting a role in vascular inflammation by reducing TNF-α-induced expression of VCAM-1 [311].

The E26 transformation-specific sequence (ETS) factors are a family of transcription factors that share a highly conserved DNA binding domain and regulate cell development, senescence, death, and tumorigenesis [312]. ETS1 is expressed in human endothelial cells and ETS1 protein expression is up-regulated by TNF-α [313]. In HUVEC, Ets-1 and Ets-2 play a fundamental role in controlling the expression of miR-126 [314]. Essential roles for miR-126 in angiogenesis and maintenance of vascular integrity have been described, and its pro-angiogenic action is in part mediated by repressing negative regulators of the VEGF pathway including the Sprouty-related protein (SPRED1) and phosphoinositol-3 kinase regulatory subunit 2 (PIK3R2) [315].

VEGF is another cytokine that is induced by TNF-α [316]. Cantaluppi et al. demonstrated a protective effect of microvesicles released from endothelial progenitor cells in experimental acute kidney injury [317]. They found that microvesicles rich in miR-126 and miR-296 activated an angiogenic program that modulated proliferation, angiogenesis and apoptosis [317]. These vesicles were reported to enhance tubular cell proliferation and reduced leukocyte infiltration, and to provide protection from chronic kidney damage progression by inhibiting capillary rarefaction, glomerulosclerosis and tubular interstitial fibrosis [317].

It is therefore possible that TNF-α treatment of CiGEnC might induce VCAM-1, miR-126 expression and microvesicle production. Induction of VCAM-1 might mediate an immediate inflammatory response through regulation of leucocyte adhesion. By contrast, increased exosomal and miR-126 production may have a protective role from future chronic damage.

The human miR-29b family includes hsa-miR-29a, hsa-miR-29b-1, hsa-miR-29b-2, and hsa-miR-29c. miR-29b-1 and miR-29b-2 have identical mature sequences, referred to collectively as miR-29b. The gene encoding the precursors of miR-29b-1 and miR-29a is located on chromosome 7q32.3, while the gene encoding miR-29b-2 and miR-29c is on chromosome 1q32.2. Different reports have shown that the miR-29 family target a variety of mRNAs that encode the extracellular matrix-related proteins: a large number of collagen isoforms, laminin γ1, fibrilin 1, elastin, matrix metalloproteinase 2, and integrin ß1 [130,318,319]. In addition, it has also been shown that expression of the miR-29 family is TGF-ß mediated [319,320]. Qin and colleagues demonstrated that miR-29 is a downstream target gene of TGF-ß/Smad3 in fibrosis, and was negatively regulated by TGF-ß/Smad3 [42]. This study also showed that miR-29 negatively regulated fibrosis by targeting the process of collagen matrix synthesis rather than by inhibiting myofibroblast accumulation [142]. Renal miR-29b overexpression in an established mouse model of unilateral ureteral obstruction (UUO) nephropathy showed a potential therapeutic effect on renal fibrosis, blocking tubulointerstitial fibrosis, collagen I and collagen III mRNA expression and protein accumulation [141].

Furthermore, it has been reported that induction of fibrosis in hepatic stellate cells correlates with a reduction of miR-29b expression and up-regulation of IGF-I and PDGF-C [321]. These data suggested that miR-29 acts as an antifibrogenic mediator by targeting collagen biosynthesis, and by interfering with profibrogenic cell communication via PDGF-C and IGF-I [321].

The above studies suggest that release of miR-126 and miR-29b by glomerular endothelial cells into the nascent glomerular ultrafiltrate may have important consequences for the downstream nephron. Further studies will be required to determine the precise consequences of this release by glomerular endothelial cells that my work uncovers. It will also be important to understand the molecular mechanisms leading to release of microRNAs.

Chapter 6 – General discussion

DN is the leading cause of CKD and the second most common cause of end-stage renal disease. Classical indicators such as determination of eGFR, presence of proteinuria and screening for microalbuminuria are neither sufficiently specific nor sensitive to predict disease outcome in individual patients. Kidney biopsy, the gold-standard diagnostic test available at present, is an invasive procedure with a 3% of risk of major complications. Therefore, identification of more effective biomarkers for early detection and better screening is highly desirable.

The aim of this thesis was to analyse miRNA expression in urine samples as a novel, non-invasive method for the diagnosis and prognosis of DN. At the start of this project in 2011, the key roles played by miRNAs in numerous physiological and pathological processes were becoming recognised. However, little was known regarding the detection of urinary miRNAs and the exploitation of this approach to identify putative DN biomarkers.

The first goal of this project was to develop a reliable and robust technique for extraction and detection of miRNAs from urine samples. The experimental data showed coefficients of variation of less than 10%, confirming that the assay was suitably robust. Furthermore, appropriate stability of endogenous urinary miRNAs was established in samples from unaffected individuals and DN patients. This first part of the study was carried out analysing two miRNAs: miR-16 and miR-192. miR-16 is expressed abundantly and ubiquitously, while previous data from the host laboratory has demonstrated down-regulation of miR-192 in severe DN and provided evidence of a potentially important role for this miRNA in renal fibrosis [136]. Data from the present study showed that both miRNAs are stable in urine samples maintained at room temperature for up to 4 hours, and demonstrated specific stabilising mechanisms for endogenous miRNAs, but not for the exogenous, spiked-in, cel-miR-39. These findings have important implications for routine analysis of urinary miRNA as disease biomarkers.

The presence of at least two populations of urinary miRNAs: those associated with microvesicles, including exosomes, and those associated with protein AGO2. Each of these associations might explain protection from RNase degradation and proteinase K digestion respectively. Previous studies have also shown that, unlike mRNAs and long ncRNAs, plasma-borne miRNAs are

resistant to endogenous RNase activity, and that their resistance to degradation may be a product of association with extracellular vesicles like exosomes, or with protein complexes [166,170,189]. Exosome-associated miRNAs have been proposed as disease-specific biomarkers [322,323]. To evaluate the utility of exosome-associated miRNA as DN biomarkers a detailed characterisation of urinary exosome-associated miRNA populations will be required.

Functionally active exosome- or protein-associated extracellular miRNAs may be taken up by recipient cells, regulating gene expression and working as cell-to-cell messengers in both local and more distant micro communication mechanisms [324]. Indeed, exosomes can mediate diverse biological functions including the transfer of mRNAs and non-coding RNAs to neighbouring or distant cells [168]. It is therefore conceivable that these extracellular miRNAs might act therapeutically or pathogenically within the nephron, depending on the local environment. Critical factors are likely to include the identity and abundance of miRNAs in exosome or protein complexes released by cells, the capacity of exosomes to transfer miRNAs to recipient cells, and the end-result of miRNA uptake in the recipient cells.

The maximum size of a molecule that can cross the healthy glomerular filtration barrier approximates to albumin, which has a molecular mass of 67 kDa. This threshold predicts that AGO2, at 97 kDa, would be excluded from the glomerular ultrafiltrate. In addition, recent evidence suggests that protein GW182 (182 kDa) may play a key role in protecting AGO-bound miRs [191]. The addition of this protein would significantly increase the miR:AGO2 complex size, making trans-glomerular filtration barrier passage even less likely. It is therefore possible to speculate that urinary AGO2:miR complexes originate largely from the urinary tract in healthy controls. It seems unlikely that this relationship will hold true in DN patients where proteinuria is greatly increased, but further work will be required.

The preliminary data generated in Chapter 3 suggested that urinary miRNAs are suitable candidates for further analysis as renal disease biomarkers. Therefore, urinary miRNA profiles were generated from samples from DN patients and healthy individuals. This analysis was carried out using a qRT-PCR-based array (TaqMan Array Human microRNA Cards A and B), permitting the simultaneous analysis of 754 small non-coding RNAs. The decision to use this

technology instead of a hybridisation array-based approach was made on the basis of previous experiments carried out in our laboratory. These previous data showed that amplification-based technology was more sensitive, producing useful miRNA expression data from FFPE renal biopsy samples from nephrology patients after storage for 8-16 years (Aleksandra Krupa's PhD thesis: The role of microRNAs in renal fibrosis).

TaqMan Array Human microRNA Card A analysis identified a significant down-regulation of 35 miRNAs expression from a total of 47. Of the miRNAs with significantly up-regulated expression in DN patients when compared to control subjects, miR-29b, miR-212, miR-126 and miR-155 showed greatest fold-changes, with miR-192 and miR-200b the corresponding down-regulated miRNAs. These results were then replicated using single, miRNA-specific, qRT-PCR assays. ROC curve analysis supported the possible utility of these miRNAs as DN biomarkers. However, for correlations between miRNAs expression and both P:Cr ratio and eGFR, the r^2 failed to exceed 0.4. Future studies analysing larger case-control cohorts will be required to clarify the association of these variables and to compare the performance of these new markers to those presently in use.

As discussed extensively in Chapter 4 (Section 4.3), different groups have investigated the role of miRNAs in DN and analysed their potential as novel biomarkers for kidney disease and other pathologies [280-283]. Validation of selected putative disease-associated miRNAs in larger DN patient cohorts will provide valuable information. Patients recruited for the present study were predominantly male, with CKD stages 3, 4 or 5. Future analyses should include increased numbers of both male and female patients at all CKD stages, including stages 1 and 2. It will also be interesting to correlate expression levels of target urinary miRNAs with disease progression and to evaluate their utility as prognostic indicators for DN.

Since diabetes is the commonest cause of DN, further work will be required to dissect miRNA disease-related components specific to DM and DN, as well as shared components. In the present study, analysis of miR-126 and miR-29b expression was carried out in three diabetes-related models: CiGEnCs cultured in

an elevated glucose concentration, diabetic NOD mice, and urine samples from PCOS females with insulin resistance. The data obtained from these models suggested that changes in expression of these miRNAs were not affected by variation in glucose concentration.

miR-29b and miR-126 were detected at low levels in control urine samples and at much higher level in the DN patients' urine. Direct involvement of miR-126 in DN has not yet been shown, but an increase in miR-126 has been demonstrated in the aortas of mice in a CKD model [307], and in urine samples from patients with low- and high-grade urothelial cancer [279]. Downregulation of miR-126 expression was observed in plasma samples of DM patients [154]. A number of reports have implicated members of the miR-29a/b/c family in the pathogenesis of renal fibrosis. In high glucose concentrations, TGF-ß1 downregulates miR-29a/b/c expression in tubular epithelium-like cells and podocytes, and these changes are associated with increased expression of collagens I, III and IV [141,143,154]. To assess the specificity of target miRNAs as biomarkers for DN, it would also be useful to investigate their expression in patients affected by other kinds of renal disease such as IgA nephropathy, polycystic kidney disease, glomerusclerosis and acute kidney disease.

In the present study, characterisation of miRNA expression in defined nephron compartments was achieved by LCM followed by miRNA detection by qRT-PCR on RNA extracts from the isolated nephron regions from 5 control biopsies. A statistically significant increase in abundance of miR-126 was detected in glomeruli when compared to proximal and distal tubular RNA extracts. Abundant miR-126 expression in LCM-dissected glomeruli was supported by almost exclusive expression of this miRNA in glomerular endothelial cells, while miR-29b expression was abundant in the glomerulus but also readily detectable in fibroblasts. These data correlated with previously published observations showing that miR-126 expression is endothelium-specific [299] and miR-29b expression is typical of fibroblasts from different origins [302-304].

However, it is important to note all LCM biopsies were taken from patients who were subsequently found to be disease-free. During this project, renal biopsy samples from DN patients were not available to analyse miRNA expression. LCM

of renal biopsy tissue from DN patients will be essential to investigate disease mechanisms and identify the sources of target miRNAs.

As discussed above, the data presented in this thesis suggest that increased miR-126 and miR-29b expression is not dependent on high glucose concentrations in the models tested. However, this effect might be due to the influence of other mechanisms that play a role in development and progression of DN. For this reason, expression of miR-29b and miR-126 was analysed in CiGEnC following treatment with VEGF, TNF-α, TGF-ß and IL-6 as *in vitro* models of DN. Statistically significant up-regulation of miR-126 expression was observed in the conditioned medium of TNF-α-treated CiGEnC and of miR-29b following TGF-ß1 treatment. These data highlight the complexity of this pathology (see Chapter 1).

The experimental data above suggest that miR-126 abundance may be involved in inflammation, while miR-29b expression is regulated by cytokines implicated in renal fibrosis. Additional studies will be needed to clarify the involvement of these miRNAs in the pathology of diabetic nephropathy, firstly to validate if miR-126 and miR-29b are regulated by TNF-α and TGF-ß1 treatment respectively, and secondly if they have a protective role in kidney damage. Up-regulated expression of these miRNAs in urine samples of DN patients, in conditioned culture medium of *in vitro* DN models and increased expression in the glomerulus of healthy subjects is also worthy of further investigation, and might provide important information on downstream signalling in the nephron.

DN is a complex condition in which a network of molecular, cellular, and physiological mechanisms play key roles in disease progression. A single miRNA can potentially regulate multiple components of one or more pathways via both autocrine and paracrine signaling. Therefore theoretically, miRNAs are credible candidates both for novel DN biomarkers and as druggable targets for disease treatment. The work presented in this thesis, together with the other published reports, provides a starting point to evaluate the use of miRNAs as future therapeutic, diagnostic and/or prognostic clinical tools.

References

1. Ross MH, Pawlina W (2010) *Histology: a text and atlas*. LWW.
2. Kurts C, Panzer U, Anders H-J, Rees AJ (2013) The immune system and kidney disease: basic concepts and clinical implications. *Nat Rev Immunol* **13**: 738–753.
3. Ballermann BJ (2005) Glomerular endothelial cell differentiation. *Kidney International* **67**: 1668–1671.
4. Bulger RE, Eknoyan G, Purcell DJ, Dobyan DC (1983) Endothelial characteristics of glomerular capillaries in normal, mercuric chloride-induced, and gentamicin-induced acute renal failure in the rat. *J Clin Invest* **72**: 128–141.
5. Levick JR, Smaje LH (1987) An analysis of the permeability of a fenestra. *Microvasc Res* **33**: 233–256.
6. Haraldsson B, Nyström J, Deen WM (2008) Properties of the glomerular barrier and mechanisms of proteinuria. *Physiol Rev* **88**: 451–487.
7. Singh A, Satchell SC, Neal CR, McKenzie EA, Tooke JE, Mathieson PW (2007) Glomerular endothelial glycocalyx constitutes a barrier to protein permeability. *J Am Soc Nephrol* **18**: 2885–2893.
8. Chesterman CN (1988) Vascular endothelium, haemostasis and thrombosis. *Blood Rev* **2**: 88–94.
9. Pober JS, Cotran RS (1990) Cytokines and endothelial cell biology. *Physiol Rev* **70**: 427–451.
10. Schlondorff D (1987) The glomerular mesangial cell: an expanding role for a specialized pericyte. *FASEB J* **1**: 272–281.
11. Alpers CE, Seifert RA, Hudkins KL, Johnson RJ, Bowen-Pope DF (1993) PDGF-receptor localizes to mesangial, parietal epithelial, and interstitial cells in human and primate kidneys. *Kidney International* **43**: 286–294.
12. Schlöndorff D (1996) Roles of the mesangium in glomerular function. *Kidney International* **49**: 1583–1585.
13. Abrass CK (1995) Diabetic nephropathy. Mechanisms of mesangial matrix expansion. *West J Med* **162**: 318–321.
14. Suleiman H, Zhang L, Roth R, Heuser JE, Miner JH, Shaw AS, Dani A (2013) Nanoscale protein architecture of the kidney glomerular basement membrane. *Elife (Cambridge)* **2**: e01149.
15. Pavenstädt H, Kriz W, Kretzler M (2003) Cell biology of the glomerular podocyte. *Physiol Rev* **83**: 253–307.
16. Smoyer WE, Mundel P (1998) Regulation of podocyte structure during the development of nephrotic syndrome. *Journal of molecular medicine* **76**: 172–183.
17. Yuan H, Takeuchi E, Salant DJ (2002) Podocyte slit-diaphragm protein nephrin is linked to the actin cytoskeleton. *Am J Physiol Renal Physiol* **282**: F585–F591.
18. Ohse T, Chang AM, Pippin JW, Jarad G, Hudkins KL, Alpers CE, Miner JH, Shankland SJ (2009) A new function for parietal epithelial cells: a second glomerular barrier. *AJP: Renal Physiology* **297**: F1566–F1574.
19. Ohse T, Pippin JW, Chang AM, Krofft RD, Miner JH, Vaughan MR, Shankland SJ (2009) The enigmatic parietal epithelial cell is finally getting noticed: a review. *Kidney International* **76**: 1225–1238.
20. Seifter J, Sloane D, Ratner A (2005) *Concepts in Medical Physiology*. Lippincott Williams & Wilkins.

21. Kierszenbaum AL, Laura L Tres MD (2012) *Histology and Cell Biology*. Mosby Incorporated.
22. Rao RM, Yang L, Garcia-Cardena G, Luscinskas FW (2007) Endothelial-dependent mechanisms of leukocyte recruitment to the vascular wall. *Circ Res* **101**: 234–247.
23. Sherwood L (2011) *Human Physiology*. Cengage Learning.
24. Lote C (2012) *Principles of renal physiology*. Springer.
25. Bell NH (1985) Vitamin D-endocrine system. *J Clin Invest* **76**: 1–6.
26. Dusso AS, Brown AJ, Slatopolsky E (2005) Vitamin D. *Am J Physiol Renal Physiol* **289**: F8–F28.
27. Stevens PE, O'Donoghue DJ, de Lusignan S, Van Vlymen J, Klebe B, Middleton R, Hague N, New J, Farmer CKT (2007) Chronic kidney disease management in the United Kingdom: NEOERICA project results. *Kidney International* **72**: 92–99.
28. Coresh J, Selvin E, Stevens LA, Manzi J, Kusek JW, Eggers P, Van Lente F, Levey AS (2007) Prevalence of chronic kidney disease in the United States. *JAMA* **298**: 2038–2047.
29. Mathew TH, Corso O, Ludlow M, Boyle A, Cass A, Chadban SJ, Joyner B, Shephard M, Usherwood T (2010) Screening for chronic kidney disease in Australia: a pilot study in the community and workplace. *Kidney Int Suppl* S9–S16.
30. Kerr M, Bray B, Medcalf J, O'Donoghue DJ, Matthews B (2012) Estimating the financial cost of chronic kidney disease to the NHS in England. *Nephrology Dialysis Transplantation* **27 Suppl 3**: iii73–iii80.
31. Levey AS, Coresh J, Balk E, Kausz AT, Levin A, Steffes MW, Hogg RJ, Perrone RD, Lau J, Eknoyan G, et al. (2003) National Kidney Foundation practice guidelines for chronic kidney disease: evaluation, classification, and stratification. *Ann Intern Med* **139**: 137–147.
32. Kopyt NP (2006) Chronic kidney disease: the new silent killer. *J Am Osteopath Assoc* **106**: 133–136.
33. Nankivell BJ (2001) Creatinine clearance and the assessment of renal function. *Australian Prescriber* **24**: 15–17.
34. Murphree DD, Thelen SM (2010) Chronic kidney disease in primary care. *J Am Board Fam Med* **23**: 542–550.
35. The National Collaborating Centre for Chronic Conditions (UK) (2008) *Chronic Kidney Disease: National Clinical Guideline for Early Identification and Management in Adults in Primary and Secondary Care*. Royal College of Physicians (UK), London.
36. TESCH GH (2010) Review: Serum and urine biomarkers of kidney disease: A pathophysiological perspective. *Nephrology* **15**: 609–616.
37. Feig DI (2009) Uric acid: a novel mediator and marker of risk in chronic kidney disease? *Curr Opin Nephrol Hypertens* **18**: 526–530.
38. Wang G, Lai FMM, Lai KB, Chow KM, Li KTP, Szeto CC (2007) Messenger RNA Expression of Podocyte-Associated Molecules in the Urinary Sediment of Patients with Diabetic Nephropathy. *Nephron Clin Pract* **106**: c169–c179.
39. Fassett RG, Venuthurupalli SK, Gobe GC, Coombes JS, Cooper MA, Hoy WE (2011) Biomarkers in chronic kidney disease: a review. *Kidney International* **80**: 806–821.
40. Chaudhary K, Phadke G, Nistala R, Weidmeyer CE, McFarlane SI, Whaley-Connell A (2010) The emerging role of biomarkers in diabetic and hypertensive chronic kidney disease. *Curr Diab Rep* **10**: 37–42.

41. Levey AS, Coresh J (2012) Chronic kidney disease. *Lancet* **379**: 165–180.
42. Klein J, Kavvadas P, Prakoura N, Karagianni F, Schanstra JP, Bascands J-L, Charonis A (2011) Renal fibrosis: insight from proteomics in animal models and human disease. *Proteomics* **11**: 805–815.
43. Ritz E, Zeng X-X, Rychlík I (2011) Clinical manifestation and natural history of diabetic nephropathy. *Contrib Nephrol* **170**: 19–27.
44. Briggs V, Wilkie M (2012) Chapter 14 Comparative audit of peritoneal dialysis catheter placement in England, Northern Ireland and Wales in 2011: a summary of progress to July 2012. *Nephron Clin Pract* **120 Suppl 1**: c261–c263.
45. Mogensen CE, Christensen CK, Vittinghus E (1983) The stages in diabetic renal disease. With emphasis on the stage of incipient diabetic nephropathy. *Diabetes* **32 Suppl 2**: 64–78.
46. Min TZ, Stephens MW, Kumar P, Chudleigh RA (2012) Renal complications of diabetes. *Br Med Bull* **104**: 113–127.
47. Wild S, Roglic G, Green A, Sicree R, King H (2004) Global prevalence of diabetes: estimates for the year 2000 and projections for 2030. *Diabetes Care* **27**: 1047–1053.
48. Schena FP, Gesualdo L (2005) Pathogenetic mechanisms of diabetic nephropathy. *Journal of the American Society of Nephrology* **16 Suppl 1**: S30–S33.
49. Fioretto P, Mauer M, Brocco E, Velussi M, Frigato F, Muollo B, Sambataro M, Abaterusso C, Baggio B, Crepaldi G, et al. (1996) Patterns of renal injury in NIDDM patients with microalbuminuria. *Diabetologia* **39**: 1569–1576.
50. Mauer SM, Steffes MW, Ellis EN, Sutherland DE, Brown DM, Goetz FC (1984) Structural-functional relationships in diabetic nephropathy. *J Clin Invest* **74**: 1143–1155.
51. ADLER S (2004) Diabetic nephropathy: Linking histology, cell biology, and genetics. *Kidney International* **66**: 2095–2106.
52. Kreisberg JI, Ayo SH (1993) The glomerular mesangium in diabetes mellitus. *Kidney International* **43**: 109–113.
53. Jacobsen P, Rossing K, Hansen BV, Bie P, Vaag A, Parving H-H (2003) Effect of short-term hyperglycaemia on haemodynamics in type 1 diabetic patients. *J Intern Med* **254**: 464–471.
54. Giacco F, Brownlee M (2010) Oxidative stress and diabetic complications. *Circ Res* **107**: 1058–1070.
55. Heilig CW, Liu Y, England RL, Freytag SO, Gilbert JD, Heilig KO, Zhu M, Concepcion LA, Brosius FC (1997) D-glucose stimulates mesangial cell GLUT1 expression and basal and IGF-I-sensitive glucose uptake in rat mesangial cells: implications for diabetic nephropathy. *Diabetes* **46**: 1030–1039.
56. Inoki K, Haneda M, Maeda S, Koya D, Kikkawa R (1999) TGF-beta 1 stimulates glucose uptake by enhancing GLUT1 expression in mesangial cells. *Kidney International* **55**: 1704–1712.
57. Di Paolo S, Gesualdo L, Ranieri E, Grandaliano G, Schena FP (1996) High glucose concentration induces the overexpression of transforming growth factor-beta through the activation of a platelet-derived growth factor loop in human mesangial cells. *Am J Pathol* **149**: 2095–2106.
58. Wolf G, Ziyadeh FN (1999) Molecular mechanisms of diabetic renal hypertrophy. *Kidney International* **56**: 393–405.

59. Galler A, Müller G, Schinzel R, Kratzsch J, Kiess W, Münch G (2003) Impact of metabolic control and serum lipids on the concentration of advanced glycation end products in the serum of children and adolescents with type 1 diabetes, as determined by fluorescence spectroscopy and nepsilon-(carboxymethyl)lysine ELISA. *Diabetes Care* **26**: 2609–2615.
60. Ohshiro Y, Lee Y, King GL (2005) Mechanism of diabetic nephropathy: role of protein kinase-C activation. *Adv Stud Med* **5**: S10–S19.
61. Forbes JM, Cooper ME, Oldfield MD, Thomas MC (2003) Role of advanced glycation end products in diabetic nephropathy. *Journal of the American Society of Nephrology* **14**: S254–S258.
62. Ayo SH, Radnik R, Garoni JA, Troyer DA, Kreisberg JI (1991) High glucose increases diacylglycerol mass and activates protein kinase C in mesangial cell cultures. *Am J Physiol* **261**: F571–F577.
63. Kang N, Alexander G, Park JK, Maasch C, Buchwalow I, Luft FC, Haller H (1999) Differential expression of protein kinase C isoforms in streptozotocin-induced diabetic rats. *Kidney International* **56**: 1737–1750.
64. Kanwar YS, Wada J, Sun L, Xie P, Wallner EI, Chen S, Chugh S, Danesh FR (2008) Diabetic Nephropathy: Mechanisms of Renal Disease Progression. *Experimental Biology and Medicine* **233**: 4–11.
65. Lynch JJ, Ferro TJ, Blumenstock FA, Brockenauer AM, Malik AB (1990) Increased endothelial albumin permeability mediated by protein kinase C activation. *J Clin Invest* **85**: 1991–1998.
66. (1988) Characterization and Localization of Calcium/Phospholipid-Dependent Protein Kinase-C during Diabetic Renal Growth. *Endocrinology* **123**: 1553–1558.
67. Cosio FG (1995) Effects of high glucose concentrations on human mesangial cell proliferation. *Journal of the American Society of Nephrology* **5**: 1600–1609.
68. Lago RM, Singh PP, Nesto RW (2007) Diabetes and hypertension. *Nat Clin Pract Endocrinol Metab* **3**: 667.
69. Tedla FM, Brar A, Browne R, Brown C (2011) Hypertension in chronic kidney disease: navigating the evidence. *Int J Hypertens* **2011**: 132405.
70. Ravera M, Re M, Deferrari L, Vettoretti S, Deferrari G (2006) Importance of blood pressure control in chronic kidney disease. *Journal of the American Society of Nephrology* **17**: S98–S103.
71. Wolf G, Ziyadeh FN (1997) The role of angiotensin II in diabetic nephropathy: emphasis on nonhemodynamic mechanisms. *Am J Kidney Dis* **29**: 153–163.
72. Van Buren PN, Toto R (2011) Hypertension in diabetic nephropathy: epidemiology, mechanisms, and management. *Adv Chronic Kidney Dis* **18**: 28–41.
73. Muniyappa R, Quon MJ (2007) Insulin action and insulin resistance in vascular endothelium. *Current Opinion in Clinical Nutrition and Metabolic Care* **10**: 523–530.
74. Mezzano S, Aros C, Droguett A, Burgos ME, Ardiles L, Flores C, Schneider H, Ruiz-Ortega M, Egido J (2004) NF-kappaB activation and overexpression of regulated genes in human diabetic nephropathy. *Nephrol Dial Transplant* **19**: 2505–2512.
75. Navarro-González JF, Mora-Fernández C, Muros de Fuentes M, García-Pérez J (2011) Inflammatory molecules and pathways in the pathogenesis of diabetic nephropathy. *Nature publishing group* **7**: 327–

340.
76. Elmarakby AA, Sullivan JC (2012) Relationship between oxidative stress and inflammatory cytokines in diabetic nephropathy. *Cardiovasc Ther* **30**: 49–59.
77. Hasegawa G, Nakano K, Sawada M, Uno K, Shibayama Y, Ienaga K, Kondo M (1991) Possible role of tumor necrosis factor and interleukin-1 in the development of diabetic nephropathy. *Kidney International* **40**: 1007–1012.
78. Sassy-Prigent C, Heudes D, Mandet C, Bélair MF, Michel O, Perdereau B, Bariéty J, Bruneval P (2000) Early glomerular macrophage recruitment in streptozotocin-induced diabetic rats. *Diabetes* **49**: 466–475.
79. Dalla Vestra M, Mussap M, Gallina P, Bruseghin M, Cernigoi AM, Saller A, Plebani M, Fioretto P (2005) Acute-phase markers of inflammation and glomerular structure in patients with type 2 diabetes. *Journal of the American Society of Nephrology* **16 Suppl 1**: S78–S82.
80. Araki S, Haneda M, Koya D, Sugimoto T, Isshiki K, Chin-Kanasaki M, Uzu T, Kashiwagi A (2007) Predictive impact of elevated serum level of IL-18 for early renal dysfunction in type 2 diabetes: an observational follow-up study. *Diabetologia* **50**: 867–873.
81. Miyauchi K, Takiyama Y, Honjyo J, Tateno M, Haneda M (2009) Upregulated IL-18 expression in type 2 diabetic subjects with nephropathy: TGF-β1 enhanced IL-18 expression in human renal proximal tubular epithelial cells. *Diabetes Res Clin Pract* **83**: 190–199.
82. Wong CK, Ho AWY, Tong PCY, Yeung CY, Kong APS, Lun SWM, Chan JCN, Lam CWK (2007) Aberrant activation profile of cytokines and mitogen-activated protein kinases in type 2 diabetic patients with nephropathy. *Clin Exp Immunol* **149**: 123–131.
83. Suzuki D, Miyazaki M, Naka R, Koji T, Yagame M, Jinde K, Endoh M, Nomoto Y, Sakai H (1995) In situ hybridization of interleukin 6 in diabetic nephropathy. *Diabetes* **44**: 1233–1238.
84. Coleman DL, Ruef C (1992) Interleukin-6: an autocrine regulator of mesangial cell growth. *Kidney International* **41**: 604–606.
85. Jevnikar AM, Brennan DC, Singer GG, Heng JE, Maslinski W, Wuthrich RP, Glimcher LH, Kelley VE (1991) Stimulated kidney tubular epithelial cells express membrane associated and secreted TNF alpha. *Kidney International* **40**: 203–211.
86. Zhang B, Ramesh G, Norbury CC, Reeves WB (2007) Cisplatin-induced nephrotoxicity is mediated by tumor necrosis factor-alpha produced by renal parenchymal cells. *Kidney International* **72**: 37–44.
87. Baud L, Perez J, Friedlander G, Ardaillou R (1988) Tumor necrosis factor stimulates prostaglandin production and cyclic AMP levels in rat cultured mesangial cells. *FEBS Letters* **239**: 50–54.
88. Mora C, Navarro JF (2006) Inflammation and diabetic nephropathy. *Curr Diab Rep* **6**: 463–468.
89. Nakamura T, Fukui M, Ebihara I, Osada S, Nagaoka I, Tomino Y, Koide H (1993) mRNA expression of growth factors in glomeruli from diabetic rats. *Diabetes* **42**: 450–456.
90. Coimbra TM, Janssen U, Gröne HJ, Ostendorf T, Kunter U, Schmidt H, Brabant G, Floege J (2000) Early events leading to renal injury in obese Zucker (fatty) rats with type II diabetes. *Kidney International* **57**: 167–182.
91. Ina K, Kitamura H, Okeda T, Nagai K, Liu ZY, Matsuda M, Fujikura Y

(1999) Vascular cell adhesion molecule-1 expression in the renal interstitium of diabetic KKAy mice. *Diabetes Res Clin Pract* **44**: 1–8.
92. Lee RC, Feinbaum RL, Ambros V (1993) The C. elegans heterochronic gene lin-4 encodes small RNAs with antisense complementarity to lin-14. *Cell* **75**: 843–854.
93. Reinhart BJ, Slack FJ, Basson M, Pasquinelli AE, Bettinger JC, Rougvie AE, Horvitz HR, Ruvkun G (2000) The 21-nucleotide let-7 RNA regulates developmental timing in Caenorhabditis elegans. *Nature* **403**: 901–906.
94. Slack FJ, Basson M, Liu Z, Ambros V, Horvitz HR, Ruvkun G (2000) The lin-41 RBCC gene acts in the C. elegans heterochronic pathway between the let-7 regulatory RNA and the LIN-29 transcription factor. *Mol Cell* **5**: 659–669.
95. Pasquinelli AE, Reinhart BJ, Slack F, Martindale MQ, Kuroda MI, Maller B, Hayward DC, Ball EE, Degnan B, Müller P, et al. (2000) Conservation of the sequence and temporal expression of let-7 heterochronic regulatory RNA. *Nature* **408**: 86–89.
96. Lagos-Quintana M, Rauhut R, Lendeckel W, Tuschl T (2001) Identification of novel genes coding for small expressed RNAs. *Science* **294**: 853–858.
97. Ramalingam P, Palanichamy JK, Singh A, Das P, Bhagat M, Kassab MA, Sinha S, Chattopadhyay P (2013) Biogenesis of intronic miRNAs located in clusters by independent transcription and alternative splicing. *RNA* **20**: 76–87.
98. Wang D, Lu M, Miao J, Li T, Wang E, Cui Q (2009) Cepred: predicting the co-expression patterns of the human intronic microRNAs with their host genes. *PLoS ONE* **4**: e4421.
99. Altuvia Y, Landgraf P, Lithwick G, Elefant N, Pfeffer S, Aravin A, Brownstein MJ, Tuschl T, Margalit H (2005) Clustering and conservation patterns of human microRNAs. *Nucleic Acids Research* **33**: 2697–2706.
100. Kim VN, Han J, Siomi MC (2009) Biogenesis of small RNAs in animals. *Nat Rev Mol Cell Biol* **10**: 126–139.
101. Winter J, Jung S, Keller S, Gregory RI, Diederichs S (2009) Many roads to maturity: microRNA biogenesis pathways and their regulation. *Nat Cell Biol* **11**: 228–234.
102. Bartel DP (2004) MicroRNAs: genomics, biogenesis, mechanism, and function. *Cell* **116**: 281–297.
103. Tétreault N, De Guire V (2013) miRNAs: their discovery, biogenesis and mechanism of action. *Clin Biochem* **46**: 842–845.
104. Macfarlane L-A, Murphy PR (2010) MicroRNA: Biogenesis, Function and Role in Cancer. *Curr Genomics* **11**: 537–561.
105. Yi R (2003) Exportin-5 mediates the nuclear export of pre-microRNAs and short hairpin RNAs. *Genes Dev* **17**: 3011–3016.
106. Kim VN (2005) MicroRNA biogenesis: coordinated cropping and dicing. *Nat Rev Mol Cell Biol* **6**: 376–385.
107. Lee Y, Ahn C, Han J, Choi H, Kim J, Yim J, Lee J, Provost P, Rådmark O, Kim S, et al. (2003) The nuclear RNase III Drosha initiates microRNA processing. *Nature* **425**: 415–419.
108. Finnegan EF, Pasquinelli AE (2013) MicroRNA biogenesis: regulating the regulators. *Crit Rev Biochem Mol Biol* **48**: 51–68.
109. Chendrimada TP, Gregory RI, Kumaraswamy E, Norman J, Cooch N, Nishikura K, Shiekhattar R (2005) TRBP recruits the Dicer complex to Ago2 for microRNA processing and gene silencing. *Nat Cell Biol* **436**:

740–744.
110. Ørom UA, Nielsen FC, Lund AH (2008) MicroRNA-10a binds the 5'UTR of ribosomal protein mRNAs and enhances their translation. *Mol Cell* **30**: 460–471.
111. Eiring AM, Harb JG, Neviani P, Garton C, Oaks JJ, Spizzo R, Liu S, Schwind S, Santhanam R, Hickey CJ, et al. (2010) miR-328 functions as an RNA decoy to modulate hnRNP E2 regulation of mRNA translation in leukemic blasts. *Cell* **140**: 652–665.
112. Gu S, Kay MA (2010) How do miRNAs mediate translational repression? *Silence* **1**: 11.
113. Wu L, Belasco JG (2008) Let me count the ways: mechanisms of gene regulation by miRNAs and siRNAs. *Mol Cell* **29**: 1–7.
114. Yang J-S, Lai EC (2011) Alternative miRNA biogenesis pathways and the interpretation of core miRNA pathway mutants. *Mol Cell* **43**: 892–903.
115. Rottiers V, Näär AM (2012) MicroRNAs in metabolism and metabolic disorders. *Nat Rev Mol Cell Biol* **13**: 239–250.
116. Weber JAJ, Baxter DHD, Zhang SS, Huang DYD, Huang KHK, Lee MJM, Galas DJD, Wang KK (2010) The microRNA spectrum in 12 body fluids. *Clin Chem* **56**: 1733–1741.
117. Sun Y, Koo S, White N, Peralta E, Esau C, Dean NM, Perera RJ (2004) Development of a micro-array to detect human and mouse microRNAs and characterization of expression in human organs. *Nucleic Acids Research* **32**: e188.
118. Harvey SJ, Jarad G, Cunningham J, Goldberg S, Schermer B, Harfe BD, McManus MT, Benzing T, Miner JH (2008) Podocyte-specific deletion of dicer alters cytoskeletal dynamics and causes glomerular disease. *J Am Soc Nephrol* **19**: 2150–2158.
119. Agrawal R, Tran U, Wessely O (2009) The miR-30 miRNA family regulates Xenopus pronephros development and targets the transcription factor Xlim1/Lhx1. *Development* **136**: 3927–3936.
120. Bai XY, Ma Y, Ding R, Fu B, Shi S, Chen XM (2011) miR-335 and miR-34a Promote Renal Senescence by Suppressing Mitochondrial Antioxidative Enzymes. *J Am Soc Nephrol* **22**: 1252–1261.
121. Bracken CP, Gregory PA, Kolesnikoff N, Bert AG, Wang J, Shannon MF, Goodall GJ (2008) A double-negative feedback loop between ZEB1-SIP1 and the microRNA-200 family regulates epithelial-mesenchymal transition. *Cancer Res* **68**: 7846–7854.
122. Sepramaniam S, Armugam A, Lim KY, Karolina DS, Swaminathan P, Tan JR, Jeyaseelan K (2010) MicroRNA 320a functions as a novel endogenous modulator of aquaporins 1 and 4 as well as a potential therapeutic target in cerebral ischemia. *Journal of Biological Chemistry* **285**: 29223–29230.
123. McClelland A, Hagiwara S, Kantharidis P (2014) Where are we in diabetic nephropathy. *Curr Opin Nephrol Hypertens* **23**: 80–86.
124. Park S-M, Gaur AB, Lengyel E, Peter ME (2008) The miR-200 family determines the epithelial phenotype of cancer cells by targeting the E-cadherin repressors ZEB1 and ZEB2. *Genes Dev* **22**: 894–907.
125. Chung AC, Yu X, Lan HY (2013) MicroRNA and nephropathy: emerging concepts. *Int J Nephrol Renovasc Dis* **6**: 169–179.
126. Zhong X, Chung ACK, Chen HY, Dong Y, Meng XM, Li R, Yang W, Hou FF, Lan HY (2013) miR-21 is a key therapeutic target for renal injury in a mouse model of type 2 diabetes. *Diabetologia* **56**: 663–674.

127. Liu Z-L, Wang H, Liu J, Wang Z-X (2013) MicroRNA-21 (miR-21) expression promotes growth, metastasis, and chemo- or radioresistance in non-small cell lung cancer cells by targeting PTEN. *Mol Cell Biochem* **372**: 35–45.
128. Wang G, Kwan BC-H, Lai FM-M, Chow K-M, Li PK-T, Szeto C-C (2012) Urinary miR-21, miR-29, and miR-93: novel biomarkers of fibrosis. *Am J Nephrol* **36**: 412–418.
129. Glowacki F, Savary G, Gnemmi V, Buob D, Van der Hauwaert C, Lo-Guidice J-M, Bouyé S, Hazzan M, Pottier N, Perrais M (2013) Increased Circulating miR-21 Levels Are Associated with Kidney Fibrosis. *PLoS ONE* **8**: e58014.
130. Liu Y, Taylor NE, Lu L, Usa K, Cowley AW, Ferreri NR, Yeo NC, Liang M (2010) Renal medullary microRNAs in Dahl salt-sensitive rats: miR-29b regulates several collagens and related genes. *Hypertension* **55**: 974–982.
131. Kantharidis P, Wang B, Carew RM, Lan HY (2011) Diabetes complications: the microRNA perspective. *Diabetes* **60**: 1832–1837.
132. Sun H, Li Q-W, Lv X-Y, Ai J-Z, Yang Q-T, Duan J-J, Bian G-H, Xiao Y, Wang Y-D, Zhang Z, et al. (2010) MicroRNA-17 post-transcriptionally regulates polycystic kidney disease-2 gene and promotes cell proliferation. *Mol Biol Rep* **37**: 2951–2958.
133. Lee S-O, Masyuk T, Splinter P, Banales JM, Masyuk A, Stroope A, Larusso N (2008) MicroRNA15a modulates expression of the cell-cycle regulator Cdc25A and affects hepatic cystogenesis in a rat model of polycystic kidney disease. *J Clin Invest* **118**: 3714–3724.
134. Kato M, Zhang J, Wang M, Lanting L, Yuan H, Rossi JJ, Natarajan R (2007) MicroRNA-192 in diabetic kidney glomeruli and its function in TGF-β-induced collagen expression via inhibition of E-box repressors. *Proc Natl Acad Sci USA* **104**: 3432.
135. Chung ACK, Huang XR, Meng X, Lan HY (2010) miR-192 mediates TGF-beta/Smad3-driven renal fibrosis. *J Am Soc Nephrol* **21**: 1317–1325.
136. Krupa A, Jenkins R, Luo DD, Lewis A, Phillips A, Fraser D (2010) Loss of MicroRNA-192 promotes fibrogenesis in diabetic nephropathy. *Journal of the American Society of Nephrology* **21**: 438–447.
137. Wang B, Herman-Edelstein M, Koh P, Burns W, Jandeleit-Dahm K, Watson A, Saleem M, Goodall GJ, Twigg SM, Cooper ME, et al. (2010) E-cadherin expression is regulated by miR-192/215 by a mechanism that is independent of the profibrotic effects of transforming growth factor-beta. *Diabetes* **59**: 1794–1802.
138. Wang J, Gao Y, Ma M, Li M, Zou D, Yang J, Zhu Z, Zhao X (2013) Effect of miR-21 on renal fibrosis by regulating MMP-9 and TIMP1 in kk-ay diabetic nephropathy mice. *Cell Biochem Biophys* **67**: 537–546.
139. Fiorentino L, Cavalera M, Mavilio M, Conserva F, Menghini R, Gesualdo L, Federici M (2013) Regulation of TIMP3 in diabetic nephropathy: a role for microRNAs. *Acta Diabetol* **50**: 965–969.
140. Szeto C-C, Ching-Ha KB, Ka-Bik L, Mac-Moune LF, Cheung-Lung CP, Gang W, Kai-Ming C, Kam-Tao LP (2012) Micro-RNA expression in the urinary sediment of patients with chronic kidney diseases. *Dis Markers* **33**: 137–144.
141. Qin W, Chung ACK, Huang XR, Meng X-M, Hui DSC, Yu C-M, Sung JJY, Lan HY (2011) TGF-β/Smad3 signaling promotes renal fibrosis by

inhibiting miR-29. *Journal of the American Society of Nephrology* **22**: 1462–1474.
142. Du B, Ma L-M, Huang M-B, Zhou H, Huang H-L, Shao P, Chen Y-Q, Qu L-H (2010) High glucose down-regulates miR-29a to increase collagen IV production in HK-2 cells. *FEBS Letters* **584**: 811–816.
143. Wang B, Komers R, Carew R, Winbanks CE, Xu B, Herman-Edelstein M, Koh P, Thomas M, Jandeleit-Dahm K, Gregorevic P, et al. (2012) Suppression of microRNA-29 expression by TGF-β1 promotes collagen expression and renal fibrosis. *J Am Soc Nephrol* **23**: 252–265.
144. Kriegel AJ, Liu Y, Fang Y, Ding X, Liang M (2012) The miR-29 family: genomics, cell biology, and relevance to renal and cardiovascular injury. *Physiol Genomics* **44**: 237–244.
145. Long J, Wang Y, Wang W, Chang BHJ, Danesh FR (2011) MicroRNA-29c is a signature microRNA under high glucose conditions that targets Sprouty homolog 1, and its in vivo knockdown prevents progression of diabetic nephropathy. Journal of Biological Chemistry **286**: 11837–11848.
146. Wang B, Koh P, Winbanks C, Coughlan MT, McClelland A, Watson A, Jandeleit-Dahm K, Burns WC, Thomas MC, Cooper ME, et al. (2011) miR-200a Prevents renal fibrogenesis through repression of TGF-β2 expression. *Diabetes* **60**: 280–287.
147. Kato M, Arce L, Wang M, Putta S, Lanting L, Natarajan R (2011) A microRNA circuit mediates transforming growth factor-β1 autoregulation in renal glomerular mesangial cells. *Kidney International* **80**: 358–368.
148. Long J, Wang Y, Wang W, Chang BHJ, Danesh FR (2010) Identification of microRNA-93 as a novel regulator of vascular endothelial growth factor in hyperglycemic conditions. *Journal of Biological Chemistry* **285**: 23457–23465.
149. Etheridge A, Lee I, Hood L, Galas D, Wang K (2011) Extracellular microRNA: a new source of biomarkers. *Mutat Res* **717**: 85–90.
150. Beltrami C, Clayton A, Phillips AO, Fraser DJ, Bowen T (2012) Analysis of urinary microRNAs in chronic kidney disease. *Biochem Soc Trans* **40**: 875–879.
151. Kato M, Castro NE, Natarajan R (2013) MicroRNAs: potential mediators and biomarkers of diabetic complications. *Free Radic Biol Med* **64**: 85–94.
152. Wang G, Chan ES-Y, Kwan BC-H, Li PK-T, Yip SK-H, Szeto C-C, Ng C-F (2012) Expression of microRNAs in the urine of patients with bladder cancer. *Clin Genitourin Cancer* **10**: 106–113.
153. Creemers EE, Tijsen AJ, Pinto YM (2012) Circulating microRNAs: novel biomarkers and extracellular communicators in cardiovascular disease? *Circ Res* **110**: 483–495.
154. Zampetaki A, Kiechl S, Drozdov I, Willeit P, Mayr U, Prokopi M, Mayr A, Weger S, Oberhollenzer F, Bonora E, et al. (2010) Plasma microRNA profiling reveals loss of endothelial miR-126 and other microRNAs in type 2 diabetes. *Circ Res* **107**: 810–817.
155. Fichtlscherer S, De Rosa S, Fox H, Schwietz T, Fischer A, Liebetrau C, Weber M, Hamm CW, Röxe T, Müller-Ardogan M, et al. (2010) Circulating microRNAs in patients with coronary artery disease. *Circ Res* **107**: 677–684.
156. Lu J, Getz G, Miska EA, Alvarez-Saavedra E, Lamb J, Peck D, Sweet-Cordero A, Ebert BL, Mak RH, Ferrando AA, et al. (2005) MicroRNA

expression profiles classify human cancers. *Nature* **435**: 834–838.
157. López-Camarillo C, Marchat LA (2013) *MicroRNAs in Cancer*. CRC Press.
158. Mraz M, Pospisilova S, Malinova K, Slapak I, Mayer J (2009) MicroRNAs in chronic lymphocytic leukemia pathogenesis and disease subtypes. *Leuk Lymphoma* **50**: 506–509.
159. Maciotta S, Meregalli M, Torrente Y (2013) The involvement of microRNAs in neurodegenerative diseases. *Front Cell Neurosci* **7**: 265.
160. Lv L-L, Cao Y-H, Ni HF, Xu M, Liu D, Liu H, Chen P-S, Liu B-C (2013) MicroRNA-29c in urinary exosome/microvesicle as a biomarker of renal fibrosis. *AJP: Renal Physiology* **305**: F1220–F1227.
161. Yang Y, Xiao L, Li J, Kanwar YS, Liu F, Sun L (2013) Urine miRNAs: potential biomarkers for monitoring progression of early stages of diabetic nephropathy. *Medical Hypotheses* **81**: 274–278.
162. Cai X, Xia Z, Zhang C, Luo Y, Gao Y, Fan Z, Liu M, Zhang Y (2013) Serum microRNAs levels in primary focal segmental glomerulosclerosis. *Pediatr Nephrol* **28**: 1797–1801.
163. Wang N, Zhou Y, Jiang L, Li D, Yang J, Zhang C-Y, Zen K (2012) Urinary microRNA-10a and microRNA-30d serve as novel, sensitive and specific biomarkers for kidney injury. *PLoS ONE* **7**: e51140.
164. Argyropoulos C, Wang K, McClarty S, Huang D, Bernardo J, Ellis D, Orchard T, Galas D, Johnson J (2013) Urinary microRNA profiling in the nephropathy of type 1 diabetes. *PLoS ONE* **8**: e54662.
165. Luo Y, Wang C, Chen X, Zhong T, Cai X, Chen S, Shi Y, Hu J, Guan X, Xia Z, et al. (2013) Increased Serum and Urinary MicroRNAs in Children with Idiopathic Nephrotic Syndrome. *Clin Chem* **59**: 658–666.
166. Mitchell PS, Parkin RK, Kroh EM, Fritz BR, Wyman SK, Pogosova-Agadjanyan EL, Peterson A, Noteboom J, O'Briant KC, Allen A, et al. (2008) Circulating microRNAs as stable blood-based markers for cancer detection. *Proc Natl Acad Sci USA* **105**: 10513–10518.
167. Chen X, Ba Y, Ma L, Cai X, Yin Y, Wang K, Guo J, Zhang Y, Chen J, Guo X, et al. (2008) Characterization of microRNAs in serum: a novel class of biomarkers for diagnosis of cancer and other diseases. *Cell Res* **18**: 997–1006.
168. Valadi H, Ekström K, Bossios A, Sjöstrand M, Lee JJ, Lötvall JO (2007) Exosome-mediated transfer of mRNAs and microRNAs is a novel mechanism of genetic exchange between cells. *Nat Cell Biol* **9**: 654–659.
169. Zernecke A, Bidzhekov K, Noels H, Shagdarsuren E, Gan L, Denecke B, Hristov M, Köppel T, Jahantigh MN, Lutgens E, et al. (2009) Delivery of microRNA-126 by apoptotic bodies induces CXCL12-dependent vascular protection. *Sci Signal* **2**: ra81.
170. Arroyo JD, Chevillet JR, Kroh EM, Ruf IK, Pritchard CC, Gibson DF, Mitchell PS, Bennett CF, Pogosova-Agadjanyan EL, Stirewalt DL, et al. (2011) Argonaute2 complexes carry a population of circulating microRNAs independent of vesicles in human plasma. *Proc Natl Acad Sci USA* **108**: 5003–5008.
171. Vickers KC, Palmisano BT, Shoucri BM, Shamburek RD, Remaley AT (2011) MicroRNAs are transported in plasma and delivered to recipient cells by high-density lipoproteins. *Nat Cell Biol* **13**: 423–433.
172. EL Andaloussi S, Mäger I, Breakefield XO, Wood MJA (2013) Extracellular vesicles: biology and emerging therapeutic opportunities. *Nat Rev Drug Discov* **12**: 347–357.

173. Lynch SF, Ludlam CA (2007) Plasma microparticles and vascular disorders. *Br J Haematol* **137**: 36–48.
174. Heijnen HF, Schiel AE, Fijnheer R, Geuze HJ, Sixma JJ (1999) Activated platelets release two types of membrane vesicles: microvesicles by surface shedding and exosomes derived from exocytosis of multivesicular bodies and alpha-granules. *Blood* **94**: 3791–3799.
175. Loyer X, Vion A-C, Tedgui A, Boulanger CM (2014) Microvesicles as cell-cell messengers in cardiovascular diseases. *Circ Res* **114**: 345–353.
176. Muralidharan-Chari V, Clancy JW, Sedgwick A, D'Souza-Schorey C (2010) Microvesicles: mediators of extracellular communication during cancer progression. *Journal of Cell Science* **123**: 1603–1611.
177. Lee Y, EL Andaloussi S, Wood MJA (2012) Exosomes and microvesicles: extracellular vesicles for genetic information transfer and gene therapy. *Hum Mol Genet* **21**: R125–R134.
178. Théry C, Ostrowski M, Segura E (2009) Membrane vesicles as conveyors of immune responses. *Nat Rev Immunol* **9**: 581–593.
179. Fang DY, King HW, LI JY, Gleadle JM (2013) Exosomes and the kidney: blaming the messenger. *Nephrology* **18**: 1–10.
180. Pegtel DM, van de Garde MDB, Middeldorp JM (2011) Viral miRNAs exploiting the endosomal-exosomal pathway for intercellular cross-talk and immune evasion. *Biochim Biophys Acta* **1809**: 715–721.
181. Mittelbrunn M, Gutiérrez-Vázquez C, Villarroya-Beltri C, González S, Sánchez-Cabo F, González MÁ, Bernad A, Sánchez-Madrid F (2011) Unidirectional transfer of microRNA-loaded exosomes from T cells to antigen-presenting cells. *Nat Commun* **2**: 282.
182. Ogata-Kawata H, Izumiya M, Kurioka D, Honma Y, Yamada Y, Furuta K, Gunji T, Ohta H, Okamoto H, Sonoda H, et al. (2014) Circulating Exosomal microRNAs as Biomarkers of Colon Cancer. *PLoS ONE* **9**: e92921.
183. Di Ieva A, Butz H, Niamah M, Rotondo F, De Rosa S, Sav A, Yousef GM, Kovacs K, Cusimano MD (2014) MicroRNAs as Biomarkers in Pituitary Tumors. *Neurosurgery* **75**: 181–189.
184. Sinha A, Yadav AK, Chakraborty S, Kabra SK, Lodha R, Kumar M, Kulshreshtha A, Sethi T, Pandey R, Malik G, et al. (2013) Exosome-enclosed microRNAs in exhaled breath hold potential for biomarker discovery in patients with pulmonary diseases. *J Allergy Clin Immunol* **132**: 219–222.
185. Street JM, Birkhoff W, Menzies RI, Webb DJ, Bailey MA, Dear JW (2011) Exosomal transmission of functional aquaporin 2 in kidney cortical collecting duct cells. *J Physiol (Lond)* **589**: 6119–6127.
186. Pisitkun T, Shen R-F, Knepper MA (2004) Identification and proteomic profiling of exosomes in human urine. *Proc Natl Acad Sci USA* **101**: 13368–13373.
187. Lv L-L, Cao Y, Liu D, Xu M, Liu H, Tang R-N, Ma K-L, Liu B-C (2013) Isolation and quantification of microRNAs from urinary exosomes/microvesicles for biomarker discovery. *Int J Biol Sci* **9**: 1021–1031.
188. Barutta F, Tricarico M, Corbelli A, Annaratone L, Pinach S, Grimaldi S, Bruno G, Cimino D, Taverna D, Deregibus MC, et al. (2013) Urinary exosomal microRNAs in incipient diabetic nephropathy. *PLoS ONE* **8**: e73798.
189. Turchinovich A, Weiz L, Langheinz A, Burwinkel B (2011)

Characterization of extracellular circulating microRNA. *Nucleic Acids Research* **39**: 7223–7233.
190. Turchinovich A, Burwinkel B (2012) Distinct AGO1 and AGO2 associated miRNA profiles in human cells and blood plasma. *RNA Biol* **9**: 1066–1075.
191. Yao B, La LB, Chen Y-C, Chang L-J, Chan EKL (2012) Defining a new role of GW182 in maintaining miRNA stability. *EMBO Rep* **13**: 1102–1108.
192. Laffont B, Corduan A, Plé H, Duchez A-C, Cloutier N, Boilard E, Provost P (2013) Activated platelets can deliver mRNA regulatory Ago2•microRNA complexes to endothelial cells via microparticles. *Blood* **122**: 253–261.
193. Olejniczak SH, La Rocca G, Gruber JJ, Thompson CB (2013) Long-lived microRNA-Argonaute complexes in quiescent cells can be activated to regulate mitogenic responses. *Proc Natl Acad Sci USA* **110**: 157–162.
194. Wang K, Zhang S, Weber J, Baxter D, Galas DJ (2010) Export of microRNAs and microRNA-protective protein by mammalian cells. *Nucleic Acids Research* **38**: 7248–7259.
195. Espina V, Wulfkuhle JD, Calvert VS, VanMeter A, Zhou W, Coukos G, Geho DH, Petricoin EF, Liotta LA (2006) Laser-capture microdissection. *Nat Protoc* **1**: 586–603.
196. Satchell SC, Tasman CH, Singh A, Ni L, Geelen J, Ruhland von CJ, O'Hare MJ, Saleem MA, van den Heuvel LP, Mathieson PW (2006) Conditionally immortalized human glomerular endothelial cells expressing fenestrations in response to VEGF. *Kidney International* **69**: 1633–1640.
197. O'Hare MJ, Bond J, Clarke C, Takeuchi Y, Atherton AJ, Berry C, Moody J, Silver AR, Davies DC, Alsop AE, et al. (2001) Conditional immortalization of freshly isolated human mammary fibroblasts and endothelial cells. *Proc Natl Acad Sci USA* **98**: 646–651.
198. Ryan MJ, Johnson G, Kirk J, Fuerstenberg SM, Zager RA, Torok-Storb B (1994) HK-2: an immortalized proximal tubule epithelial cell line from normal adult human kidney. *Kidney International* **45**: 48–57.
199. Jones S, Jones S, Phillips AO (2001) Regulation of renal proximal tubular epithelial cell hyaluronan generation: implications for diabetic nephropathy. *Kidney International* **59**: 1739–1749.
200. Tian Y-C, Fraser D, Attisano L, Phillips AO (2003) TGF-beta1-mediated alterations of renal proximal tubular epithelial cell phenotype. *Am J Physiol Renal Physiol* **285**: F130–F142.
201. Saleem MA, O'Hare MJ, Reiser J, Coward RJ, Inward CD, Farren T, Xing CY, Ni L, Mathieson PW, Mundel P (2002) A conditionally immortalized human podocyte cell line demonstrating nephrin and podocin expression. *Journal of the American Society of Nephrology* **13**: 630–638.
202. Andreasen D, Fog JU, Biggs W, Salomon J, Dahslveen IK, Baker A, Mouritzen P (2010) Improved microRNA quantification in total RNA from clinical samples. *Methods* **50**: S6–S9.
203. Livak KJ, Schmittgen TD (2001) Analysis of relative gene expression data using real-time quantitative PCR and the 2(-Delta Delta C(T)) Method. *Methods* **25**: 402–408.
204. Laemmli UK (1970) Cleavage of structural proteins during the assembly of the head of bacteriophage T4. *Nature* **227**: 680–685.
205. Shannon P, Markiel A, Ozier O, Baliga NS, Wang JT, Ramage D, Amin

N, Schwikowski B, Ideker T (2003) Cytoscape: a software environment for integrated models of biomolecular interaction networks. *Genome Res* **13**: 2498–2504.

206. Lewis BP, Shih I-H, Jones-Rhoades MW, Bartel DP, Burge CB (2003) Prediction of mammalian microRNA targets. *Cell* **115**: 787–798.
207. Uil TG, Vellinga J, de Vrij J, van den Hengel SK, Rabelink MJWE, Cramer SJ, Eekels JJM, Ariyurek Y, van Galen M, Hoeben RC (2011) miRTarBase: a database curates experimentally validated microRNA-target interactions. *Nucleic Acids Research* **39**: D163–D169.
208. Xiao F, Zuo Z, Cai G, Kang S, Gao X, Li T (2009) miRecords: an integrated resource for microRNA-target interactions. *Nucleic Acids Research* **37**: D105–D110.
209. Wu J, Chen Y-D, Gu W (2010) Urinary proteomics as a novel tool for biomarker discovery in kidney diseases. *J Zhejiang Univ Sci B* **11**: 227–237.
210. Bravo V, Rosero S, Ricordi C, Pastori RL (2007) Instability of miRNA and cDNAs derivatives in RNA preparations. *Biochem Biophys Res Commun* **353**: 1052–1055.
211. Mraz M, Malinova K, Mayer J, Pospisilova S (2009) MicroRNA isolation and stability in stored RNA samples. *Biochem Biophys Res Commun* **390**: 1–4.
212. Bernardo BC, Charchar FJ, Lin RCY, McMullen JR (2012) A microRNA guide for clinicians and basic scientists: background and experimental techniques. *Heart Lung Circ* **21**: 131–142.
213. Hanke M, Hoefig K, Merz H, Feller AC, Kausch I, Jocham D, Warnecke JM, Sczakiel G (2010) A robust methodology to study urine microRNA as tumor marker: microRNA-126 and microRNA-182 are related to urinary bladder cancer. *Urol Oncol* **28**: 655–661.
214. Yamada Y, Enokida H, Kojima S, Kawakami K, Chiyomaru T, Tatarano S, Yoshino H, Kawahara K, Nishiyama K, Seki N, et al. (2010) MiR-96 and miR-183 detection in urine serve as potential tumor markers of urothelial carcinoma: correlation with stage and grade, and comparison with urinary cytology. *Cancer Science* **102**: 522–529.
215. Wang G, Kwan BC-H, Lai FM-M, Chow K-M, Kam-Tao LP, Szeto C-C (2010) Expression of microRNAs in the urinary sediment of patients with IgA nephropathy. *Dis Markers* **28**: 79–86.
216. Chan RW-Y, Tam L-S, Li EK-M, Lai FM-M, Chow K-M, Lai K-B, Li PK-T, Szeto C-C (2003) Inflammatory cytokine gene expression in the urinary sediment of patients with lupus nephritis. *Arthritis & Rheumatism* **48**: 1326–1331.
217. Chan RW-Y, Lai FM-M, Li EK-M, Tam L-S, Wong TY-H, Szeto CY-K, Li PK-T, Szeto C-C (2004) Expression of chemokine and fibrosing factor messenger RNA in the urinary sediment of patients with lupus nephritis. *Arthritis & Rheumatism* **50**: 2882–2890.
218. Yu Z, Hecht NB (2008) The DNA/RNA-binding protein, translin, binds microRNA122a and increases its in vivo stability. *J Androl* **29**: 572–579.
219. Martin J, Jenkins RH, Bennagi R, Krupa A, Phillips AO, Bowen T, Fraser DJ (2011) Post-transcriptional regulation of Transforming Growth Factor Beta-1 by microRNA-744. *PLoS ONE* **6**: e25044.
220. Krupa AA, Jenkins RR, Luo DDD, Lewis AA, Phillips AA, Fraser DD (2010) Loss of MicroRNA-192 promotes fibrogenesis in diabetic nephropathy. *Audio, Transactions of the IRE Professional Group on* **21**:

438–447.
221. Sugiyama RH, Blank A, Dekker CA (1981) Multiple ribonucleases of human urine. *Biochemistry* **20**: 2268–2274.
222. Raposo G, Nijman HW, Stoorvogel W, Liejendekker R, Harding CV, Melief CJ, Geuze HJ (1996) B lymphocytes secrete antigen-presenting vesicles. *J Exp Med* **183**: 1161–1172.
223. Diederichs S, Haber DA (2007) Dual role for argonautes in microRNA processing and posttranscriptional regulation of microRNA expression. *Cell* **131**: 1097–1108.
224. Li L, Zhu D, Huang L, Zhang J, Bian Z, Chen X, Liu Y, Zhang C-Y, Zen K (2012) Argonaute 2 complexes selectively protect the circulating microRNAs in cell-secreted microvesicles. *PLoS ONE* **7**: e46957.
225. Diehl P, Fricke A, Sander L, Stamm J, Bassler N, Htun N, Ziemann M, Helbing T, El-Osta A, Jowett JBM, et al. (2012) Microparticles: major transport vehicles for distinct microRNAs in circulation. *Cardiovasc Res* **93**: 633–644.
226. Gallo A, Tandon M, Alevizos I, Illei GG (2012) The majority of microRNAs detectable in serum and saliva is concentrated in exosomes. *PLoS ONE* **7**: e30679.
227. Cheng Y, Wang X, Yang J, Duan X, Yao Y, Shi X, Chen Z, Fan Z, Liu X, Qin S, et al. (2012) A translational study of urine miRNAs in acute myocardial infarction. *J Mol Cell Cardiol* **53**: 668–676.
228. Gray SPS, Cooper MEM (2011) Diabetic nephropathy in 2010: Alleviating the burden of diabetic nephropathy. *Nat Rev Nephrol* **7**: 71–73.
229. Molitch ME, DeFronzo RA, Franz MJ, Keane WF, Mogensen CE, Parving H-H, Steffes MW, American Diabetes Association (2004) Nephropathy in diabetes. *Diabetes Care* **27 Suppl 1**: S79–S83.
230. Hewitt SM, Dear J, Star RA (2004) Discovery of protein biomarkers for renal diseases. *Journal of the American Society of Nephrology* **15**: 1677–1689.
231. Tsalamandris C, Allen TJ, Gilbert RE, Sinha A, Panagiotopoulos S, Cooper ME, Jerums G (1994) Progressive decline in renal function in diabetic patients with and without albuminuria. *Diabetes* **43**: 649–655.
232. Kanwar YS, Sun L, Xie P, Liu F-Y, Chen S (2011) A glimpse of various pathogenetic mechanisms of diabetic nephropathy. *Annu Rev Pathol* **6**: 395–423.
233. Farris AB, Colvin RB (2012) Renal interstitial fibrosis: mechanisms and evaluation. *Curr Opin Nephrol Hypertens* **21**: 289–300.
234. Bail S, Swerdel M, Liu H, Jiao X, Goff LA, Hart RP, Kiledjian M (2010) Differential regulation of microRNA stability. *RNA* **16**: 1032–1039.
235. Schena FP, Serino G, Sallustio F (2014) MicroRNAs in kidney diseases: new promising biomarkers for diagnosis and monitoring. *Nephrology Dialysis Transplantation* **29**: 755–763.
236. Gottardo FF, Liu CGC, Ferracin MM, Calin GAG, Fassan MM, Bassi PP, Sevignani CC, Byrne DD, Negrini MM, Pagano FF, et al. (2007) Micro-RNA profiling in kidney and bladder cancers. *Urol Oncol* **25**: 387–392.
237. Yokoi T, Nakajima M (2011) Toxicological implications of modulation of gene expression by microRNAs. *Toxicol Sci* **123**: 1–14.
238. Tili EE, Michaille J-JJ, Gandhi VV, Plunkett WW, Sampath DD, Calin GAG (2007) miRNAs and their potential for use against cancer and other diseases. *Pharmacogenomics* **3**: 521–537.
239. Li WY, Jin J, Chen J, Guo Y, Tang J, Tan S (2014) Circulating

microRNAs as potential non-invasive biomarkers for the early detection of hypertension-related stroke. *J Hum Hypertens* **28**: 288–291.

240. Ben-Dov IZ, Tan Y-C, Morozov P, Wilson PD, Rennert H, Blumenfeld JD, Tuschl T (2014) Urine microRNA as potential biomarkers of autosomal dominant polycystic kidney disease progression: description of miRNA profiles at baseline. *PLoS ONE* **9**: e86856.
241. Neal CS, Michael MZ, Pimlott LK, Yong TY, Li JYZ, Gleadle JM (2011) Circulating microRNA expression is reduced in chronic kidney disease. *Nephrol Dial Transplant* **26**: 3794–3802.
242. Andersen CL, Jensen JL, Ørntoft TF (2004) Normalization of real-time quantitative reverse transcription-PCR data: a model-based variance estimation approach to identify genes suited for normalization, applied to bladder and colon cancer data sets. *Cancer Res* **64**: 5245–5250.
243. Shen Y, Li Y, Ye F, Wang F, Wan X, Lu W, Xie X (2011) Identification of miR-23a as a novel microRNA normalizer for relative quantification in human uterine cervical tissues. *Exp Mol Med* **43**: 358–366.
244. Davoren PA, McNeill RE, Lowery AJ, Kerin MJ, Miller N (2008) Identification of suitable endogenous control genes for microRNA gene expression analysis in human breast cancer. *BMC Mol Biol* **9**: 76.
245. Peltier HJ, Latham GJ (2008) Normalization of microRNA expression levels in quantitative RT-PCR assays: identification of suitable reference RNA targets in normal and cancerous human solid tissues. *RNA* **14**: 844–852.
246. Coulouarn C, Factor VM, Andersen JB, Durkin ME, Thorgeirsson SS (2009) Loss of miR-122 expression in liver cancer correlates with suppression of the hepatic phenotype and gain of metastatic properties. *Oncogene* **28**: 3526–3536.
247. Wang S, Qiu L, Yan X, Jin W, Wang Y, Chen L, Wu E, Ye X, Gao GF, Wang F, et al. (2012) Loss of microRNA 122 expression in patients with hepatitis B enhances hepatitis B virus replication through cyclin G1-modulated P53 activity. *Hepatology* **55**: 730–741.
248. Waidmann O, Bihrer V, Pleli T, Farnik H, Berger A, Zeuzem S, Kronenberger B, Piiper A (2011) Serum microRNA-122 levels in different groups of patients with chronic hepatitis B virus infection. *Journal of Viral Hepatitis* **19**: e58–e65.
249. Zhang Y, Jia Y, Zheng R, Guo Y, Wang Y, Guo H, Fei M, Sun S (2010) Plasma MicroRNA-122 as a Biomarker for Viral-, Alcohol-, and Chemical-Related Hepatic Diseases. *Clin Chem* **56**: 1830–1838.
250. Ji X, Takahashi R, Hiura Y, Hirokawa G, Fukushima Y, Iwai N (2009) Plasma miR-208 as a Biomarker of Myocardial Injury. *Clin Chem* **55**: 1944–1949.
251. Wang S, Aurora AB, Johnson BA, Qi X, McAnally J, Hill JA, Richardson JA, Bassel-Duby R, Olson EN (2008) The endothelial-specific microRNA miR-126 governs vascular integrity and angiogenesis. *Developmental Cell* **15**: 261–271.
252. Wanet A, Tacheny A, Arnould T, Renard P (2012) miR-212/132 expression and functions: within and beyond the neuronal compartment. *Nucleic Acids Research* **40**: 4742–4753.
253. Eskildsen TV, Jeppesen PL, Schneider M, Nossent AY, Sandberg MB, Hansen PBL, Jensen CH, Hansen ML, Marcussen N, Rasmussen LM, et al. (2013) Angiotensin II Regulates microRNA-132/-212 in Hypertensive Rats and Humans. *Int J Mol Sci* **14**: 11190–11207.

254. Ucar A, Gupta SK, Fiedler J, Erikci E, Kardasinski M, Batkai S, Dangwal S, Kumarswamy R, Bang C, Holzmann A, et al. (2012) The miRNA-212/132 family regulates both cardiac hypertrophy and cardiomyocyte autophagy. *Nat Commun* **3**: 1078.
255. Brennecke J, Stark A, Russell RB, Cohen SM (2005) Principles of microRNA-target recognition. *PLoS Biol* **3**: e85.
256. Vo N, Klein ME, Varlamova O, Keller DM, Yamamoto T, Goodman RH, Impey S (2005) A cAMP-response element binding protein-induced microRNA regulates neuronal morphogenesis. *Proc Natl Acad Sci USA* **102**: 16426–16431.
257. Impey S, McCorkle SR, Cha-Molstad H, Dwyer JM, Yochum GS, Boss JM, McWeeney S, Dunn JJ, Mandel G, Goodman RH (2004) Defining the CREB regulon: a genome-wide analysis of transcription factor regulatory regions. *Cell* **119**: 1041–1054.
258. Ucar A, Vafaizadeh V, Jarry H, Fiedler J, Klemmt PAB, Thum T, Groner B, Chowdhury K (2010) miR-212 and miR-132 are required for epithelial stromal interactions necessary for mouse mammary gland development. *Nat Genet* **42**: 1101–1108.
259. Lee S-T, Chu K, Im W-S, Yoon H-J, Im J-Y, Park J-E, Park K-H, Jung K-H, Lee SK, Kim M, et al. (2011) Altered microRNA regulation in Huntington's disease models. *Exp Neurol* **227**: 172–179.
260. Zhang Z, Chang H, Li Y, Zhang T, Zou J, Zheng X, Wu J (2010) MicroRNAs: potential regulators involved in human anencephaly. *Int J Biochem Cell Biol* **42**: 367–374.
261. Kim AH, Reimers M, Maher B, Williamson V, McMichael O, McClay JL, van den Oord EJCG, Riley BP, Kendler KS, Vladimirov VI (2010) MicroRNA expression profiling in the prefrontal cortex of individuals affected with schizophrenia and bipolar disorders. *Schizophr Res* **124**: 183–191.
262. Li Y, Zhang D, Chen C, Ruan Z, Li Y, Huang Y (2012) MicroRNA-212 displays tumor-promoting properties in non-small cell lung cancer cells and targets the hedgehog pathway receptor PTCH1. *Mol Biol Cell* **23**: 1423–1434.
263. Incoronato M, Garofalo M, Urso L, Romano G, Quintavalle C, Zanca C, Iaboni M, Nuovo G, Croce CM, Condorelli G (2010) miR-212 increases tumor necrosis factor-related apoptosis-inducing ligand sensitivity in non-small cell lung cancer by targeting the antiapoptotic protein PED. *Cancer Res* **70**: 3638–3646.
264. Hatakeyama H, Cheng H, Wirth P, Counsell A, Marcrom SR, Wood CB, Pohlmann PR, Gilbert J, Murphy B, Yarbrough WG, et al. (2010) Regulation of heparin-binding EGF-like growth factor by miR-212 and acquired cetuximab-resistance in head and neck squamous cell carcinoma. *PLoS ONE* **5**: e12702.
265. O'Connell RM, Taganov KD, Boldin MP, Cheng G, Baltimore D (2007) MicroRNA-155 is induced during the macrophage inflammatory response. *Proc Natl Acad Sci USA* **104**: 1604–1609.
266. Hulsmans M, Holvoet P (2013) MicroRNA-containing microvesicles regulating inflammation in association with atherosclerotic disease. *Cardiovasc Res* **100**: 7–18.
267. Faraoni I, Antonetti FR, Cardone J, Bonmassar E (2009) miR-155 gene: a typical multifunctional microRNA. *Biochim Biophys Acta* **1792**: 497–505.

268. Squadrito ML, Etzrodt M, De Palma M, Pittet MJ (2013) MicroRNA-mediated control of macrophages and its implications for cancer. *Trends Immunol* **34**: 350–359.
269. Hartmann G, Wagner H (2013) *Innate Immunity: Resistance and Disease-Promoting Principles*. Karger Medical and Scientific Publishers.
270. Su C, Hou Z, Zhang C, Tian Z, Zhang J (2011) Ectopic expression of microRNA-155 enhances innate antiviral immunity against HBV infection in human hepatoma cells. *Virol J* **8**: 354.
271. Zhu N, Zhang D, Chen S, Liu X, Lin L, Huang X, Guo Z, Liu J, Wang Y, Yuan W, et al. (2011) Endothelial enriched microRNAs regulate angiotensin II-induced endothelial inflammation and migration. *Atherosclerosis* **215**: 286–293.
272. Suárez Y, Wang C, Manes TD, Pober JS (2010) Cutting edge: TNF-induced microRNAs regulate TNF-induced expression of E-selectin and intercellular adhesion molecule-1 on human endothelial cells: feedback control of inflammation. *J Immunol* **184**: 21–25.
273. Wang H, Peng W, Shen X, Huang Y, Ouyang X, Dai Y (2012) Circulating levels of inflammation-associated miR-155 and endothelial-enriched miR-126 in patients with end-stage renal disease. *Braz J Med Biol Res* **45**: 1308–1314.
274. Oba S, Kumano S, Suzuki E, Nishimatsu H, Takahashi M, Takamori H, Kasuya M, Ogawa Y, Sato K, Kimura K (2010) miR-200b precursor can ameliorate renal tubulointerstitial fibrosis. *PLoS ONE* **5**: e13614.
275. Xiong M, Jiang L, Zhou Y, Qiu W, Fang L, Tan R, Wen P, Yang J (2012) The miR-200 family regulates TGF-β1-induced renal tubular epithelial to mesenchymal transition through Smad pathway by targeting ZEB1 and ZEB2 expression. *AJP: Renal Physiology* **302**: F369–F379.
276. Hyun S, Lee JH, Jin H, Nam J, Namkoong B, Lee G, Chung J, Kim VN (2009) Conserved MicroRNA miR-8/miR-200 and its target USH/FOG2 control growth by regulating PI3K. *Cell* **139**: 1096–1108.
277. Jenkins RH, Martin J, Phillips AO, Bowen T, Fraser DJ (2012) Transforming growth factor β1 represses proximal tubular cell microRNA-192 expression through decreased hepatocyte nuclear factor DNA binding. *Biochem J* **443**: 407–416.
278. Jenkins RH, Martin J, Phillips AO, Bowen T, Fraser DJ (2012) Pleiotropy of microRNA-192 in the kidney. *Biochem Soc Trans* **40**: 762–767.
279. Snowdon J, Boag S, Feilotter H, Izard J, Siemens DR (2012) A pilot study of urinary microRNA as a biomarker for urothelial cancer. *Can Urol Assoc J* 1–5.
280. Zhou X, Mao A, Wang X, Duan X, Yao Y, Zhang C (2013) Urine and serum microRNA-1 as novel biomarkers for myocardial injury in open-heart surgeries with cardiopulmonary bypass. *PLoS ONE* **8**: e62245.
281. Bryant RJ, Pawlowski T, Catto JWF, Marsden G, Vessella RL, Rhees B, Kuslich C, Visakorpi T, Hamdy FC (2012) Changes in circulating microRNA levels associated with prostate cancer. *British Journal of Cancer* **106**: 768–774.
282. Wang G, Tam L-S, Kwan BC-H, Li EK-M, Chow K-M, Luk CC-W, Li PK-T, Szeto C-C (2012) Expression of miR-146a and miR-155 in the urinary sediment of systemic lupus erythematosus. *Clin Rheumatol* **31**: 435–440.
283. QI J, Wang J, KATAYAMA H, SEN S, LIU SM (2012) Circulating microRNAs (cmiRNAs) as novel potential biomarkers for hepatocellular carcinoma. *Neoplasma*.

284. Ciesla M, Skrzypek K, Kozakowska M, Loboda A, Jozkowicz A, Dulak J (2011) MicroRNAs as biomarkers of disease onset. *Anal Bioanal Chem* **401**: 2051–2061.
285. Wang G, Kwan BC-H, Lai FM-M, Chow K-M, Li PK-T, Szeto C-C (2011) Elevated levels of miR-146a and miR-155 in kidney biopsy and urine from patients with IgA nephropathy. *Dis Markers* **30**: 171–179.
286. Wang Q, Wang Y, Minto AW, Wang J, Shi Q, Li X, Quigg RJ (2008) MicroRNA-377 is up-regulated and can lead to increased fibronectin production in diabetic nephropathy. *FASEB J* **22**: 4126–4135.
287. Kato M, Putta S, Wang M, Yuan H, Lanting L, Nair I, Gunn A, Nakagawa Y, Shimano H, Todorov I, et al. (2009) TGF-beta activates Akt kinase through a microRNA-dependent amplifying circuit targeting PTEN. *Nat Cell Biol* **11**: 881–889.
288. Chen YQY, Wang XXX, Yao XMX, Zhang DLD, Yang XFX, Tian SFS, Wang NSN (2012) Abated microRNA-195 expression protected mesangial cells from apoptosis in early diabetic renal injury in mice. *J Nephrol* **25**: 566–576.
289. Landgraf P, Rusu M, Sheridan R, Sewer A, Iovino N, Aravin A, Pfeffer S, Rice A, Kamphorst AO, Landthaler M, et al. (2007) A mammalian microRNA expression atlas based on small RNA library sequencing. *Cell* **129**: 1401–1414.
290. Soldatos G, Cooper ME (2008) Diabetic nephropathy: important pathophysiologic mechanisms. *Diabetes Res Clin Pract* **82 Suppl 1**: S75–S79.
291. Cooper ME (2001) Interaction of metabolic and haemodynamic factors in mediating experimental diabetic nephropathy. *Diabetologia* **44**: 1957–1972.
292. Zatz R, Dunn BR, Meyer TW, Anderson S, Rennke HG, Brenner BM (1986) Prevention of diabetic glomerulopathy by pharmacological amelioration of glomerular capillary hypertension. *J Clin Invest* **77**: 1925–1930.
293. Emmert-Buck MR, Bonner RF, Smith PD, Chuaqui RF, Zhuang Z, Goldstein SR, Weiss RA, Liotta LA (1996) Laser capture microdissection. *Science* **274**: 998–1001.
294. Grupp C, Müller GA (1999) Renal fibroblast culture. *Exp Nephrol* **7**: 377–385.
295. Demircan N, Safran BG, Soylu M, Ozcan AA, Sizmaz S (2006) Determination of vitreous interleukin-1 (IL-1) and tumour necrosis factor (TNF) levels in proliferative diabetic retinopathy. *Eye (Lond)* **20**: 1366–1369.
296. Navarro JF, Mora C (2005) Role of inflammation in diabetic complications. *Nephrol Dial Transplant* **20**: 2601–2604.
297. Kohda Y, Murakami H, Moe OW, Star RA (2000) Analysis of segmental renal gene expression by laser capture microdissection. *Kidney International* **57**: 321–331.
298. Kriegel AJ, Liu Y, Liu P, Baker MA, Hodges MR, Hua X, Liang M (2013) Characteristics of microRNAs enriched in specific cell types and primary tissue types in solid organs. *Physiol Genomics* **45**: 1144–1156.
299. Lagos-Quintana M, Rauhut R, Yalcin A, Meyer J, Lendeckel W, Tuschl T (2002) Identification of Tissue-Specific MicroRNAs from Mouse. *Current Biology* **12**: 735–739.
300. Wienholds E, Kloosterman WP, Miska E, Alvarez-Saavedra E, Berezikov

E, de Bruijn E, Horvitz HR, Kauppinen S, Plasterk RHA (2005) MicroRNA expression in zebrafish embryonic development. *Science* **309**: 310–311.

301. Asgeirsdottir SA, van Solingen C, Kurniati NF, Zwiers PJ, Heeringa P, van Meurs M, Satchell SC, Saleem MA, Mathieson PW, Banas B, et al. (2012) MicroRNA-126 contributes to renal microvascular heterogeneity of VCAM-1 protein expression in acute inflammation. *Am J Physiol Renal Physiol* **302**: F1630–F1639.
302. Li N, Cui J, Duan X, Chen H, Fan F (2012) Suppression of type I collagen expression by miR-29b via PI3K, Akt, and Sp1 pathway in human Tenon's fibroblasts. *Invest Ophthalmol Vis Sci* **53**: 1670–1678.
303. Abonnenc M, Nabeebaccus AA, Mayr U, Barallobre-Barreiro J, Dong X, Cuello F, Sur S, Drozdov I, Langley SR, Lu R, et al. (2013) Extracellular Matrix Secretion by Cardiac Fibroblasts: Role of MicroRNA-29b and MicroRNA-30c. *Circ Res* **113**: 1138–1147.
304. Jeppesen PL, Christensen GL, Schneider M, Nossent AY, Jensen HB, Andersen DC, Eskildsen T, Gammeltoft S, Hansen JL, Sheikh SP (2011) Angiotensin II type 1 receptor signalling regulates microRNA differentially in cardiac fibroblasts and myocytes. *Br J Pharmacol* **164**: 394–404.
305. Meng S, Cao JT, Zhang B, Zhou Q, Shen CX, Wang CQ (2012) Downregulation of microRNA-126 in endothelial progenitor cells from diabetes patients, impairs their functional properties, via target gene Spred-1. *J Mol Cell Cardiol* **53**: 64–72.
306. Oglesby IK, Bray IM, Chotirmall SH, Stallings RL, O'Neill SJ, McElvaney NG, Greene CM (2010) miR-126 is downregulated in cystic fibrosis airway epithelial cells and regulates TOM1 expression. *J Immunol* **184**: 1702–1709.
307. Taïbi F, Metzinger-Le Meuth V, M'baya-Moutoula E, Djelouat MSEI, Louvet L, Bugnicourt J-M, Poirot S, Bengrine A, Chillon J-M, Massy ZA, et al. (2013) Possible involvement of microRNAs in vascular damage in experimental chronic kidney disease. *Biochim Biophys Acta* **1842**: 88–98.
308. He A, Zhu L, Gupta N, Chang Y, Fang F (2007) Overexpression of Micro Ribonucleic Acid 29, Highly Up-Regulated in Diabetic Rats, Leads to Insulin Resistance in 3T3-L1 Adipocytes. *Molecular Endocrinology* **21**: 2785–2794.
309. de Jong OG, VERHAAR MC, Chen Y, Vader P, Gremmels H, Posthuma G, Schiffelers RM, Gucek M, van Balkom BWM (2012) Cellular stress conditions are reflected in the protein and RNA content of endothelial cell-derived exosomes. *J Extracell Vesicles* **1**:.
310. Alon R, Kassner PD, Carr MW, Finger EB, Hemler ME, Springer TA (1995) The integrin VLA-4 supports tethering and rolling in flow on VCAM-1. *J Cell Biol* **128**: 1243–1253.
311. Harris TA, Yamakuchi M, Ferlito M, Mendell JT, Lowenstein CJ (2008) MicroRNA-126 regulates endothelial expression of vascular cell adhesion molecule 1. *Proc Natl Acad Sci USA* **105**: 1516–1521.
312. Oettgen P (2006) Regulation of vascular inflammation and remodeling by ETS factors. *Circ Res* **99**: 1159–1166.
313. McLaughlin F, Ludbrook VJ, Kola I, Campbell CJ, Randi AM (1999) Characterisation of the tumour necrosis factor (TNF)-(alpha) response elements in the human ICAM-2 promoter. *Journal of Cell Science* **112 (Pt 24)**: 4695–4703.
314. Harris TA, Yamakuchi M, Kondo M, Oettgen P, Lowenstein CJ (2010)

Ets-1 and Ets-2 regulate the expression of microRNA-126 in endothelial cells. *Arteriosclerosis, Thrombosis, and Vascular Biology* **30**: 1990–1997.
315. Fish JE, Santoro MM, Morton SU, Yu S, Yeh R-F, Wythe JD, Ivey KN, Bruneau BG, Stainier DYR, Srivastava D (2008) miR-126 regulates angiogenic signaling and vascular integrity. *Developmental Cell* **15**: 272–284.
316. Ohba T, Haro H, Ando T, Wako M, Suenaga F, Aso Y, Koyama K, Hamada Y, Nakao A (2009) TNF-α-induced NF-κB signaling reverses age-related declines in VEGF induction and angiogenic activity in intervertebral disc tissues. *J Orthop Res* **27**: 229–235.
317. Cantaluppi V, Gatti S, Medica D, Figliolini F, Bruno S, Deregibus MC, Sordi A, Biancone L, Tetta C, Camussi G (2012) Microvesicles derived from endothelial progenitor cells protect the kidney from ischemia-reperfusion injury by microRNA-dependent reprogramming of resident renal cells. *Kidney International* **82**: 412–427.
318. Li Z, Hassan MQ, Jafferji M, Aqeilan RI, Garzon R, Croce CM, van Wijnen AJ, Stein JL, Stein GS, Lian JB (2009) Biological functions of miR-29b contribute to positive regulation of osteoblast differentiation. *J Biol Chem* **284**: 15676–15684.
319. van Rooij E, Sutherland LB, Thatcher JE, DiMaio JM, Naseem RH, Marshall WS, Hill JA, Olson EN (2008) Dysregulation of microRNAs after myocardial infarction reveals a role of miR-29 in cardiac fibrosis. *Proc Natl Acad Sci USA* **105**: 13027–13032.
320. Cushing L, Kuang PP, Qian J, Shao F, Wu J, Little F, Thannickal VJ, Cardoso WV, Lü J (2011) miR-29 is a major regulator of genes associated with pulmonary fibrosis. *Am J Respir Cell Mol Biol* **45**: 287–294.
321. Kwiecinski M, Elfimova N, Noetel A, Töx U, Steffen H-M, Hacker U, Nischt R, Dienes HP, Odenthal M (2012) Expression of platelet-derived growth factor-C and insulin-like growth factor I in hepatic stellate cells is inhibited by miR-29. *Lab Invest* **92**: 978–987.
322. Taylor DD, Gercel-Taylor C (2008) MicroRNA signatures of tumor-derived exosomes as diagnostic biomarkers of ovarian cancer. *Gynecol Oncol* **110**: 13–21.
323. Kloecker GH, Rabinowits G, Gercel-Taylor C, Day JM, Taylor DD (2008) Exosomal microRNA: A Diagnostic Marker for Lung Cancer. *Clinical Lung Cancer* **9**: 295.
324. Hergenreider E, Heydt S, Tréguer K, Boettger T, Horrevoets AJG, Zeiher AM, Scheffer MP, Frangakis AS, Yin X, Mayr M, et al. (2012) Atheroprotective communication between endothelial cells and smooth muscle cells through miRNAs. *Nat Cell Biol* **14**: 249–256.